NYS00484A
Submitted: June 9, 2015

U.S.NRC
United States Nuclear Regulatory Commission
Protecting People and the Environment

NUREG/CR-7153, Vol. 2
ORNL/TM-2013/532

Expanded Materials Degradation Assessment (EMDA)

Volume 2: Aging of Core Internals and Piping Systems

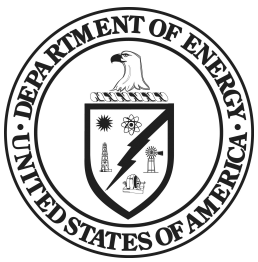

Office of Nuclear Regulatory Research

AVAILABILITY OF REFERENCE MATERIALS IN NRC PUBLICATIONS

NRC Reference Material

As of November 1999, you may electronically access NUREG-series publications and other NRC records at NRC's Public Electronic Reading Room at http://www.nrc.gov/reading-rm.html. Publicly released records include, to name a few, NUREG-series publications; *Federal Register* notices; applicant, licensee, and vendor documents and correspondence; NRC correspondence and internal memoranda; bulletins and information notices; inspection and investigative reports; licensee event reports; and Commission papers and their attachments.

NRC publications in the NUREG series, NRC regulations, and Title 10, "Energy," in the *Code of Federal Regulations* may also be purchased from one of these two sources.

1. The Superintendent of Documents
   U.S. Government Printing Office
   Mail Stop SSOP
   Washington, DC 20402–0001
   Internet: bookstore.gpo.gov
   Telephone: 202-512-1800
   Fax: 202-512-2250
2. The National Technical Information Service
   Springfield, VA 22161–0002
   www.ntis.gov
   1–800–553–6847 or, locally, 703–605–6000

A single copy of each NRC draft report for comment is available free, to the extent of supply, upon written request as follows:

Address: U.S. Nuclear Regulatory Commission
Office of Administration
Publications Branch
Washington, DC 20555-0001
E-mail: DISTRIBUTION.RESOURCE@NRC.GOV
Facsimile: 301–415–2289

Some publications in the NUREG series that are posted at NRC's Web site address http://www.nrc.gov/reading-rm/doc-collections/nuregs are updated periodically and may differ from the last printed version. Although references to material found on a Web site bear the date the material was accessed, the material available on the date cited may subsequently be removed from the site.

Non-NRC Reference Material

Documents available from public and special technical libraries include all open literature items, such as books, journal articles, transactions, *Federal Register* notices, Federal and State legislation, and congressional reports. Such documents as theses, dissertations, foreign reports and translations, and non-NRC conference proceedings may be purchased from their sponsoring organization.

Copies of industry codes and standards used in a substantive manner in the NRC regulatory process are maintained at—

The NRC Technical Library
Two White Flint North
11545 Rockville Pike
Rockville, MD 20852–2738

These standards are available in the library for reference use by the public. Codes and standards are usually copyrighted and may be purchased from the originating organization or, if they are American National Standards, from—

American National Standards Institute
11 West 42nd Street
New York, NY 10036–8002
www.ansi.org
212–642–4900

Legally binding regulatory requirements are stated only in laws; NRC regulations; licenses, including technical specifications; or orders, not in NUREG-series publications. The views expressed in contractor-prepared publications in this series are not necessarily those of the NRC.

The NUREG series comprises (1) technical and administrative reports and books prepared by the staff (NUREG–XXXX) or agency contractors (NUREG/CR–XXXX), (2) proceedings of conferences (NUREG/CP–XXXX), (3) reports resulting from international agreements (NUREG/IA–XXXX), (4) brochures (NUREG/BR–XXXX), and (5) compilations of legal decisions and orders of the Commission and Atomic and Safety Licensing Boards and of Directors' decisions under Section 2.206 of NRC's regulations (NUREG–0750).

U.S.NRC
United States Nuclear Regulatory Commission
Protecting People and the Environment

NUREG/CR-7153, Vol. 2
ORNL/TM-2013/532

Expanded Materials Degradation Assessment (EMDA)

Volume 2: Aging of Core Internals and Piping Systems

Manuscript Completed: October 2013
Date Published: October 2014

Prepared by Expert Panel
Peter Andresen, General Electric; Koji Arioka, Institute of Nuclear Safety Systems; Steve Bruemmer, Pacific Northwest National Laboratory; Jeremy Busby, Oak Ridge National Laboratory; Robin Dyle, Electric Power Research Institute; Peter Ford, General Electric-Retired, Karen Gott, Swedish Nuclear Power Inspectorate-Retired; Amy Hull, U.S. Nuclear Regulatory Commission; and Roger Staehle, Staehle Consulting

On behalf of
Oak Ridge National Laboratory
Managed by UT-Battelle, LLC

J. T. Busby, DOE-NE LWRS EMDA Lead

P. G. Oberson and C. E. Carpenter, NRC Project Managers
M. Srinivasan, NRC Technical Monitor

Office of Nuclear Regulatory Research

ABSTRACT

In NUREG/CR-6923, "Expert Panel Report on Proactive Materials Degradation Assessment," referred to as the PMDA report, NRC conducted a comprehensive evaluation of potential aging-related degradation modes for core internal components, as well as primary, secondary, and some tertiary piping systems, considering operation up to 40 years. This document has been a very valuable resource, supporting NRC staff evaluations of licensees' aging management programs and allowing for prioritization of research needs.

This report describes an expanded materials degradation assessment (EMDA), which significantly broadens the scope of the PMDA report. The analytical timeframe is expanded to 80 years to encompass a potential second 20-year license-renewal operating-period, beyond the initial 40-year licensing term and a first 20-year license renewal. Further, a broader range of structures, systems, and components (SSCs) was evaluated, including core internals, piping systems, the reactor pressure vessel (RPV), electrical cables, and concrete and civil structures. The EMDA uses the approach of the phenomena identification and ranking table (PIRT), wherein an expert panel is convened to rank potential degradation scenarios according to their judgment of susceptibility and current state of knowledge. The PIRT approach used in the PMDA and EMDA has provided the following benefits:

- Captured the status of current knowledge base and updated PMDA information,
- Identified gaps in knowledge for a SSC or material that need future research,
- Identified potential new forms of degradation, and
- Identified and prioritized research needs.

As part of the EMDA activity, four separate expert panels were assembled to assess four main component groups, each of which is the subject of a volume of this report.

- Core internals and piping systems (i.e., materials examined in the PMDA report) – Volume 2
- Reactor pressure vessel steels (RPV) – Volume 3
- Concrete civil structures – Volume 4
- Electrical power and instrumentation and control (I&C) cabling and insulation – Volume 5

This volume summarizes the results of expert panel assessment of the aging and degradation of core internals and piping materials of nuclear power plants (NPPs). The work was conducted via a partnership between the NRC and the DOE's Light Water Reactor Sustainability (LWRS) program to extend NRC's Proactive Materials Degradation Assessment (PMDA), NUREG/CR-6923. The main objective of the work described herein was to identify core internal and primary piping components of NPPs where degradation is likely to occur, or may have occurred, to define relevant aging and degradation modes and mechanisms, and to perform systematic assessment of the effects of this aging related degradation on the future life of those components, drawing on the knowledge and expertise of the above-cited panel. The approach adopted by the panel is based on the Phenomena Identification and Ranking Table (PIRT) process.

FOREWORD

According to the provisions of Title 10 of the *Code of Federal Regulations* (CFR), Part 54, "Requirements for Renewal of Operating Licenses for Nuclear Power Plants," licensees may apply for twenty-year renewals of their operating license following the initial forty-year operating period. The majority of plants in the United States have received the first license renewal to operate from forty to sixty years and a number of plants have already entered the period of extended operation. Therefore, licensees are now assessing the economic and technical viability of a second license renewal to operate safely from sixty to eighty years. The requirements of 10 CFR, Part 54 include the identification of passive, long-lived structures, systems, and components which may be subject to aging-related degradation, and the development of aging management programs (AMPs) to ensure that their safety function is maintained consistent with the licensing basis during the extended operating period. NRC guidance on the scope of AMPs is found in NUREG-1800 "Standard Review Plan for Review of License Renewal Applications for Nuclear Power Plants" (SRP-LR) and NUREG-1801, "Generic Aging Lessons Learned (GALL) Report."

In anticipation to review applications for reactor operation from sixty to eighty years, the Office of Nuclear Reactor Regulation (NRR) requested the Office of Nuclear Regulatory Research (RES) to conduct research and identify aging-related degradation scenarios that could be important in this timeframe, and to identify issues for which enhanced aging management guidance may be warranted and allowing for prioritization of research needs. As part of this effort, RES agreed to a Memorandum of Understanding with the U.S. Department of Energy (DOE) to jointly develop an Expanded Materials Degradation Assessment (EMDA) at Oak Ridge National Laboratory (ORNL). The EMDA builds upon work previously done by RES in NUREG/CR-6923, "Expert Panel Report on Proactive Materials Degradation Assessment." Potential degradation scenarios for operation up to forty years were identified using an expert panel to develop a phenomena identification and ranking table (PIRT). NUREG/CR-6923 mainly addressed primary system and some secondary system components. The EMDA covers a broader range of components, including piping systems and core internals, reactor pressure vessel, electrical cables, and concrete structures. To conduct the PIRT and to prepare the EMDA report, an expert panel for each of the four component groups was assembled. The panels included from 6 to 10 members including representatives from NRC, DOE national laboratories, industry, independent consultants, and international organizations. Each panel was responsible for preparing a technical background volume and a PIRT scoring assessment. The technical background chapters in each volume summarizes the current state of knowledge concerning degradation of the component group and highlights technical issues deemed to be the most important for subsequent license renewal.

Detailed background discussions, PIRT findings, assessments, and comprehensive analysis for each of these component groups are presented in the following chapters.

CONTENTS

FIGURES

TABLES

ACKNOWLEDGMENTS

This work was performed jointly under contract with the U.S. Nuclear Regulatory Commission (NRC) Office of Nuclear Regulatory Research (RES) and under the U.S. DOE Office of Nuclear Energy Light Water Reactor Sustainability Program. The authors thank R. Reister, the DOE-NE LWRS Program Manager; K. McCarthy, the DOE-NE LWRS Technical Integration Office Lead, and J. Busby, the DOE-NE LWRS Technical Manager; P. G. Oberson and C. E. Carpenter, the NRC Project Managers; M. Srinivasan, the NRC Technical Monitor; and J. Stringfield, the Oak Ridge National Laboratory (ORNL) NRC Program Manager for support and guidance. J. Busby, T. Rosseel, and D. Williams at ORNL provided helpful suggestions that were essential in the execution of the panel discussion and incorporation of the results into the report. Many valuable review comments were received from NRC staff members of RES and the Division of Engineering. The authors also wish to thank W. Koncinski, A. Harkey, K. Jones, and S. Thomas at ORNL for assistance in formatting and preparing the final document. G. West at ORNL deserves special attention and thanks for his assistance in developing a database to compile, sort, and format the extensive data generated in the PIRT process. Professor G. Was at the University of Michigan was a key participant in the writing of the technical background assessments and his contribution to this work is greatly appreciated.

ABBREVIATED TERMS

%, percent

°C, degrees Celsius

°F, degrees Fahrenheit

γ, gamma

γ′, gamma prime

Δ, delta; denotes change

$\Delta\sigma_y$, change in yield strength

σ, sigma; denotes variability

τ, UMD recovery time

ϕ, flux

ϕt, fluence

$<T_{dam}>$, total average damage energy per atom

0.5T, ½T compact tension specimen

1TC(T), 1T compact tension specimen

3/4-t, three-quarters of the way through the vessel

3DAP, three-dimensional atom probe

41J, 41 joules (absorbed energy level in which Charpy v-notch specimen reaches the ductile-to-brittle transition temperature)

AAR, alkali-aggregate reaction

ADP, annealing demonstration project

AERE, Atomic Energy Research Establishment (UK)

AFCEN, French Society for Design and Construction and In-Service Inspection Rules for Nuclear Islands

AMP, aging management program

AMR, aging management review

ANO-1, Arkansas Nuclear One Unit 1

APT, atom probe tomography

ASME, American Society of Mechanical Engineers

ASTM, American Society for Testing and Materials

at %, atomic percent

ATI, ATI Consulting

ATR, Advanced Test Reactor

B&W, Babcox and Wilcox

BAC, boric acid corrosion

BR3, Belgian reactor 3

BWR, boiling water reactor

C, carbon

C&LAS, carbon and low alloy steels

CASS, cast austenitic stainless steel

CFR, *Code of Federal Regulations*

Cl^-, chloride ion

cm, centimeter

Cr, chromium

CR, cold rolled

CRD, control rod drive

CRDM, control rod drive mechanism

CREEP, thermal creep

CREV, crevice corrosion

CRIEPI, Central Research Institute of Electric Power Industry (Japan)

CRP, Cu-rich precipitates

Cu, copper

CUF, cumulative fatigue usage factor

CVCS, chemical and volume control system

CVN, Charpy V-notch

CW, cold-worked

DBTT, ductile-to-brittle transition temperature

DEBOND, debonding

DH, dissolved hydrogen

DOE, U.S. Department of Energy

dpa, displacements per atom

E, neutron spectrum flux

EBSD, electron backscatter diffraction

EC, erosion–corrosion

ECCS, emergency core cooling system

ECP, electric chemical potential

E_d, displacement threshold energy

EDF, Electricite de France

EDS, energy-dispersive X-ray spectroscopy

EK, Erickson Kirk

Emb., Embrittlement

EMDA, Extended Materials Degradation Assessment

Env., environmental

EONY, Eason, Odette, Nanstad, and Yamamoto

EPMDA, Extended Proactive Materials Degradation Assessment

EPR, electrochemical potentiokinetic reactivation

EPRI, Electric Power Research Institute

eV, electron volt

FAC, flow-accelerated corrosion

FAT, corrosion fatigue

Fe, iron

f_p, volume fraction

FR, fracture resistance

GALL, generic aging lessons learned

GALV, galvanic corrosion

GC, general corrosion

h, hour

HAZ, heat-affected zone

HC, high cycle

HSSI, Heavy-Section Steel Irradiation

HSST, Heavy Section Steel Technology

HWC, hydrogen water chemistry

HWR, heavy water reactor

I&C, instrumentation and controls

IA, irradiation assisted

IAEA, International Atomic Energy Agency

IASCC, irradiation-assisted stress corrosion cracking

IC, irradiation creep

IG, intergranular

IGC, intergranular corrosion

IGF, intergranular fracture

IGSCC, intergranular stress corrosion cracking

IMP, Implementation

IMT, Issue Management Table

in., inch

INL, Idaho National Laboratory

IPA, integrated plant assessment

IVAR, irradiation variables

JAEA, Japan Atomic Energy Agency

JAERI, Japan Atomic Energy Research Institute

JMTR, Japan Materials Testing Reactor

JNES, Japan Nuclear Safety Organization

JPDR, Japan Power Demonstration Reactor

K, stress intensity

keV, thousand electron volt

K_{Ia}, crack-arrest toughness

K_{Ic}, fracture toughness

K_{Jc}, elastic-plastic fracture toughness at onset of cleavage fracture

LAS, low alloy steel

LBP, late-blooming phase

LC, low cycle

LMC, lattice Monte Carlo

LRO, long-range ordering

LTCP, low-temperature crack propagation

LTO, long-term operation

LWR, light water reactor

LWRS, Light-Water Reactor Sustainability

LWRSP, Light Water Reactor Sustainability Program

MA, mill-anneal

MDM, materials degradation matrix

MeV, million electron volts

MIC, microbially induced corrosion

MF, matrix feature

MIG, metal inert gas (welding)

Mn, manganese

MO, Mader and Odette

Mo, molybdenum

MOU, memorandum of understanding

MOY, Mader, Odette, and Yamamoto

MPa√m, stress intensity factor; fracture toughness in units of megapascal square root meter

MPC, Materials Properties Council

n/cm², fluence

n/cm²·s, flux

NE, DOE Office of Nuclear Energy

NEI, Nuclear Energy Institute

Ni, nickel

NMCA, noble metal chemical addition

NOSY, Nanstad, Odette, Stoller, and Yamamoto

NPP, nuclear power plant

NRC, U.S. Nuclear Regulatory Commission

NWC, normal water chemistry

ORNL, Oak Ridge National Laboratory

P, phosphorous

PA, proton annihilation

PIA, postirradiation annealing

PIRT, phenomenon identification and ranking technique

PIT, pitting

PLIM, Nuclear Power Plant Integrity Management

PMDA, Proactive Materials Degradation Assessment

PMMD, proactive management of materials degradation

PNNL, Pacific Northwest National Laboratory

PRA, primary recoil atom

PRE, Prediction of Radiation Embrittlement

PREDB, Power Reactor Engineering Database

PSF, Poolside Facility

PT, penetration test

PTS, pressurized thermal shock

PWHT, post-weld heat treatment

PWR, pressurized water reactor

PWROG, Pressurized Water Reactor Owners Group

PWSCC, primary water stress corrosion cracking

R&D, research and development

RADAMO, SCK-CEN TR model and corresponding TR database

RCS, reactor coolant system

RES, NRC Office of Nuclear Research

RHRS, residual heat removal system

RIS, radiation-induced segregation

RPV, reactor pressure vessel

RSE-M, Rules for In-Service Inspection of Nuclear Power Plant Components (France)

RT, reference temperature

SA, solution anneal

SANS, small-angle neutron scattering

SCC, stress corrosion cracking

SCK-CEN, Studiecentrum voor Kernenergie—Centre d'Etude de l'Énergie Nucléaire (Belgian Nuclear Research Centre)

SE(B), single-edge, notched bend

SEM, scanning electron microscopy

SG, steam generator

SIA, self-interstitial atom

SIS, safety injection system

SM, Stationary Medium Power

SMF, stable matrix feature

SR, stress relaxation

SS, stainless steel

SSC, system, structure, and component

SSRT, slow strain rate test

SW, swelling

$\mathbf{T_0}$, fracture toughness reference temperature

$\mathbf{T_{41J}}$, ductile-to-brittle transition temperature measured at 41 joules of Charpy impact energy

TEM, transmission electron microscopy

TG, transgranular

Th, thermal

$\mathbf{T_i}$, irradiation temperature

TIG, tungsten inert gas (welding)

TiN, titanium nitride

TLAA, time-limited aging analysis

TMS, The Minerals, Metals and Materials Society

TR, test reactor

TT, reference transition temperature; thermal treatment

TTS, transition temperature shift

UCSB, University of California, Santa Barbara

UK, United Kingdom

UMD, unstable matrix defect

UNS, Unified Numbering System

U.S., United States

USE, upper-shelf energy

UT, ultrasonic test

VS, void swelling

VVER, Voda-Vodyanoi Energetichesky Reaktor (Water-Water Energetic Reactor)

WEAR, fretting/wear

Wstg., wastage

wt %, weight percent

Zn, zinc

1. INTRODUCTION

Ensuring safe operation of NPPs for a first, and any subsequent, license renewal period (i.e., 60–80+ years) will require an in-depth knowledge of the various modes of materials degradation that could impact the long-lived systems, structures, and components (SSC) of concern. Identifying and evaluating the effects of emerging degradation mechanisms on the expected service life is vital. The key to any adequate aging management program (AMP) is identifying and controlling the degradation of the constituent materials of the SSC. The U.S. Nuclear Regulatory Commission (NRC) Office of Nuclear Regulatory Research (RES) agreed to a memorandum of understanding (MOU) [1] with the U.S. Department of Energy (DOE) Office of Nuclear Energy (NE) to cooperate on research activities related to the long-term operation of licensed commercial nuclear power plants (NPPs). The NRC and DOE have now completed an Expanded Materials Degradation Assessment (EMDA), involving a comprehensive analysis of degradation mechanisms that may affect the functionality of (i) primary and secondary piping materials and core internals, (ii) concrete civil structures, (iii) reactor pressure vessels (RPVs), and (iv) electrical power and instrumentation and control (I&C) cable insulations during the second, and further subsequent periods of extended operation. The outcome of this research is prioritization of needed research to inform the development of technical basis for such extended reactor operation. The main objective of the EMDA report is to provide a technical basis for regulatory assessments and safety evaluations regarding subsequent license renewal. The EMDA was performed using the same methodology, including an expert panel discussion and PIRT scoring process, as in the original Proactive Materials Degradation Assessment (PMDA), formally presented in *Expert Panel Report on Proactive Materials Degradation Assessment,* NUREG/CR-6923 [2].

1.1 MATERIALS DEGRADATION IN CORE INTERNALS AND PIPING SYSTEMS

Aging-related materials degradation can lead to increased maintenance, downtime, and economic uncertainty for the nuclear power industry as well as increased oversight for the regulatory authorities. Thus, there is a need to resolve materials issues for reactor pressure vessels (RPV) and primary piping, core internals, secondary systems, weldments, concrete, electrical power and instrumentation and control cable insulation, and buried piping. This report deals with core internals and piping systems.

The components, structures and systems of nuclear reactors are exposed to very harsh environments during their service. Components within a reactor core must tolerate high temperature water, stress, vibration, and an intense neutron field. Degradation of materials in this environment can lead to reduced performance, and in some cases, unexpected early failure. Materials degradation within a nuclear power plant is very complex. There are many different types of materials within the reactor itself: over 25 different metal alloys can be found within the primary and secondary systems, not to mention the concrete containment vessel, instrumentation and control, and other support facilities. When this diverse set of materials is placed in the complex and harsh environment coupled with load, degradation over an extended life is indeed quite complicated.

Clearly, materials degradation will impact reactor reliability, availability and, potentially, safe operation. Routine surveillance and component replacement can mitigate these factors, although failures still occur. With reactor life extensions to 60 years or beyond many components must

tolerate the reactor environment for even longer times and when coupled with power uprates reactor conditions may also become more severe (e.g. higher temperatures, increased flow, or higher neutron fluxes). This may increase susceptibility of most components and may introduce new degradation modes. While all components (except perhaps the reactor vessel) can be replaced, it may not be economically favorable. Therefore, understanding, detecting, mitigating, and preventing materials degradation processes with adequate repair and replacement are key priorities for extended reactor operation and power uprate considerations.

The reactor core is a very adverse environment, combining the effects of stress, corrosion, and irradiation. Components in this environment are also often the most critical for safe and reliable operation as the failure of a core internal component may have very severe consequences. Service life beyond 60 years will increase time at temperature and neutron fluence, in general leading to increased susceptibility and severity with respect to known degradation mechanisms (although new mechanisms are also possible). Therefore, understanding the materials performance and degradation mechanisms is one of the key elements for aging management. The issues described below represent those that may warrant additional attention for life beyond 60 years and are grouped into three key areas: corrosion, thermal aging embrittlement and fatigue, and irradiation-induced aging effects. While the material susceptibilities to these key aging effects are highly dependent upon specific material and environment combinations, these aging effects have been observed in service for many key components. These elements are described in considerably more detail in following chapters, organized by key classes of materials.

1.1.1 Corrosion and Stress Corrosion Cracking

In addition to elevated temperatures, intense neutron fields, and stress, components must also be able to withstand a corrosive environment. Temperatures typically range from 288 ºC (550 ºF) in a BWR up to 360 ºC (680 ºF) in a PWR, although other water chemistry variables differ more significantly between the BWR and PWRs.

Corrosion is a complex form of degradation that is strongly dependent on temperature, material condition, material composition, water purity, water pH, water impurities, and gas concentrations. The operating corrosion mechanism will vary from location to location within the reactor vessel and piping system and a number of different mechanisms may be operative simultaneously. These may include general corrosion mechanisms such as uniform corrosion, boric acid corrosion (BAC), flow-accelerated corrosion (FAC), and/or erosion corrosion. Generally speaking, material degradation due to these corrosion mechanisms occurs over a reasonably large area in a fairly homogenous manner. By contrast, localized corrosion modes occurs over much smaller areas, but at much higher rates than general corrosion and includes crevice corrosion, pitting, galvanic corrosion, and microbially-induced corrosion (MIC). Finally, environmentally assisted cracking (EAC) includes other forms of degradation, which are assisted by localized or general corrosion with the additional contribution of stress. In a LWR, a number of different environmentally assisted cracking mechanisms are observed: intergranular stress corrosion cracking (IGSCC), transgranular stress corrosion cracking (TGSCC), primary water stress corrosion cracking (PWSCC), irradiation-assisted stress corrosion cracking (IASCC) and low-temperature crack propagation (LTCP).

While all forms of corrosion are important in developing an appropriate aging management program, IASCC has received considerable attention over the last four decades due to both its severity and unpredictability. Despite over thirty years of international study, the underlying mechanism of IASCC is still unknown, although more recent work led by groups such as the

Cooperative IASCC Research Group* has identified important controlling parameters. This will be discussed in considerably more detail below.

Clearly, unmonitored corrosion (in all the various forms) is not acceptable for the safe and reliable operation of a reactor. With extended lifetimes, components must resist degradation due to additional time in contact with the coolant. As a result, the various corrosion mechanisms must all be understood and evaluated for different reactor component and sub-systems to ensure safe extended service. The *NUREG/CR-6923* report provides a clear and in-depth review of all these mechanisms for the current LWR fleet. Additional effort is required to evaluate the importance of each with further license renewal.

Components in the secondary (steam generator) side of a PWR are also subject to degradation. While the secondary side of the reactor does not have the added complications of an intense neutron irradiation field, the combined action of corrosion and stress can create many different forms of failure. The majority of steam generator systems in U.S. power plants today originally used Alloy 600 (a Ni-Cr-Fe alloy) for tubes and some other components, although service experience showed many failures in tubes through the 1970s. In the last 20 years, most steam generators with Alloy 600 tubes have been replaced with units that have Alloy 690 tubes, which contain higher Cr content and exhibits more resistance SCC. In addition to the base material, there are weldments, joints, and varying water chemistry conditions leading to a very complex component. Indeed, the array of modes of degradation varies with location. In a single steam generator examined by Staehle and Gorman [3], twenty-five different modes of corrosion degradation were identified. Stress corrosion cracking is found in several different forms, and may be the limiting factor for extended service. The integrity of these components is critical for reliable power generation in extended operation, and as a result, understanding and mitigating these forms of degradation is important. Adding additional service period to these components will allow more time for corrosion to occur. The various forms of corrosion must be evaluated as in the PMDA report, with a special attention to those that may be life limiting in extended service.

1.1.2 Thermal Aging and Fatigue

The effects of elevated temperature service in metal alloys have been examined for many years. Possible effects include phase transformations that can adversely affect mechanical properties. Extended time at elevated temperature may permit even very slow phase transformations to occur. This is of particular concern for cast stainless steel components where the formation of a brittle alpha-phase can result in a loss of fracture toughness and lead to brittle failure. The effects of aging on other components are also of concern and should be examined. The effort required for identifying possible problems can be reduced, though, by using modern materials science modeling techniques and experience from other industries.

Fatigue refers to an aging degradation mechanism where components undergo cyclic stress. Typically, these are either low-load, high frequency stresses or high-load, low frequency stresses generated by thermal cycling, vibration, seismic events, or loading transients. Environmental factors may accelerate fatigue and eventually may result in a component failure. In a light water reactor, components such as the pressure vessel, pressurizer, steam generator shells, steam separators, pumps, and piping are among the components that may be affected. The PMDA

* An international collaboration, based in Halden, Norway, among utilities, vendors, regulators, and research organizations to develop IASCC data.

report identified fatigue as an issue for a number of different components and subsystems for both PWR and BWR. This area of degradation was also identified by the panelists of this effort and is discussed in considerable detail in the background Chapters in this Volume..

Due to the potential for thermal aging and fatigue damage during extended lifetimes, the assumptions and limits considered at the design phase for core internal structures should also be examined. During the initial plant design, each component was designed with a load to expected and specific lifetimes and operating conditions using established guidelines (typically those in Section III of the ASME Boiler and Pressure Vessel Code). An 80-year reactor period of operation corresponds to over 600,000 hours of service (at a 90% service factor) while most long-term mechanical performance data used in design comes from tests operating much less than 100,000 hours. The extension of period of operations beyond these initial design considerations should be carefully examined.

1.1.3 Irradiation-induced Effects

Over the forty-year lifetime of a light water reactor, internal structural components may experience neutron flux to ~10^{22} n/cm^2/s in a BWR and ~10^{23} n/cm^2/s in a PWR (E > 1 MeV), corresponding to accumulated neutron dose of ~7 displacements per atom (dpa) and 70 dpa, respectively. Extending the operating period of a reactor will increase the total neutron fluence to each component. Fortunately, radiation effects in stainless steels (the most common core constituent) are also the most examined as these materials are also of interest in fast-spectrum fission and fusion reactors where higher fluences are encountered. A brief summary of key irradiation-induced changes is listed below, however a much more detailed assessment is provided in Chapter 8 below.

The neutron irradiation field can produce large property and dimensional changes in materials. This occurs primarily via one of five radiation damage processes: Radiation-induced hardening and embrittlement, phase instabilities from radiation-induced or -enhanced segregation and precipitation, irradiation creep due to unbalanced absorption of interstitials vs. vacancies at dislocations, volumetric swelling from cavity formation, and high temperature helium embrittlement due to formation of helium-filled cavities on grain boundaries. For light water reactor systems, high temperature embrittlement and creep are not common problems due to the relatively (for creep) lower reactor operating temperature. However, radiation embrittlement, phase transformation, segregation, and swelling have all been observed in reactor components.

Radiation-induced segregation and phase transformations: Under irradiation, the large concentrations of radiation-induced defects will diffuse to defect sinks such as grain boundaries and free surfaces. These concentrations are far in excess of thermal-equilibrium values and can lead to coupled-diffusion with particular atoms. In engineering metals such as stainless steel, this results in radiation-induced segregation of elements within the steel. For example, in Type 316 stainless steel (SS), chromium (important for corrosion resistance) can be depleted at areas while elements like nickel and silicon are enriched to levels well above the starting, homogenous composition. While radiation-induced segregation does not directly cause component failure, it can influence corrosion behavior in a water environment. Further, this form of degradation can accelerate the thermally-driven phase transformations mentioned above and also result in phase transformations that are not favorable under thermal aging (such as gamma or gamma-prime phases observed in stainless steels). Additional fluence may exacerbate radiation-induced phase transformations and should be considered. The wealth of data generated for fast-breeder reactor studies and more recently in LWR-related analysis will be beneficial in this effort.

Radiation-induced swelling and creep: The diffusion of radiation-induced defects can also result in the clustering of vacancies, creating voids. If gas atoms such as He enter the void, it becomes a bubble. While swelling is typically a greater concern for fast reactor applications where it can be life-limiting, voids have recently been observed in LWR components such as baffle bolts. The motion of vacancies can also greatly accelerate creep rates, resulting in stress relaxation and deformation. Irradiation-induced swelling and creep effects can be synergistic and their combined influence must be considered. Longer reactor component lifetimes may increase the need for a more thorough evaluation of swelling as a limiting factor in LWR operation. As above, data, theory, and simulations generated for fast reactor and fusion applications can be used to help identify potentially problematic components.

Radiation-induced embrittlement: Irradiation may lead to a change in material properties, characterized by a loss of fracture toughness and resistance to crack growth. Radiation embrittlement is typically concurrent with in an increase in the yield and ultimate tensile strength of the material. This increase in strength comes with a corresponding decrease in ductility. This hardening and embrittlement can be caused by the changes in the alloy's microstructure including radiation-induced segregation, phase transformations, and swelling. Although they are different measures of material properties or performance, the irradiation effects community often refers to hardening and embrittlement synonymously, due to their concurrent occurrence and root causes. Extended reactor lifetimes may lead to increased embrittlement issues.

1.2 EMDA PROCESS AND IDENTIFICATION OF RESEARCH NEEDS FOR EXTENDED OPERATING PERIODS

As noted above, materials degradation in the core and primary piping is complex and involves many variables including alloy, environment, stress state, irradiation, and time. The *NUREG/CR-6923* effort provided a systematic and detailed assessment of the susceptibility and knowledge for many of those material, environment, and degradation combinations. When evaluating service to potential 80 years, a similar systematic analysis is required to highlight key needs in research. This document provides an expert panel assessment of corrosion, stress corrosion cracking, thermal effects and irradiation for key material systems in core internal and piping systems. Here, an expanded PMDA methodology was again utilized to provide systematic assessment of aging-related degradation for the extended period of operation up to 80 years. This approach benefits all stakeholders in providing a comprehensive analysis of degradation modes and identifying potential gaps, which may need to be addressed by further research to provide additional data and information for assurance of safe and efficient extended operation.

The expert elicitation process conducted for each expert panel in the EMDA project is based on the Phenomena Identification and Ranking Table (PIRT) process. This process has been used in many nuclear applications for ranking and prioritizing any number of issues. The PIRT process provides a systematic means of obtaining information from experts by generating and analyzing lists (tables) of degradation phenomena. In this process, "phenomena" can refer to a particular reactor condition, a physical or engineering approximation, a reactor component or parameter, or anything else that might influence some relevant figure-of-merit, which is related to reactor safety. The process usually involves the ranking of these phenomena using a series of scoring criteria. The results of the scoring can be assembled to lead to a quantitative ranking of issues or needs.

Each PIRT application has been unique in some respect and the current project is unique in its application. The current PIRT can be described in terms of several key steps. These are

described for the generic process below, although each expert panel made minor adjustments, based on the needs of that material system, and such adjustments will also be described below.

As part of this activity, an expert panel was assembled and, included up to 9 leading experts with a variety of perspectives (including regulatory, academia, industry, and international experience). The panelists selected for this core internals and piping panel had an average of over 40 years experience in the field and many had participated earlier in the NUREG/CR-6923 activity. Selection and assembly of panel experts was performed with NRC and DOE input and approval.

Initial technical background assessments of key degradation modes were then developed and used as a starting foundation for broader discussion, evaluation, and ranking. For this volume, the existing *NUREG/CR-6923* was used as a starting point and additional discussion on the potential changes that might be experienced during subsequent operating periods. Each chapter of the technical background assessment was written by a single panelist and then peer-reviewed by the entire panel. Subsequent discussion amongst the entire panel was also used to identify key themes and revisions to the technical background assessments were made accordingly.

It is important to note that these background assessments are not intended to encompass all of the particular degradation modes or material systems. Detailed texts and background assessments exist in other publications and it is beyond the scope of this project to reproduce them here. Rather, the discussions presented in this report are intended to introduce the subject and context for the evaluation of key modes of degradation for subsequent operating periods.

Based on the input from the technical background chapters (Chapters 2-8 of this volume) the panel then developed a PIRT matrix with a list of degradation scenarios to score. A degradation scenario generally encompasses a particular material, system, component, or subcomponent (depending on the categorization scheme devised by the panel), the environmental condition to which that material is exposed, and the degradation mode, which that material may experience, based on laboratory and operational data. If a certain material is exposed to multiple environments or may experience multiple degradation modes, those are listed and scored as distinct scenarios.

After the scoring matrix was developed, panelists independently scored the degradation scenarios in three categories: Susceptibility, Confidence, and Knowledge. These categories are the same as were used for *NUREG/CR-6923*. Subsequent to the completion of panelists scoring, all scores were compiled and the average of Susceptibility and Knowledge were calculated. Since Confidence is a measure of personal confidence, the average is less meaningful and was not calculated.

After completion of scoring and identification of “outliers,” the panels were reassembled for discussion of the scoring. During this discussion, each degradation mode and related scoring was discussed with the “outliers” being of highest priority. In these discussions, the scoring panelist presented rationale for any scores that differed from the average. The objective was not to develop a consensus score or force conformity among the panelists. The primary goal of this discussion was to foster comprehensive assessments and exchange differing points of view. This discussion among panelists was an important part of the process to ensure all points of view were considered, including consideration of any new information on the subject area which was not previously considered, and accounted for in the final scoring. After compiling any changes in scoring following this debate, the PIRT scoring was tabulated to determine relative research needs and priorities.

Finally, the results of the PIRT scoring were compared to the background technical chapters to ensure all of the important modes of degradation and technical discussion points were captured. Revisions were then made to the supporting chapters and analysis to ensure adequate discussion of key topics, outcomes, and underlying causes. Thus, the technical basis information for conducting PIRT and the results of the PIRT were re-iterated to ensure that coverage and consistency is maintained in the various PIRT subject areas.

1.3 ORGANIZATION OF THIS EMDA VOLUME

This EMDA volume on core internals and piping systems is broad and is an extension of *NUREG/CR-6923*, which covered the same material systems. These material systems include low alloy and carbon steels, wrought stainless steels (SS), Alloy 600 and its weldments, Alloy 690 and its weldments, CASS, and liner materials. These materials serve in a variety of environments spanning a broad range of water chemistry and stress conditions. For many components, irradiation may also occur. The expert panel considered and scored over 1,000 different material/environment/degradation combinations (451 for PWR and 599 for BWR). This document represents the expert panel deliberations and PIRT findings for reactor core internals and primary piping systems.

Chapters 2 through 7 present the technical background assessments for key material systems. These include chapters covering

- Alloy 600 and its weldments
- Alloy 690 and its weldments
- Low alloy and carbon steels
- Wrought stainless steels
- Cast-austenitic stainless steels
- Containment liners

In addition, a separate assessment (Chapter 8) covering irradiation effects is presented as a crosscutting issue covering many of the specific material systems. Each technical background assessment provides a limited amount of background into key material specifications and operating regimes along with an assessment of key degradation modes. Each background assessment also includes a summary of key modes of degradation or knowledge gaps that may exist for subsequent operating periods.

Chapter 9 provides a more detailed description of the PIRT process used by this panel. The overlap and differences with the original PMDA in *NUREG/CR-6923* is also provided. The findings of the PIRT scoring are presented and the results are compared with the findings of the technical background assessments.

Finally, Chapter 10 provides a summary of key knowledge gaps that were identified by the expert panel as well as recommendations and conclusions.

1.4 REFERENCES*

1. NRC, "Memorandum of Understanding between U.S. Nuclear Regulatory Commission and U.S. Department of Energy on Cooperative Nuclear Safety Research," ADAMS ML083370612, U.S. Nuclear Regulatory Commission, April 20, 2009.
2. P. L. Andresen et al., *Expert Panel Report on Proactive Materials Degradation Analysis,* NUREG/CR-6923 (BNL-NUREG-77111-2006), U.S. Nuclear Regulatory Commission, February 2007.
3. R. W. Staehle and J. A. Gorman, "Quantitative Assessment of Submodes of Stress Corrosion Cracking on the Secondary Side of Steam Generator Tubing in Pressurized Water Reactors: Part 2," *Corrosion* **60**(1): 5–63 (2004).

* Inclusion of references in this report does not necessarily constitute NRC approval or agreement with the referenced information.

2. WROUGHT STAINLESS STEELS

Koji Arioka
Institute of Nuclear Safety Systems, Inc.*

2.1 INTRODUCTION

There are over 150 different grades of stainless steel in current commercial use, of which 15 are commonly used in LWRs. Of these, 304 SS and 316 SS are the most common with specific applications of 308 SS, 309 SS, 321 SS, and 347 SS. Both 304 SS and 316 SS are widely used in nuclear reactor applications as well as 321 SS and 347 SS grades. Decades of experience in both commercial LWRs and fast breeder reactors have resulted in further refinement of stainless steel compositions for reactor applications. Past experience in both LWRs and fast breeder reactors has shown that 316 SS offers higher performance and greater reliability than 304 SS, particularly in aqueous corrosion and radiation damage resistance, which will be discussed in more detail in a later chapter.

Type 316 and 304 SS are used for pressure-retaining piping for primary and secondary systems in PWRs. Stabilized stainless steel (Type 347 SS) was used in steam generator tubing in PWRs during the 1960s and is still used in stems of reactor coolant pumps. Types 308L SS and 316L SS are used as the filler metals between stainless steels components and stainless steel piping. The chemical compositions of the Fe-based stainless steels used in LWRs are described in Table 2.1. In BWRs, type 304 SS and 316 SS are utilized as core internal structures including core shrouds, guides, plates, and supports. These grades are also utilized as pressure-retaining piping and coolant pumps. As in PWRs, Type 308 SS and 309 SS are used as weld filler metals (316 SS is used as weld filler in some applications in other countries). Types 308 SS and 309 SS are also utilized for vessel cladding applications.

The background on the choice of these materials is described in the *Corrosion and Wear Handbook for Water-Cooled Reactors* [1], which contains a materials database and explains the concept for material selection for the first nuclear-powered submarine (USS *Nautilus*) and the first commercial PWR (Shippingport, Pennsylvania). The main criteria for the material selection were (a) high corrosion resistance in a readily available alloy for the small purification system needed in a submarine; (b) good fabrication characteristics; and (c) extensive experience with the alloys in other industries, such as petrochemical and fossil power, to avoid unexpected failures and fully leverage the previous research and literature review results.

* Wholly owned by Kansai Electric Power Co., Inc. (KEPCO), Japan.

Table 2.1. Chemical compositions of stainless steels used in LWRs (wt %) (balance is Fe)

	C	Nb	Cr	Cu	Mn	Mo	Ni	P	S	Si
Type 316	0.08 max.	—	16.0-18.0	—	2.0 max.	2.0-3.0	10.0-14.0	0.045 max.	0.03 max.	1.0 max.
Type 316L	0.03 max.	—	16.0-18.0	—	2.0 max.	2.0-3.0	10.0-14.0	0.045 max.	0.03 max.	1.0 max.
Type 304	0.08 max.	—	18.0-20.0	—	2.0 max.	—	8.0-10.5	0.045 max.	0.03 max.	1.0 max.
Type 304L	0.03 max.	—	18.0-20.0	—	2.0 max.	—	8.0-12.0	0.045 max.	0.03 max.	1.0 max.
Type 347	0.08 max.	10xC min.	17.0-19.0	—	2.0 max.	—	9.0-13.0	0.045 max.	0.03 max.	1.0 max.
Type 308L	0.04 max.	—	18.0-21.0	0.75 max.	0.5-2.5	0.75 max.	9.0-11.0	0.04 max.	0.03 max.	0.90 max.
Type 309L	0.04 max.	—	22.0-25.0	0.75 max.	0.5-2.5	0.75 max.	12.0-14.0	0.04 max.	0.03 max.	0.90 max.
Type 403	0.15 max.	—	11.5-13.0	—	1.0 max.	—	—	0.04 max.	0.03 max.	0.5 max
Type 410	0.15 max.	—	11.5-13.5	—	1.0 max.	—	—	0.04 max.	0.03 max.	1.0 max
Type 630	0.07 max.	0.15-0.45	15.0-17.5	3.0-5.0	1.0 max.	—	3.0-5.0	0.04 max.	0.03 max.	1.0 max.

Reproduced from [1].

The stainless steels listed in Table 2.1 are used in the primary systems in a variety of forms, including seamless piping, forgings, castings, and plates. The specific stainless steel–component combinations vary among reactor designs and manufacturers but in general share the following traits:

- Main coolant piping and elbows for PWR primary circuits are cast 316 SS (CF8M). Seamless Type 316 SS is also used for main coolant piping in some PWRs. Cast grades are discussed in detail in Chapter 7 below.
- The inner surfaces of the RPV, pressurizer, and steam generator channel head are clad with Type 308L SS; they are then stress-relieved during a post-weld heat treatment (PWHT) at 595 °C (1,103 °F) to 620 °C (1,148 °F) for 1 hour per 25 mm thickness of steel.
- Pump and valve casings are generally made of cast stainless steel (CF8). Type 410 and Type 630 SS is used for the valve stem. Type 347 SS is used for the reactor coolant pump stem.
- Type 410 and Type 403 SS are used for stem and parts of the control rod drive mechanism, such as the plunger.
- Main coolant piping, elbows, joints and elbows for BWR circuits are comprised for 304 and 316 SS grades.
- Like PWRs the inner surfaces of the RPV are clad with stainless steel, typically 309 or 308L SS grades.
- Core internal structures in BWRs are made of wrought 304 SS and 316 SS.

The history of material degradation in LWRs supports the need for proactive research to identify potential problems before they manifest in the field, and sharing the research results among the stakeholders enables appropriate countermeasures to be taken. Various types of corrosion, such as general corrosion, crevice corrosion, SCC, and corrosion product transport in the primary

system, were studied in the stainless steels described above in hydrogenated and oxygenated high-temperature water to determine their suitability for use in the *Nautilus* and in the first commercial PWRs. The following recommendations were made with regard to expected material degradation at the time of the first commercial nuclear power plants.

2.1.1 Effect of Cold Work on SCC in Primary Systems

Before 1957, SCC had been found in non-sensitized and cold-worked >10% Type 304 SS that had been exposed to oxygenated pure water at 316 °C (601 °F) (see Table 2.2). However, at that time, SCC had not been found in cold-worked non-sensitized Type 304 SS, 310 SS, 316 SS, or 347 SS in hydrogenated pure water after testing for 120 days. Based on those results, it was recommended that cold-worked stainless steels not be used as spring materials in primary systems.

2.1.2 Effect of Secondary Water Chemistry and Sensitization on SCC of Steam Generator Tubing

An initial major concern was cracking in the secondary side of steam generator tubing made of stainless steel when exposed to seawater, especially onboard a submarine. To reduce SCC, non-sensitized stainless steel (Type 347 SS) was recommended as a less susceptible tubing material. Water treatments with phosphate (PO_4^{3-}) as an inhibitor and sulfite ($Na_2SO_3^{2-}$) as an oxygen scavenger were recommend for the secondary water based on the results described in Tables 2.3 and 2.4.

The U.S. Navy decided to change the steam generator tubing material to a Ni-based alloy (Alloy 600) in 1962 to minimize the occurrence of SCC on the secondary side. However, before then in 1959, Coriou et al. [2] reported experimental results to show the SCC susceptibility of Alloy 600 in high-temperature deuterated pure water environments. At present, the materials used to make steam generator tubing are Alloy 690, Alloy 800, and Alloy 600. Alloy 600 is now being phased out in commercial power plants because of IGSCC occurrence on both the primary and secondary sides.

Table 2.2. Influence of cold work and oxygen concentration on SCC susceptibility of austenitic stainless steels in high temperature water

Autoclave SCC tests in Primary water with simple beam specimens of AISI austenitic stainless steels

Water condition			AISI Type	Condition	Stress (psi)	Days	SCC
Temp. (°F)	Gas content	Velocity (ft/sec)					
500	5-10 ppm O2	0	302	Annealed	10,000	90	No
500	do	0	302	do	30,000	90	No
500	do	0	302	do	> yield stress	90	No
500	do	0	302	Sensitized 2h, 1200°F	10,000	90	No
500	do	0	302	do	30,000	90	No
500	do	0	302	do	>yield stress	90	No
500	0.5-4.6 ml/liter O2	11	304	Annealed	30,000	90	No
500	20-30 ml/liter O2	11	304	do	30,000	120	No
600	5-10 ppm O2	0	304	10% Cold worked, annealed	30,000	74	Yes
600	do	0	304	do	50,000	74	Yes
600	do	0	304	50% Cold worked, annealed	30,000	74	Yes
600	do	0	304	do	50,000	74	No
600	do	0	304	10% Cold worked	60,000	74	Yes
600	do	0	304	do	80,000	74	Yes
600	do	0	304	20% Cold worked	70,000	30	No
600	do	0	304	do	90,000	74	Yes
600	do	0	304	30% Cold worked	95,000	30	Yes
600	do	0	304	do	110,000	30	No
600	do	0	304	40% Cold worked	110,000	30	No
600	do	0	304	do	125,000	30	Yes
600	do	0	304	50% Cold worked	130,000	30	No
600	do	0	304	do	150,000	30	No
600	200 ml/ liter H2	0	304	10% Cold worked	60,000	38	No
600	do	0	304	do	80,000	38	No
600	do	0	304	20% Cold worked	70,000	38	No
600	do	0	304	do	90,000	38	No
600	do	0	304	30% Cold worked	95,000	38	**
600	do	0	304	do	110,000	38	**
600	do	0	304	40% Cold worked	110,000	38	No
600	do	0	304	do	125,000	38	**
600	do	0	304	50% Cold worked	130,000	38	No
600	do	0	304	do	150,000	38	No
500	0.5-4.6 ml/liter O2	11	310	Annealed	29,800	30	No
500	20-30 ml/liter O2	11	310	do	29,800	120	No
500	0.5-4.6 ml/liter O2	11	316	do	28,300	30	No
500	20-30 ml/liter O2	11	316	do	28,300	120	No
500	0.5-4.6 ml/liter O2	11	347	do	31,500	30	No
500	20-30 ml/liter O2	11	347	do	31,500	120	No
600	Degassed *	25	347	do	22,400	34	No

Water velocity obtained by rotation of specimens in water or circulating of water past specimen.

* : Degassed means air purge by boiling autoclave before sealing

** : Slight defect parallel to direction of stress; Apparantly associated with a rolling seam ; doubtful if associated with stress corrosion

Reproduced from [1].

Table 2.3. Influence of phosphate treatment on SCC susceptibility of austenitic stainless steels in high temperature water

Autoclave SCC tests of AISI type austenitic stainless steel U-Bend specimens submerged in various alkaline phosphase treated waters (steels annealed before testing)

Cl (ppm)	Nominal O2 ppm	AISI type	Days of test in water with pH *			Total days in tests	Temp, °F	Number of specimens	SCC
			10.6	11	11.3				
High **	Degassed	347	14			14	500	2	No
High **	do	347			14	14	500	2	No
553	Saturated	347	15			15	467	2	No
553	30	347	7			7	500	3	No
553	0.1-0.7	347	30			30	467	2	No
553	0.06	347	7			7	500	3	No
553	Degassed	347	15			15	467	4	No
550	0.05-0.5	304	7		55	62	500	40	No
550	do	347	7	24	51	82	500	50	No
530	Saturated	304	15			15	500	1	Yes ***
530	do	305	15			15	500	1	Yes ***
530	do	347	15			15	500	1	Yes ***
530	do	304			15	15	500	1	No
530	do	347			15	15	500	1	No
530	Aerated	304	90			90	500	1	No
530	do	347	90			90	500	2	No
530	Degassed	347	14			14	470	1	No
500	do	347	15			15	467	1	No
400	do	347	15			15	467	1	No
350	<1.0	347	15			15	500	2	No
350	Degassed	347	15			15	467	1	No
336	Aerated	347			30	30	500	2	No
336	Degassed	347			30	30	470	1	No
336	do	347			30	30	500	2	No
300	do	347	15			15	467	1	No
200	0.05-0.5	304	21	9	35	65	500	40	No
200	do	347	21	53	31	105	500	50	No
150	Degassed	347	15			15	467	1	No
100	<1.0	347	15			15	500	2	No
50	0.05-0.5	304	35		43	78	500	40	No
50	do	347	49	39	52	140	500	50	No
10	do	304	33		83	116	500	40	No
10	do	347	42		74	116	500	50	No
2	do	304	36		67	103	500	40	No
2	do	347	59	14	66	139	500	50	No
1	200	347	15			15	500	2	No
1	30	347	15			15	500	2	No
total								495	Yes : 3 No : 492

Degassed means oxygen removed by boiling and venting autoclave. Aerated means no atempt was made to remove air before sealing autoclave.
Saturatede means oxygen was bubbled through autoclave before sealing. Actual or calculated oxygen contents are given where data are available.
* Water conposition were: pH 10.6 : 50 ppm PO4, pH 11 : 120 ppm PO4, pH 11.3 : 200 ppm PO4
** Exact cholide unknown. High chlorode contained by boiling off to full saturation a solution originally containinng 530 ppm Cl, 50 ppm PO4, and pH 10
*** Vessel was inverted momentarily twice each day, thus exposing the specimens to the vapor phase for short periods.

Reproduced from [1].

Table 2.4. Influence of sensitization on SCC susceptibility under phosphate treatment of austenitic stainless steels

Autocleva SCC tests of sensitized type 304 stainless steel, U bend specimens submerged in 500°F Alkaline-Phosphate treated water containing 0.05-0.5 ppm oxygen

Time sensitized at 1,200F, hr	Cl, ppm	Days of test in water with pH *			Total days in tests	Number of specimens	Number of specimens with IGSCC
		10.6	11	11.3			
1	550	7			7	10	10
1	200	21	9	35	65	10	2
1	50	7		35	42	10	10
1	10	33		69	102	10	None
1	2	36		67	103	10	None
2	550			40	40	4	4
2	550			28	28	10	6
2	50			29	29	10	None

* : Water compositions were, pH 10.6 : 50 ppm PO4, pH 11 : 120 ppm PO4, pH 11.3 : 200 ppm PO4

Reproduced from [1].

2.1.3 Crevice Corrosion in Primary Systems

Crevice corrosion has not yet been experienced in crevice joints, such as socket welds or flange joints, in the presence of hydrogen-bearing water.

2.1.4 Key Modes of Degradation of Stainless Steel in Water Reactor Applications

The degradation of stainless steel in water reactors has been examined for decades and many forms of degradation are well known. Irradiation effects for austenitic stainless steels are well studied and material changes can occur in a number of forms. These are described in detail in Chapter 8 below.

Environmentally assisted cracking (EAC) is also a known form of degradation for stainless steels provided the material is in a susceptible state, a corrosive environment, and under stress. In LWR conditions, the coolant can be very aggressive with high temperatures, high electrochemical potentials [in BWR normal water chemistry (NWC)], with the potential for impurities in sufficient concentration to alter corrosion processes. Stress states are typically complex for most reactor components. Stainless steel is also known to be susceptible to several forms of degradation caused by cold working, embrittlement, sensitization, and weldments and heat-affected zones. For stainless steels in an LWR, a number of different cracking mechanisms are observed: intergranular stress corrosion cracking (IGSCC), transgranular stress corrosion cracking (TGSCC), primary water stress corrosion cracking (PWSCC) and irradiation-assisted stress corrosion cracking (IASCC) have all been observed.

2.2 POTENTIAL FOR DEGRADATION OF STAINLESS STEELS IN LWRS BEYOND 60 YEARS OF OPERATION

Overall, the service experience with wrought stainless steel has been positive to date, although there have been a number of degradation issues in the past.

As noted widely in the open literature, conventional wrought austenitic stainless steels such as 304 SS and 316 SS are susceptible to IGSCC in BWRs when the material was sensitized during

fabrication (either through heat treatment or welding processes), particularly in the high electrochemical potential in NWC environments for BWRs. Proactive countermeasures to reduce the electrochemical potential of the environment and improve the resistance of the alloy via refined alloy chemistry and management of residual stress have greatly reduced cracking observations in BWR piping. Incidents of IGSCC in stainless steel piping in BWRs are now rare.

While IGSCC in BWR piping is well known and largely addressed in the U.S. fleet, EAC in BWR reactor core internals is still observed today. A number of ongoing industry, regulatory, and academia programs are underway around the world to understand the mechanisms and key factors driving susceptibility. Mitigation techniques such as hydrogen water chemistry (HWC) are being utilized to reduce the potential of BWR water and reduce cracking. Noble metal chemical additions have also been successful in reducing cracking incidence in austenitic stainless steel core internals. The long-term effectiveness of these techniques in core internal environments is still being evaluated.

Wrought stainless steels used in PWR reactor coolant systems and reactor internals have an excellent history of service performance. The absence of systematic IGSCC in piping in PWR applications is different than experience in BWR systems and this difference is attributed to the low oxygen content and hydrogen overpressure in PWR reactor coolant. Indeed, this observation was a key motivation for the development of HWC in BWR applications. The relatively limited numbers of problems that have occurred in stainless steel parts in PWRs have generally been due to either mechanical or thermal fatigue, to high levels of cold work, or to the development in stagnant areas of aggressive environments with chlorides, concentrated boric acid and entrapped oxygen.

When considering the potential for operation beyond 60 years of service, there are a number of possible EAC degradation factors and open questions that must be addressed. EAC in oxidizing, high-potential environments like BWR-NWC are well-known phenomena and currently well mitigated for piping applications. Mitigation results from operation in lower electrochemical corrosion potential (ECP) environments such as PWR or even BWR-HWC environments. The following sections are primarily focused on low-ECP hydrogenated water environments, as they will be the most common for extended operating periods.

Potential for the degradation of stainless steel reactor components beyond 60 years of operation may occur due to following phenomena (which are also discussed in more detail in later sections of this document):

- SCC in a low-electrochemical-potential environment typically requires a long-term incubation time or a precursor, becoming apparent after extended times.

- SCC in a high-electrochemical-potential environment (such as oxygen-stagnant areas in PWRs) and possibly impurities such as chloride. Such conditions may occur during plant start-up because the residual air might not be adequately removed before plant start-up. Therefore, the cumulative number of times permitted under such an aggressive environment might exceed after extended operation.

- Potential for the acceleration in more mechanistic degradation processes and ultimately, SCC susceptibility might occur due to a change in the local grain boundary or surface properties during long-term operation, such as chemical composition changes (primarily driven by radiation-induced segregation although thermal processes are also possible) or cavity formation.

Two degradation modes for stainless steels are addressed in the following sections in terms of (a) the past and current plant experience; (b) the current prediction capabilities (e.g., parametric dependency, mechanistic-based models) that expand the analysis time; and based on (c) the long-term (beyond 60 years) concerns that address both the onset of new degradation modes and/or inadequacies in the current mitigation/plant management actions, based on information from both current plant experience and prediction capabilities.

2.2.1 SCC in a Low-Electrochemical-Potential Environment

2.2.1.1 Past and current plant experience

There have been a few reports of PWR component failures due to SCC: canopy seal welds resulting from SCC of austenitic stainless steel in oxygen-stagnant areas [3], the upstream side of the final check valve in the Safety Injection System (SIS) [4], and IASCC [5–9]. The main cause of SCC is assumed to be degradation under high-electrochemical-potential environments due to the residual oxygen in case of the first two incidents. Moreover, the main cause of IASCC is usually assumed to be material irradiation in low-electrochemical-potential environments. To date, the number of incidents caused by SCC in low-electrochemical-potential environments is very few. However, the following incidents caused by SCC on cold-worked 316 SS were reported recently in low-electrochemical-potential environments in PWR primary systems besides IASCC.

SCC in the HAZ of the safe end welded with steam generator inlet nozzle and main coolant piping

Circumferential shallow intergranular cracking was identified in Mihama unit 2 in 2008 [10]. The cracks were located at the safe end made from forged 316 SS. The safe end was welded with the steam generator inlet nozzle and main coolant piping in the primary system. The temperature at the inlet nozzle is about 320 °C (608 °F) during operation. The inner surface was machined and surface-ground after welding. The surface hardness was reported to be ~400 (H_v 1g load) [10]. The maximum depth of the cracking was 0.9 mm. The cracking was located about 3 to 5 mm away from the weld fusion line. An example of the fracture surface and cross-sectional view of the cracking is shown in Figure 2.1. The steam generator in Mihama unit 2 was replaced in the beginning of 1990. The replacement was outfitted with Alloy 690TT tubing. The plant resumed operation in 1994. Therefore, the cracking near the safe end weld is thought to have developed between 1994 and 2008. Significant sensitization was not observed by electrochemical potentiokinetic reactivation method (EPR) and by transmission electron microscope (TEM) observation. Since before 1994, the diaphragm of the make-up tank in Mihama unit 2 has been covered by N_2 gas to keep the oxygen concentration low. Consequently, the influence of oxygen ingress on the cracking of Mihama unit 2 is not postulated to be very significant.

Figure 2.1. Fracture surface and cross-sectional view of the cracking observed at the safe end in Mihama unit 2, after [10].

SCC on the heater sheath in the pressurizer

Since 1997, several occurrences of longitudinal IGSCC have been identified in France on the heater sheaths in pressurizers. Some of them had leaked [11]. The heater sheaths were made from 316L SS and 304L SS, and the cracking initiated from the cold-worked surface. The reported surface hardness via Vickers hardness testing was between 280 and 411 (Hv 0.05g load). No trace of impurity was identified for the removed heater sheath. Based on field results and on laboratory tests, Electricite de France (EdF) concluded that strain localization and associated cold working are necessary conditions for SCC and that IGSCC may be promoted by low strain rate and an increase of alkalinity. EDF developed the stress-relieved heater sheath to decrease the surface hardness, which occurred during manufacturing process. EDF has used the alternative heater sheaths as replacements since the beginning of 2011 [12]. Similar stress-relieving heater sheaths have been used in other countries, such as Japan.

2.2.1.2 Current prediction capabilities

The dependency of a variety of variables on SCC growth behavior has been researched [13–17] in PWR primary water coolant environments using cold-worked austenitic stainless steels and weld metals. The dependence of variables on SCC growth, such as cold work, temperature, stress intensity factor, material composition of forged materials (316, 304 SS) and weld metals (308L SS, 316L SS), electrochemical potential, the extent of sensitization, and rolling direction have been examined. Furthermore, water chemistry variables, such as hydrogen, lithium, and boron concentration, have also been examined [15, 18]. With such information, dissimilarities and similarities in SCC growth behaviors in PWRs and BWRs could be compared, factoring the possible inadequacy of sources and the amount of data.

However, there has been little research to date on the crack initiation phenomena of stainless steels in BWR or PWR primary systems. Lifetime prediction depends on an understanding of the processes occurring during crack initiation and propagation. Consequently, detailed studies on the processes of crack initiation are necessary for reliable estimates of cracking susceptibility during long-term operation.

Present knowledge on the important factors on growth of SCC is summarized as follows to assess the present prediction capabilities and limitations.

Cold work and electrochemical potential

Dependence of electrochemical potential on SCC growth was observed on cold-worked non-sensitized 316 SS and 304 SS in high-temperature water. This trend is quite similar to the results shown in Table 2.1. However, significant IGSCC growth did occur, even in hydrogenated PWR primary water on cold-worked non-sensitized 316 SS and 304 SS, as shown in Figure 2.2.

The growth rate of IGSCC increased with an increasing degree of cold work (which leads to an increase in YS). This result suggested that the growth rate of SCC increases with increasing the residual strain in the materials, such as in the HAZ, heater sheath, and cold-worked piping.

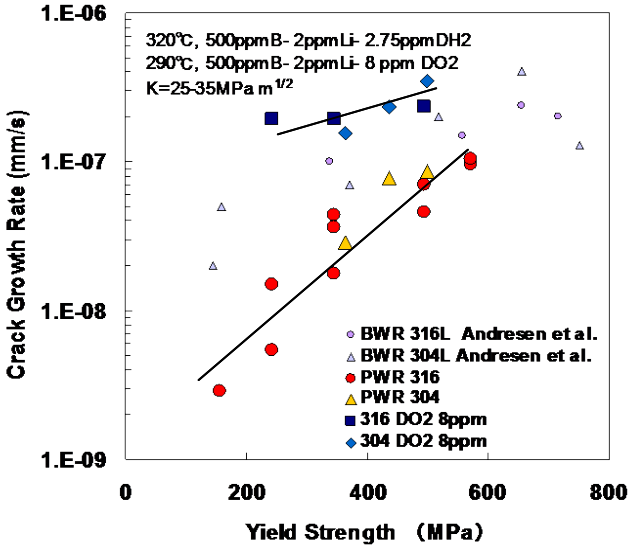

Figure 2.2. Dependence of cold work (measured by yield stress here) and potential on growth of IGSCC of non-sensitized 316 SS and 304 SS [15].

The residual strain caused by shrinkage during the welding process is considered to be strongly dependent on the heat input and the number of passes made during welding. Therefore, the residual strain at weld HAZs is dependent on the thickness or diameter of the piping. Consequently, the rate of SCC growth at the weld HAZ is affected by the pipe diameter and heat input. Examples of major piping in PWR systems and their respective outer diameters are given in Table 2.5.

Table 2.5 Key piping in PWR systems

System piping	Outer Diameter (mm)
Reactor coolant system and safe end	800
Safety injection	165
Residual heat removal	165
Chemical and volume control	89

Given the test results shown in Figure 2.2 and the information on the size of the piping used in PWRs, the weld HAZ in the Reactor Coolant System (RCS) and safe end might show high SCC susceptibility in PWRs. In other words, the SCC susceptibility in the other systems is assumed to be lower. The residual strain also depends on the manufacturing process. The degree of cold work of the through-wall cracked heater sheath was reported as around 30%, judging from its hardness measurement. Given this operating information and results shown in Figure 2.2, one of the major causes of the failure of the heater sheath is considered to be the heavy cold work during manufacturing. A stress-relieved heater sheath is recommended to maintain reliability. Stress-relieved heater sheaths have been put into service in some countries (e.g., Japan and France).

The growth rate of SCC in PWRs is low compared with that in high potential environment such as under NWC condition in BWRs judging from the literature data, such as shown in Figure 2.2. Furthermore, the number of incidents caused by SCC is a few in PWRs except for the cases described in above, to date. However, a few field experiences described here suggested that it is necessary to recognize that it is not immune even in low potential environment such as BWR HWC or PWRs, if material was heavily cold worked. Therefore, detailed studies of SCC initiation are important for precise prediction after long-term operation to keep reliability of components made from heavily cold-worked stainless steels after long-term operation in high tensile stress conditions.

Temperature and cold work

The effect of temperature on IGSCC growth of cold-worked austenitic stainless steels exposed to PWR primary water is shown in Figure 2.3. The growth rate of IGSCC of non-sensitized 20% cold worked 316 [20% cold-worked (CW) 316 SS] increased with increasing temperature in the range 250 °C (482 °F) to 340 °C (644 °F) and then decreased at 360 °C (680 °F) in a PWR primary environment. Also, the growth rate of IGSCC of non-sensitized 10% CW and 15% CW 316 SS increased with increasing temperature up to 330 °C (626 °F) and then decreased at 340 °C (644 °F) and 360 °C (680 °F). However, the detailed mechanism is not clear on this temperature dependence with peak. Simple 1/T type temperature dependence is observed below 330 °C (626 °F) in either case, the apparent activation energy is about 100 kJ/mol. The results seem to suggest that significant crack growth does not occur in the pressurizer [~343 °C (650 °F)], if the degree of cold work does not exceed 20%. Considering the small diameter and thin thickness of the piping in the pressurizer, the residual strain at the weld HAZ is assumed to be low, so the SCC susceptibility and growth rate are assumed to be low in the pressurizer except for heavily cold-worked heater sheath that has not been stress-relieved. The highest operating temperature in Chemical Volume Control System (CVCS) is about 290 °C from the outlet of RCS until the first regenerative heater, and then the temperature decreased. The highest temperature is also about 290 °C in Safety Injection System (SIS) and Residual Heat Removal System (RHRS), even if cavity flow occurs from the RCS, and then temperature decreases. On the upstream side of the separator valve of RHR system, the operating temperature is usually less than about 177 °C (351 °F). Given the operating temperature in CVCS, SIS and RHRS, the SCC susceptibility and SCC growth rate at the weld HAZ in those systems are assumed to be low compared with the hot-leg side of the RCS [~320 °C (608 °F)] based on the literature data such as shown in Figure 2.3. Furthermore, the size and thickness of the piping in CVCS, SIS, and RHRS is smaller and thinner than main coolant piping in RCS, consequently the residual strain caused by welding is assumed to be smaller in weld HAZ in CVCS, SIS, and RHRS than that in RCS. These results suggested that SCC susceptibility in these systems (CVCS, SIS, RHRS) will be lower than that of the safe end welded area in main coolant piping, which was described in Section 1.2.1.1.

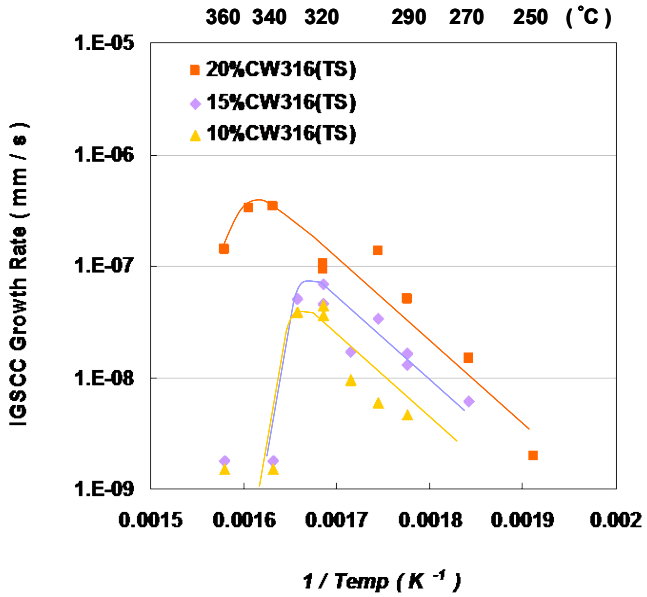

Figure 2.3. Dependence of temperature and cold work on the growth of IGSCC of non-sensitized 316 SS [16]. "TS" in the legend refers to cold-work direction.

Stress intensity factor and cold work

The effect of the stress intensity factor (K) on the crack growth rate of IGSCC in the PWR primary environment is shown in Figure 2.4. Within the test period (~2 months), no significant growth was observed for 15% and 20% cold-worked 316 SS with a K of less than 10 MPa $m^{1/2}$ at 320 °C (608 °F), or for 5% and 10% cold-worked 316 SS with a K of less than 20 MPa $m^{1/2}$ at 320 °C. The results indicated that the growth rate of SCC was insignificant in the HAZ of piping under low-K conditions.

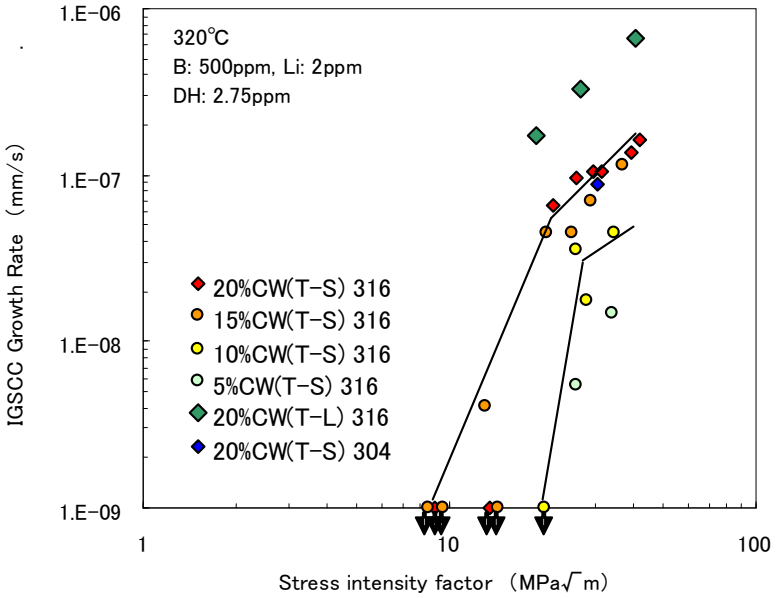

Figure 2.4. Dependence of IGSCC growth rate on stress intensity factor for non-sensitized 316 SS and 304 SS [15].

Sensitization and electrochemical potential

Significant IGSCC growth was not observed for sensitized 20% cold-worked 316 SS in a PWR primary environment in the temperature range between 250 °C (482 °F) and 340 °C (644 °F), as shown in Figure 2.5. This trend is completely different from the IGSCC behavior in high-potential environments such as in BWRs. Furthermore, a similar trend was observed in the hydrogen range between 0 and 30 cc/kg of H_2O, as shown in Figure 2.6. This result suggested that stress relieving does not have any harmful effect on IGSCC propagation in stainless steels in a PWR primary coolant environment except for case in oxygen stagnant area.

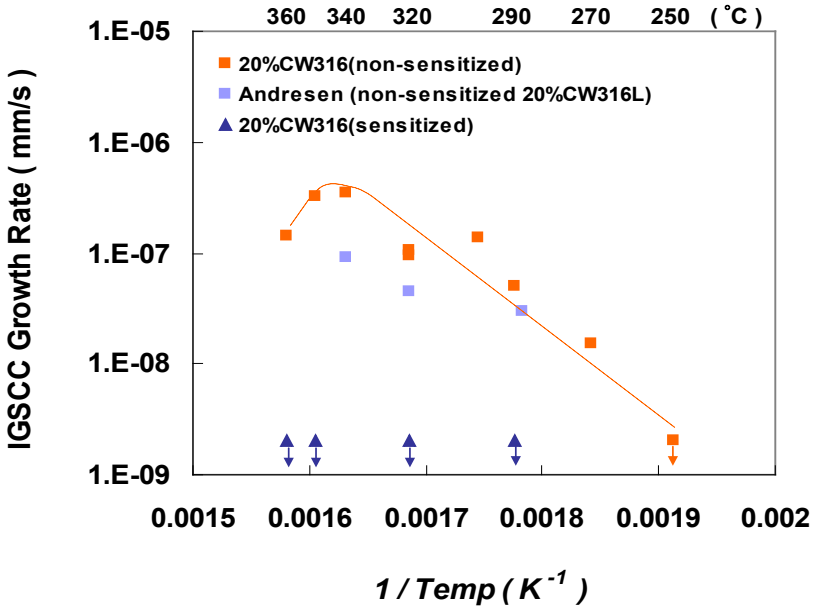

Figure 2.5. Influence of sensitization on IGSCC growth in the PWR primary environment [16].

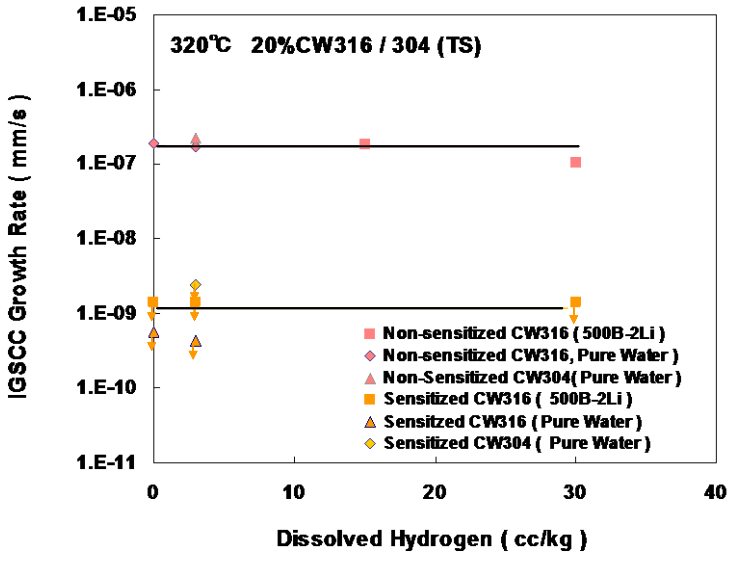

Figure 2.6. Influence of sensitization on IGSCC growth in the PWR primary environment [16].

In other words, this result seems to suggest that stress relieving might become a future countermeasure to retard IGSCC susceptibility in low-potential environments by removing any residual stresses in a component. However, much more fundamental information is necessary, including the mechanistic cause of the effect of sensitization on IGSCC growth in a low-potential environment.

Weld metal and electrochemical potential

High SCC resistance of weld metal (308L SS, 316L SS) was reported [17] for samples exposed to low-potential PWR primary water, although so far the data are limited. Significant SCC growth was not observed for a 10% CW weld metal (308L SS, 316L SS) specimen in a PWR primary environment at 320 °C (608 °F). This behavior is different from that observed forged austenitic stainless steels as discussed above. On the other hand, SCC growth was observed at ferrite and austenite boundaries for 10% cold-worked 308 SS and 316L SS specimens in oxygenated high-temperature water containing lithium and boric acid. Preferential oxidation was observed in the ferrite phase in a high-potential environment although it is not clear whether this is one of the causes of SCC in a high-potential environment. A significant difference in the growth rate in the high-potential environment was not observed between weld metal (308L SS and 316L SS) and forged 316 SS and 304 SS specimens in the high-potential environment. Furthermore, the effect of spinodal decomposition during long term operation on SCC growth was reported [17] using weld and cast stainless steel in both a high- and a low-potential environment. These research data on weld stainless steels has indicated a high resistance to SCC in a low-potential PWR primary environment. However, the data is very limited to data for the precise prediction. To improve the prediction capability on SCC behavior of stainless steel weld metals and cast stainless steels, many more studies are needed. In addition, mechanistic knowledge, such as the mechanistic cause of the difference in SCC susceptibility between stainless steel forgings and stainless steel welds in a low-potential environment and the reason why SCC growth rates are dependent on the potential could potentially enable informed understanding for taking corrective measures

The probability that IGSCC will occur in low potential environment is relatively low for both of non-sensitized and sensitized stainless steels, mainly due to the differences in the electrochemical potential in the respective environments judging from the data shown in Figures 2.2 through 2.6. However, the combined knowledge, based on laboratory data and a few recent field experiences, indicates that heavily cold-worked non-sensitized stainless steels under conditions of high tensile stress condition and high temperature are not immune to SCC, even in a low-potential PWR environment.

When cracking has been observed, it has been related to the combined effects of

- heavy cold work and high residual stress and strain due to high heat input during welding,
- high tensile residual stress and/or stress concentration due to poor weld design, and
- lack of effective stress-relief treatment.

2.2.1.3 Long-term concerns

As described in previously, the probability of occurrence of IGSCC in a low-potential environment is low for both sensitized and non-sensitized stainless steel. However, we should realize that these grades of steel are not immune even in PWR primary low potential environment, if material was heavily cold worked. Therefore, there are concerns for operation extended for more than 60

years. A maintenance program based on information that addresses those concerns should be established to maintain the reliability of components made with these materials in BWRs and PWRs. Those concerns are detailed in the following sections.

Crack initiation process during long-term operation

Steady IGSCC propagation is assumed to start with shallow cracking (~50 to 100 μm deep), although the depth may depend on a number of variables, such as the type of material, degree of cold work, presence of residual stress, and environmental conditions (e.g. service temperature, and coolant chemistry). In other words, even though SCC may be observed in some area in some system (such as safe end weld HAZ), SCC may not occur in piping in other systems (such as SIS, CVCS and RHRS). However, studies on SCC initiation processes in LWR environments are limited to date. From an engineering point of view, detailed studies to consider what locations are susceptible and not susceptible to SCC would be beneficial.

Criteria for arresting the IGSCC propagation

In some cases, the surfaces of HAZ in the welded zone are machined and surface-ground. Shallow local oxidation penetration may occur in these cold-worked regions exposed to PWR environments during long-term operation as judged from the results of removed piping examination [10]. It might be difficult to control the local penetration of corrosion into the cold-worked layer beyond 60 years. However, some cracks are likely to stop growing, even after shallow oxide penetration into the cold-worked layer; in other cases, cracking may continue to grow after shallow crack penetration into the cold worked layer. These different growth behaviors are assumed to depend on the difference in the residual stress and residual strain in the material.

Residual stress and strain in the HAZ strongly depend on the welding procedures, such as the number of passes of welding and heat input. Consequently, if the residual stress in the HAZ is low enough, the crack stops growing, even after shallow crack penetration into the cold-worked surface layer. If the residual stress is high, the crack could potentially grow just after shallow crack penetration into the cold-worked surface layer. Therefore, studies to focus on the criteria for arresting IGSCC propagation would be useful for establishing a reasonable maintenance program to extend reliability beyond 60 years.

Crack growth behavior in weld metal after long-term operation

Hardness and mechanical strength of the ferrite phase change with time due to the spinodal decomposition during operation. Consequently, the local stress and local chemical composition can be expected to change with time. Thermal aging and potential influences on SCC were studied using thermal aged 316L SS, 308L SS, and CF8M test coupons [17–19]. An increase in SCC growth rates was observed after long term aged cast stainless steel (40,000 h at 400 °C (752 °F) in comparison with the crack growth rate of non-aged cast stainless steel in a high potential environment with B and Li at 320 °C (608 °F). On the other hand, no SCC growth was observed in low potential PWR primary environment in the same aged material. However, the data are very limited, especially for the PWR primary environment (service stress, temperature, and coolant chemistry and its composition). Furthermore, the cause of the difference in SCC growth between stainless steel weld and forged stainless steel materials is not well known. More detailed studies on SCC growth and initiation in weld stainless steels may provide technical data and basis to provide the material and component performance assessments for reactor operation beyond 60 years.

Potential for change in local grain-boundary and surface properties during long-term operation

In general, the lattice diffusivity in face centered cubic materials (fcc) is slower than that of body centered cubic material (bcc) such as steel. Therefore, the influence of lattice diffusion on changes in local chemical composition in fcc is assumed to be low at LWR operating temperatures. On the other hand, it's well known that cold work enhances the lattice diffusivity. However, little has been published describing the effect of cold work on diffusivity of austenitic stainless steel and other fcc materials at low temperature less than 600 °C (1,112 °F), and thus not enough information is available about the local change in the materials at PWR operating temperatures. Estimating the possible change in local properties such as the local chemical composition of grain boundaries during long-term operation (beyond 60 years) is not presently available.

Cavity formation was identified at grain boundaries not only for bcc material but also for fcc materials in recent research using cold-worked Alloy 690 (fcc), cold-worked Alloy 600 (fcc), and cold-worked carbon steel (bcc) after testing in the temperature range between 360 °C (680 °F) to 475 °C (887 °F) [20, 21]. An example is shown in Figure 2.7. These cavities are proposed to form as a result of the diffusion of vacancies induced by cold work and driven by a stress gradient. Targeted research may provide information on the possibility that changes in the grain boundary properties (such as changes in grain boundary bonding strength and in chemical composition of grain boundary) have an effect on IGSCC initiation and growth during long-term operation, especially for cold-worked materials.

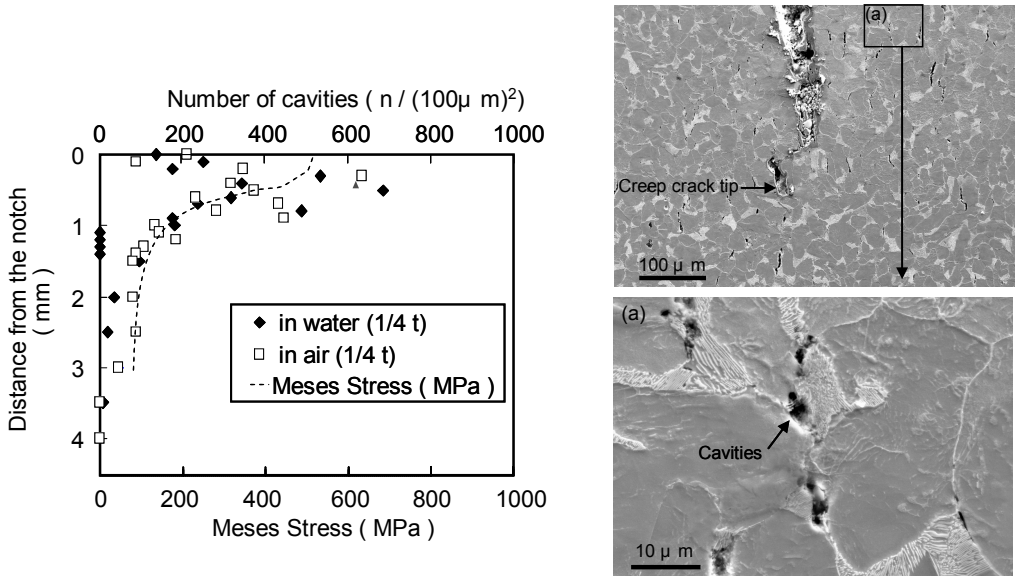

Figure 2.7. Cavity formation at grain boundaries of 30% cold-worked carbon steel after test in at 360 °C [20].

2.2.2 SCC in a High-Electrochemical-Potential Environment (Oxygen-Stagnant Area)

2.2.2.1 Past and current plant experience

There have been some reports of incidents in PWR components resulting from SCC of austenitic stainless steel in oxygen-stagnant areas, such as canopy seal welds [3], the upstream side of the final check valve in the safety injection line [4], and the heater sleeve of the pressurizer [22]. The major cause of the SCC was due to the presence of residual oxygen in the affected area. In these cases, the affected area was exposed to a high electrochemical potential during every plant start-up due to the presence of air in the crevice unless a special plant start-up procedure was applied, such as an air removal procedure using vacuum pumping before plant start-up. Consequently, cracking occurs if the cumulative number of times that an aggressive environment forms during plant start-up exceeds some threshold quantity. Therefore, this type of SCC in an oxygen stagnant area in low-potential environments is one of concerns when determining how to maintain reliability for more than 60 years.

Stress corrosion cracking at the canopy seal weld in the control rod drive mechanism

Small leakage occurred at the lower canopy seal of some PWR plants in 1980 [3]. The canopy seal ensures the leak tightness of threaded joints between the top of the vessel head penetrations and the CRDM housing and is typically fabricated from Type 304. Destructive examination of the affected seals was performed on five PWR plants. In almost all cases, TGSCC from the inside the canopy seal was found. It was concluded that the cause of the cracking was a combination of a corrosive medium, most likely chloride, and oxygen in the “dead end cavity” that is formed by the canopy seal.

Stress corrosion cracking at the heater sleeve in the pressurizer

During a 2006 outage at Braidwood Unit 1, a leak was detected in the upper socket weld connected to a pressurizer heater [22]. The sleeve material was Type 316 SS with 0.08% C. Based on destructive examination, the leak was determined to be the result of circumferential IGSCC, which initiated from the inner surface. The crack propagated through the HAZ of the multipass socket weld. Significant sensitization was confirmed, and it was reported that qualitative energy-dispersive X-ray spectroscopy (EDS) evaluations identified high oxygen content on the crack deposits, indicating that the crevice was exposed to an oxygenated environment. Given the structure of the heater sleeve, it is not easy to remove all the residual air before plant start-up. Based on the observed structure, the cause of the cracking was concluded to be due to a combination of the presence of residual oxygen in the socket weld during start-up and high degree of sensitization of the material.

Stress corrosion cracking at the upstream side of the final check valve in the SIS

Cracking was found by routine ultrasonic examination at Sequoyah Unit 2 during an outage in 1996 [4]. IGSCC was located at the HAZ adjacent to the weld in the piping on the upstream side of the final check valve between SIS and RCS. The piping was made from 316 SS with 0.077% C. The results of examination conducted according to ASTM test standard A262 [23] revealed that the HAZ was sensitized to high levels. No evidence of contaminants or aggressive elements, such as chlorine, was reported; it was concluded that the IGSCC was caused by the exposure to the oxygenated water and a high concentration of boric acid in the SIS.

2.2.2.2 Current prediction capabilities

The slow strain rate test (SSRT) has been used in an environment that simulates the oxygen-stagnant areas in PWR primary systems to investigate the susceptibility of austenitic stainless steels to SCC. The essential variables, such as temperature, electrochemical potential, sensitization, and the effect of lithium and boron were examined [24–27].

The current knowledge of these important variables affecting susceptibility to SCC is summarized in the following subsections of this chapter to assess the current capabilities and limitations to predict potential occurrence of SCC during extended reactor operation.

Effect of temperature, LiOH, and boric acid

The susceptibility of sensitized 304 SS to IGSCC in oxygenated water with LiOH and boric acid below 200 °C (392 °F) increases with increasing temperature. Below 150 °C (302 °F), sensitized 304 SS is less susceptible to IGSCC in water containing 2 ppm Li than it is in pure water without Li and B or in water containing low concentrations of B (500 ppm). Below 200 °C, the IGSCC susceptibility of sensitized 304 SS is also suppressed by B concentrations greater than 1,500 ppm B (Figure 2.8). However, no significant difference in IGSCC susceptibility was identified at high temperature (above 200 °C) in a high-potential environment.

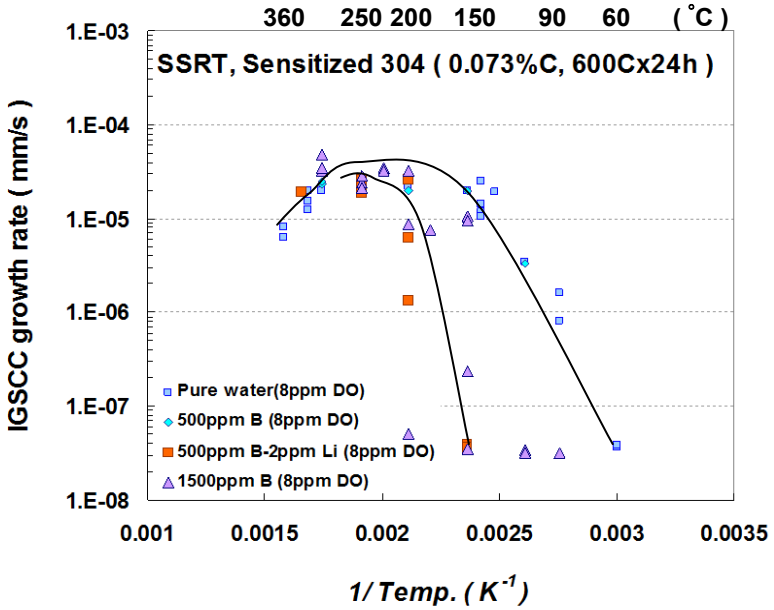

Figure 2.8. Influence of temperature and LiOH and $B(OH)_3$ concentrations on IGSCC susceptibility in an oxygen-stagnant environment [26].

Generally, LiOH and boric acid additions retard the IGSCC susceptibility of sensitized stainless steels compared with that in oxygenated pure water at temperature less than 150 °C. However, no significant effect of LiOH and B addition was observed at high temperature (above 200 °C). This result suggests that the probability of IGSCC occurrence in an oxygen-stagnant area in PWRs is low at temperatures <150 °C compared with that in oxygenated pure water. This result also suggests that it could be difficult to prevent SCC occurrence in an oxygen-stagnant area in PWRs during long-term operation especially at high temperature (>200 °C) conditions, such as canopy seal weld and heater sleeve. Consequently, to improve the prediction capability on SCC

occurrence during extended service, detailed evaluations of the SCC susceptibility for each stagnant area are necessary to consider the measures to keep reliability during extended operation. In addition, based on the results of the evaluation described above, applications of appropriate countermeasures, such as residual air removal, would likely benefit maintaining reliability of PWRs for long-term operation.

Effect of sensitization

The effect of sensitization on SCC was examined to consider the potential SCC in simulated oxygen-stagnant areas. The sensitization of the materials was measured by EPR method. The result is shown in Figure 2.9. This trend is quite similar to that in BWR environment. Similar sensitization dependence was also observed at low temperature [100 °C (212 °F)]. In addition, the critical potential for the IGSCC susceptibility of sensitized 304 SS and 316 SS was studied in a B-Li environment [24, 25] and was summarized as a function of temperature.

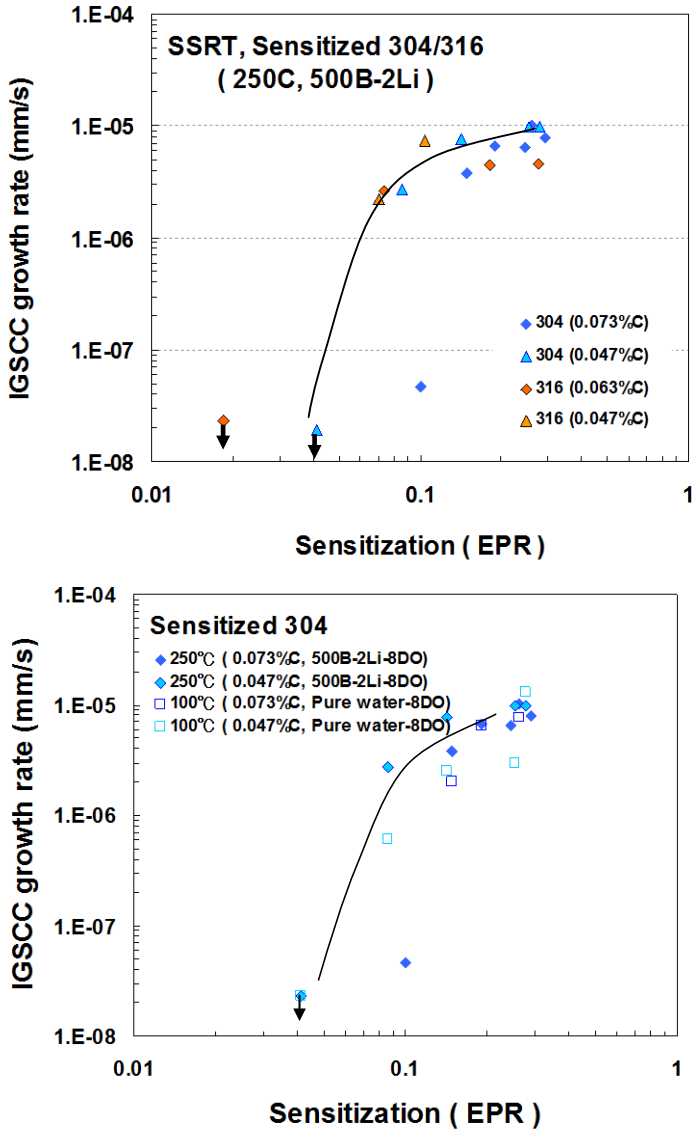

Figure 2.9. Sensitization-dependence on IGSCC-susceptibility in an oxygen-stagnant environment [26].

These test results suggested that sensitization enhanced the IGSCC susceptibility in an oxygen-stagnant areas in PWR piping and internals at high and low temperatures. These results suggest that replacement of the sensitized stainless steels with sensitization-resistant stainless steels will mitigate IGSCC in the oxygen-stagnant areas of PWR piping systems.

Effect of oxygen and hydrogen on electrochemical potential

Hydrogen addition affects electrochemical potential significantly, mainly due to its high exchange current density (Figure 2.10). This result suggests that the potential in oxygen-stagnant areas is controlled by the combination of the concentrations of hydrogen and oxygen, and the temperature. In other words, the potential is controlled by how rapidly hydrogen was supplied to the oxygen stagnant area during plant start-up as shown in Figure 2.10. Therefore, one of the ways for evaluation of SCC susceptibility in an oxygen stagnant area is to evaluate the local potential and then to compare it with the critical potential for the occurrence of SCC [25, 27]. Dotted lines in Figure 2.10 are the calculated results of the potential based on the revised mix potential model [18]. In other words, the change in potential during plant start-up could be estimated using this type of calculation model if we can better determine the oxygen and hydrogen concentration behavior in the stagnant area.

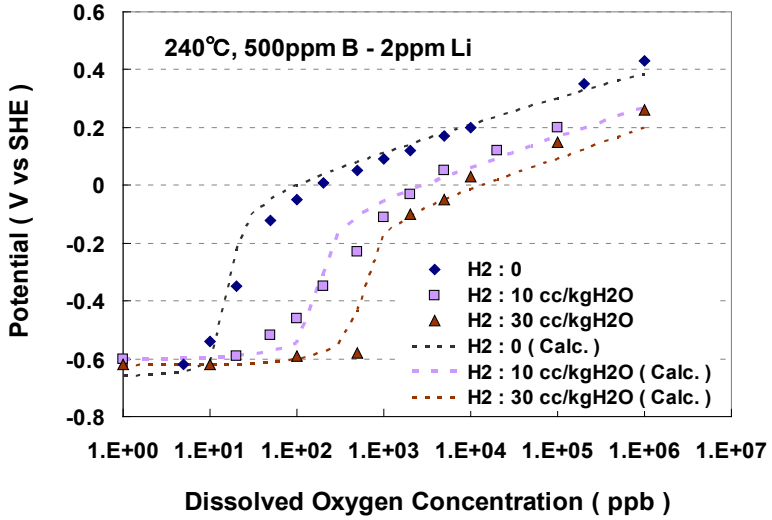

Figure 2.10. Influence of hydrogen concentration on the potential of stainless steel at 240 °C [18].

One example, the potential for the upper part of a canopy sealed crevice, is shown in Figure 2.11. The calculated result suggests that the potential exceeds the critical potential for IGSCC in about 300 h beginning from start-up for a plant, if residual air is not removed before plant start-up. A comparison of the results for the upper part of a canopy sealed crevice with the results for the lower part is shown in Figure 2.12. The duration exceeding the critical potential is much longer in the lower part. Thus, the duration exceeding the critical potential seems to depend on the design and manufacturing process, such as length of diffusion pass of oxygen and hydrogen and temperature. However, past operational experience, has shown that it is difficult to remove residual oxygen in such stagnant areas before plant start-up.

In essence, based on the combined knowledge of operating experience, laboratory results, and mechanistic understanding, detailed studies would inform proper evaluation of the possibility of

crack initiation and propagation beyond 60 years in the oxygen-stagnant areas in PWRs if residual air is not adequately removed before plant start-up. Furthermore, some studies on appropriate countermeasures, such as residual air removal or replacement of the non-sensitized stainless steels, might provide additional information to help maintain the reliability of LWRs for long-term operation.

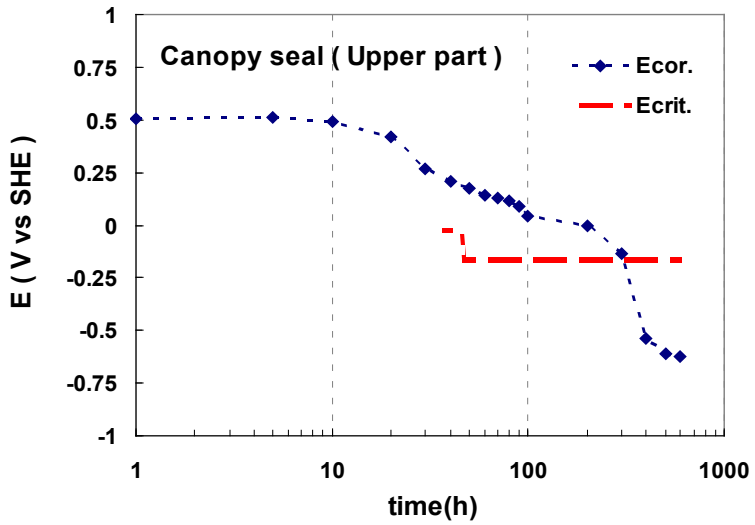

Figure 2.11. Assumed electrochemical potential behavior during plant start-up in canopy seal [18].

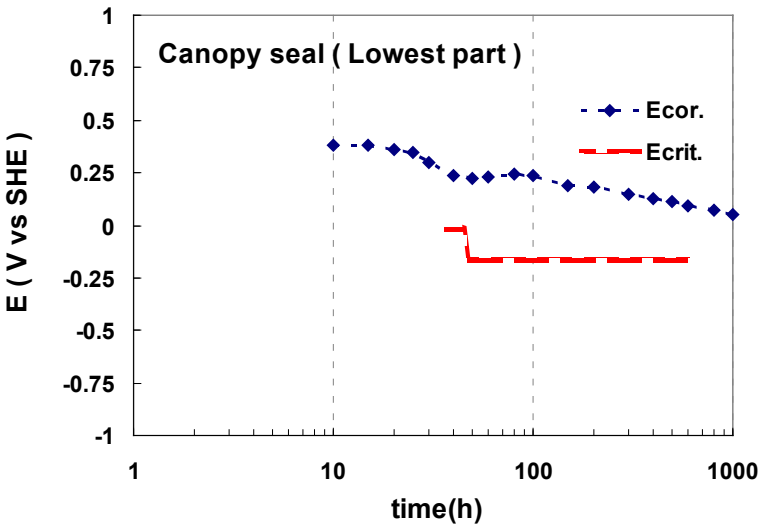

Figure 2.12. Assumed electrochemical potential behavior during plant start-up in canopy seal [18].

2.2.2.3 Long-term concerns

Based on information presented above, some potential technical issues for extended operations to beyond 60 years have been identified. These issues are as follows.

- ***Detailed evaluation of SCC susceptibility in each stagnant area.*** Studies on the SCC susceptibility in each stagnant area will inform a complete evaluation of the possibility of SCC occurrence during extended operation to maintain reliability.
- ***Effective residual air removal procedure before plant start-up.*** Studies for effective residual air removal procedure before plant start-up would provide additional information to maintain the stagnant area.
- ***Stress relief.*** Stress relieving and replacement with non-sensitized materials are considered to be other types of countermeasures to retard SCC susceptibility in oxygen stagnant areas.

2.3 REFERENCES*

1. D. J. DePaul (ed.), *Corrosion and Wear Handbook for Water-Cooled Reactors,* United States Atomic Energy Commission, McGraw-Hill, New York, 1957.
2. H. Coriou, L. Grall, and V. Gall, *Colloque de Metallugie, Sacley (1959)*, North Holland Publishing, Amsterdam, 1960, pp.161–169.
3. C. M. Pezze and I. L. W. Wilson, *Proc. 4th Int. Symp. Environmental Degradation of Materials in Nuclear Power Systems—Water Systems,* Jekyll Island, Aug. 6–10, 1989, D. Cubicciotti (ed.), National Association of Corrosion Engineers, 1990, p. 4-164.
4. G. V. Rao, D. E. Boyle, and R. Phillips, *Proc. Fontevraud 4 Int. Symp.: Contribution of Materials Investigation to the Resolution of Problems Encountered in Pressurized Water Reactors*, F. de Keroulas and Ph. Berge (Meeting Chairs), Société Française d'Energie Nucléaire, Paris, Sept. 14–18, 1998.
5. R. Cauvin, O. Goltrant, Y. Rouillon, E. Cazus, P. Dubuisson, P. Poitrenaud, and S. Bellet, *Proc. Fontevraud 3 Int. Symp.: Contribution of Materials Investigation to the Resolution of Problems Encountered in Pressurized Water Reactors,* F. de Keroulas and Ph. Berge (Meeting Chairs), Société Française d'Energie Nucléaire, Paris, Sept. 12–16, 1994, p. 54.
6. G. Pironet, A. Heuze, O. Goltrant, and R. Cauvin, *Proc. Fontevraud 4 Int. Symp.: Contribution of Materials Investigation to the Resolution of Problems Encountered in Pressurized Water Reactors*, F. de Keroulas and Ph. Berge (Meeting Chairs), Société Française d'Energie Nucléaire, Paris, Sept. 14–18, 1998, p. 195.
7. M. Nakano, K. Fukuya, K. Fujii, M. Kodama, and T. Torimaru, *Proc. 11th Int. Symp. Environmental Degradation of Materials in Nuclear Power Systems—Water Reactor,* Stevenson, Aug. 10–14, 2003, Gary S. Was and L. Nelson (eds.), American Nuclear Society, 2003.
8. T. Yonezawa, K. Arioka, H. Kanasaki, K. Fujimoto, S. Urata, and H. Mizuta, *Proc. Fontevraud 4 Int. Symp.: Contribution of Materials Investigation to the Resolution of Problems Encountered in Pressurized Water Reactors*, F. de Keroulas and Ph. Berge (Meeting Chairs), Société Française d'Energie Nucléaire, Paris, Sept. 14–18, 1998, p. 237.
9. T. Yonezawa, K. Arioka, H. Kanasaki, K. Fujimoto, K. Ajiki, T. Matsuoka, S. Urata, and H. Mizuta, "Intergranular cracking mechanism in baffle former bolt materials for PWR core internals," *Journal of the Atomic Energy Society of Japan* **42,** 212–217 (2000).

* Inclusion of references in this report does not necessarily constitute NRC approval or agreement with the referenced information.

10. T. Shoji, K. Sakaguchi, Z. Lu, S. Hirano, Y. Hasegawa, T. Kobayashi, K. Fujimoto, and Y. Nomura, *Proc. Fontevraud 7 Int. Symp.: Contribution of Materials Investigations to Improve the Safety and Performance of LWRs,* Société Française d'Energie Nucléaire, Avignon, Sept. 26–30, 2010.

11. T. Couvant, P. Moulart, L. Legras, P. Bordes, J. Capelle, Y. Rouillon, and T. Balon, *Proc. Fontevraud 6 Int. Symp.: Contribution of Materials Investigations to Improve the Safety and Performance of LWRs,* Société Française d'Energie Nucléaire, Paris, Sept. 18–22, 2006, p. 67.

12. J. Champredonde, Y. Thebault, P. Moulart, T. Couvant, K. Dubourgnoux, Y. Neau, J. Fageon, D. Lecharpetier, A. Breiul, and V. Derouet, *Proc. 15th Int. Conf. Environmental Degradation in Nuclear Power Systems—Water Reactors,* Colorado Springs, J. Busby and G. Ilevbare (eds.), The Metallurgical Society, 2011.

13. K. Arioka, Y. Yamada, T. Terachi, and Roger W. Staehle, "Intergranular Stress Corrosion Cracking Behavior of Austenitic Stainless Steels in Hydrogenated High-Temperature Water," *Corrosion* **62,** 74 (2006).

14. K. Arioka, T. Yamada, T. Terachi, and G. Chiba, "Influence of Carbide Precipitation and Rolling Direction on Intergranular Stress Corrosion Cracking of Austenitic Stainless Steels in Hydrogenated High-Temperature Water," *Corrosion* **62,** 568 (2006).

15. K. Arioka, T. Yamada, T. Terachi, and G. Chiba, "Cold Work and Temperature Dependence of Stress Corrosion Crack Growth of Austenitic Stainless Steels in Hydrogenated and Oxygenated High-Temperature Water," *Corrosion* **63,** 1114 (2007).

16. K. Arioka, T. Yamada, T. Terachi, and T. Miyamoto, "Dependence of Stress Corrosion Cracking for Cold-Worked Stainless Steel on Temperature and Potential, and Role of Diffusion of Vacancies at Crack Tips," *Corrosion* **64,** 691 (2008).

17. T. Yamada, T. Terachi, K. Arioka, Proc. *14th Int. Conf. Environmental Degradation in Nuclear Power Systems—Water Reactors,* Virginia Beach, T. Allen and J. Busby (eds.), American Nuclear Society, 2010.

18. K. Arioka, T. Yamada, T. Terachi, and T. Fukumura, *SCC Behaviors of Stainless Steels in PWR Primary Environments*, INSS Monograph No. 5, Institute of Nuclear Safety Systems, Japan (2012).

19. K. Arioka, *Proc. Fontevraud 5 Int. Symp.: Contribution of Materials Investigation to the Resolution of Problems Encountered in Pressurized Water Reactors,* F. de Keroulas and F. Hedin (Meeting Chairs), Société Française d'Energie Nucléaire, Paris, Sept. 23–27, 2002.

20. K. Arioka, T. Miyamoto, T. Yamada, and T. Terachi, "Formation of Cavities Prior to Crack Initiation and Growth on Cold-Worked Carbon Steel in High-Temperature Water," *Corrosion* **66,** 015008 (2010).

21. K. Arioka, T. Miyamoto, T. Yamada, and T. Terachi, "Dependence of Stress Corrosion Cracking of Alloy 690 on Temperature, Cold Work, and Carbide Precipitation—Role of Diffusion of Vacancies at Crack Tips," *Corrosion* **67,** 035006 (2011).

22. NRC, *Circumferential Cracking in the Stainless Steel Pressurizer Heater Sleeves of Pressurized Water Reactors,* NRC Information Notice 2006-27, ADAMS ML062500219, U.S. Nuclear Regulatory Commission, Dec. 11, 2006.

23. ASTM, *Standard Practices for Detecting Susceptibility to Intergranular Attack in Austenitic Stainless Steels,* ASTM A262–10, ASTM International.

24. K. Arioka, M. Hourai, S. Okamoto, and K. Onimura, “The effects of boric acid, solution temperature, and sensitization on SCC behavior under elevated temperature water,” *Corrosion’83,* Paper 135, National Association of Corrosion Engineers, USA, 1983.

25. K. Arioka, T. Nojima, T. Kanechiku, C. G. Schmidt, and D. D. Macdonald, “Critical potential of IGSCC for sensitized stainless steels under PWR environment,” *3rd Int. Conf. Nuclear Engineering,* Kyoto, Japan, 1995.

26. K. Arioka, M. Hourai, S. Noguchi, and K. Onimura, “Studies on analytical method and non-destructive measurement method for sensitization of 304 and 316 stainless steels,” *Corrosion’83,* Paper 134, National Association of Corrosion Engineers, USA, 1983.

27. H. C. Park, G. Cragnolino, and D. D. Macdonald, *1st Int. Conf. Environment Degradation of Materials in Nuclear Power Systems—Water Reactors,* Myrtle Beach, Aug. 22–25, 1983, J. Roberts and W. Berry (eds.), National Association of Corrosion Engineers, 1984.

3. DEGRADATION VULNERABILITIES OF ALLOY 600 AND ALLOY 182/82 WELD METALS IN LIGHT WATER REACTORS

Peter Andresen
General Electric Global Research, Niskayuna, New York

3.1 INTRODUCTION

Nickel alloys and weld metals were chosen for LWR components because of low corrosion rate, resistance to SCC, and thermal expansion coefficient that is similar to that of low alloy RPV steel. Components containing Alloy 600 and Alloy 182 and 82 weld metals are listed in Figure 3.1 and Table 3.1 for BWRs, and in Figure 3.2 and Table 3.2 for PWRs. Table 3.3 contains data on the compositions of Alloy 600 and its weld metals, and Alloy X-750. Alloy 800 is preferred to Alloy 600 in Canadian and some German steam generators, and it possesses some attractive properties. However, it is an iron-base alloy (30Ni-21Cr) and is not covered in this section.

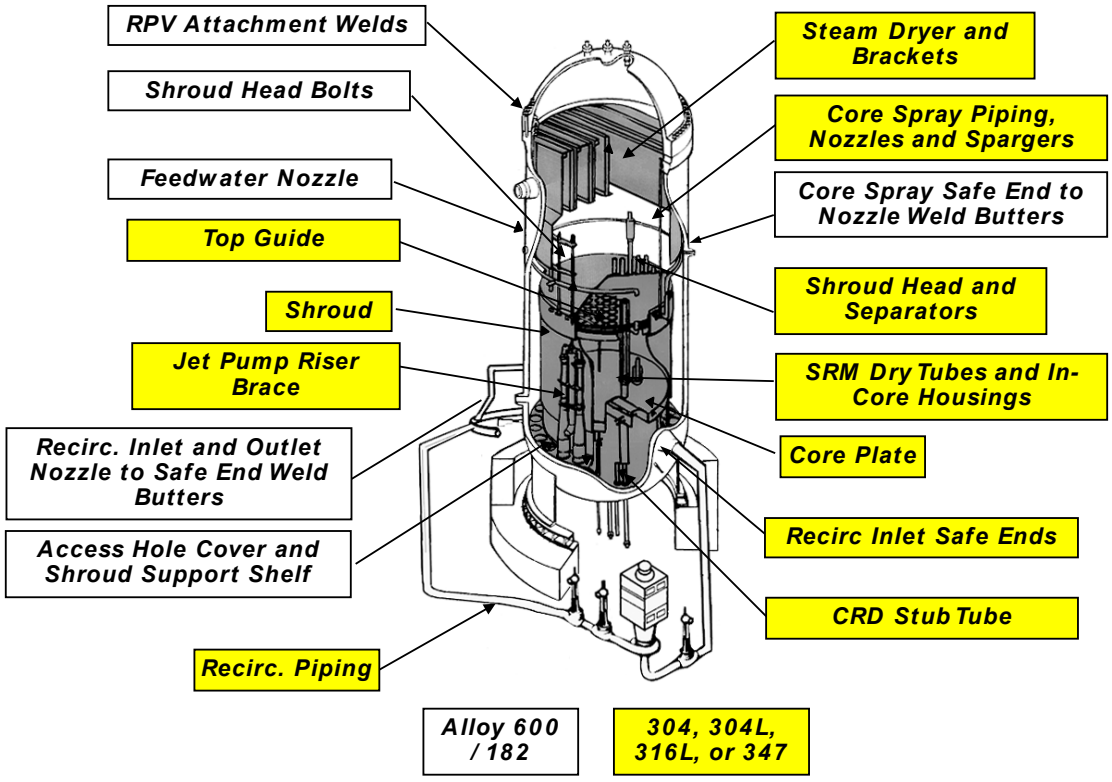

Figure 3.1. BWR components containing Alloy 600 and alloy 182 and 82 weld metals (white boxes). Austenitic stainless steels are shown in yellow boxes.

Table 3.1. BWR components fabricated from Ni alloys

BWR Component	Nickel Alloy Designation
BWR shroud head bolts	Alloy 600
Pressure vessel attachment pads	Alloy 182
Control rod penetrations	Alloy 600
Control rod penetration welds	Alloy 182
Core shroud support welds	Alloy 182
Pressure vessel nozzles	Alloys 182 and 82
Safe ends	Alloy 600
Weld metal deposits	Alloys 82 and 182
Jet pump beams	Alloy X-750
Fuel rod spacers	Alloy X-750

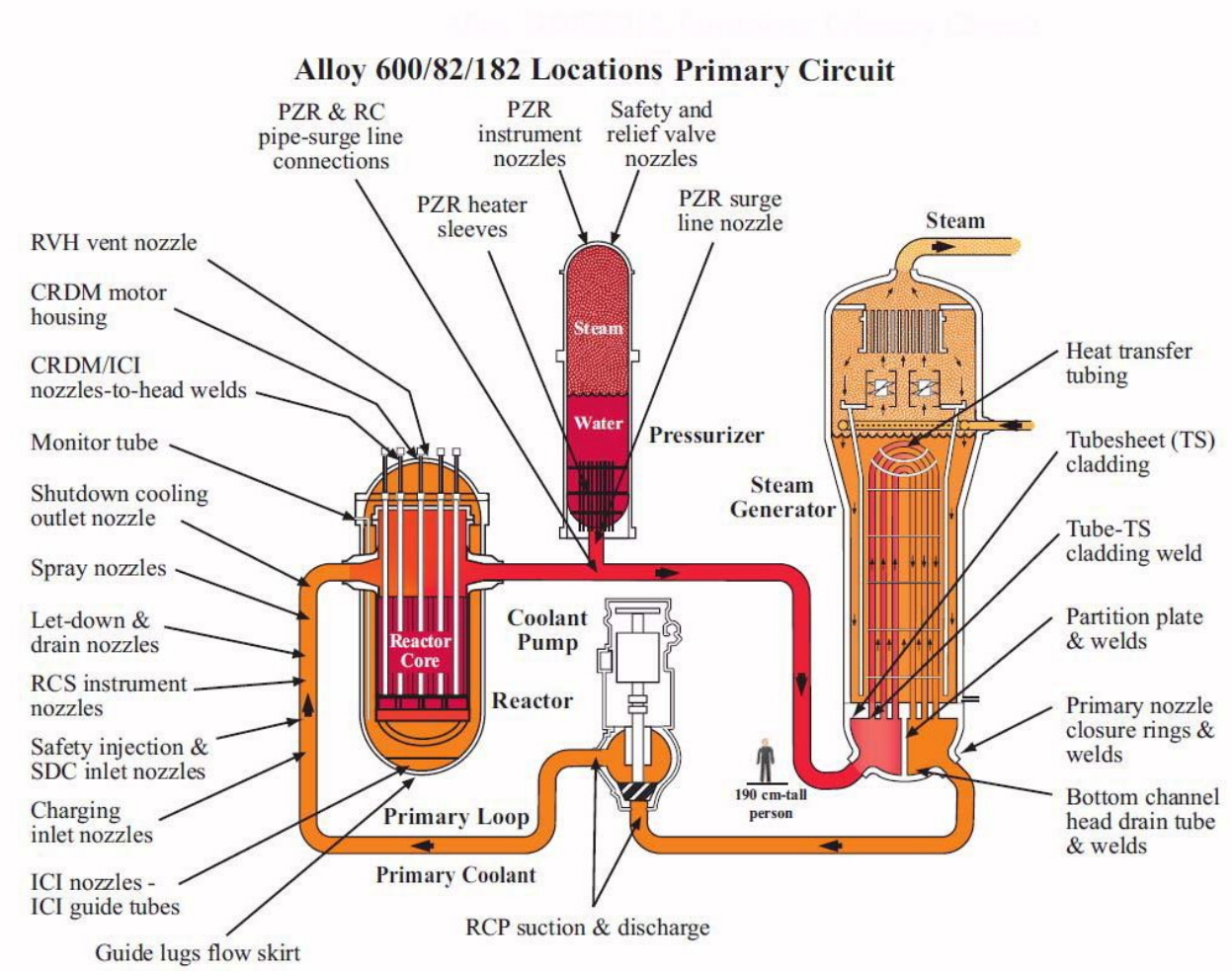

Figure 3.2. PWR components containing Alloy 600 and Alloy 182 and 82 weld metals [1, 2].

Table 3.2. PWR components fabricated from Ni alloys

PWR Component	Nickel Alloy Designation
Steam generator tubes	Alloy 600 (mill annealed and thermally treated)
Steam generator divider plates	Alloy 600
Upper head penetrations	Alloy 600
Lower head penetrations	Alloy 600
Core supports	Alloy 600
Pressurizer nozzles	Alloy 600
Safe ends	Alloy 600
Weld metal deposits	Alloys 82 and 182

Table 3.3. Compositions of common Ni alloys used in LWRs

	Alloy 600	Alloy 182	Alloy 82	Alloy X-750
Nickel (Ni)	Bal.	Bal.	Bal.	Bal.
Chromium (Cr)	14-17	13-17	18-22	15-17
Iron (Fe)	6-10	≤10.0	≤3.00	8-9
Titanium (Ti)		≤1.0	≤0.75	2.5-3.0
Aluminum (Al)				0.7-1.0
Niobium (Nb) plus tantalum (Ta)		1.0-2.5	2.0-3.0	0.8-1
Carbon (C)	≤0.05	≤0.10	≤0.10	0.05-0.08
Manganese (Mn)	≤1.0	5.0-9.5	2.5-3.5	0.1
Sulfur (S)	≤0.015	≤0.015	≤0.015	<0.03
Phosphorous (P)		≤0.030	≤0.030	<0.03
Silicon (Si)	≤0.5	≤1.0	≤0.50	0.1-0.2
Copper (Cu)	≤0.5	≤0.50	≤0.50	<0.50
Cobalt (Co)	≤0.10	≤0.12	≤0.10	<0.10

Degradation modes and related concerns in Ni alloys and weld metals include:

- SCC
- environmentally assisted fatigue, and
- environmentally assisted fracture.

For weld metals, potential issues also include:

- welding defects, such as hot cracking, ductility dip cracking, and lack of fusion;
- thermal aging;
- dilution effects (and cracking along the weld interface); and
- the growth of cracks through weld metal attachment pads and interface and into the underlying low alloy steel.

Significant cracking of Ni alloys was discovered in BWR components in the 1970s, and SCC has become the primary materials issue for Ni alloys in LWRs [1, 3–10]. Although cracking occurred initially in crevices and/or cold-worked components, it has spread to other areas and components, and has especially manifested in Alloy 182 welds. The SCC growth rates of Alloy 82 weld are not consistently different from Alloy 182 weld metal.

In PWR water (deaerated and/or hydrogenated), the susceptibility of Alloy 600 to intergranular stress corrosion cracking (IGSCC) was first revealed in laboratory testing in 1959 and then surfaced in operational service in plant in the early 1970s. IGSCC that occurs during exposure to PWR primary water is today commonly referred to as primary water stress corrosion cracking (PWSCC) [3, 4]. Highly cold-worked components were affected earlier, including the tight U-bends in steam generator tubes and cold-worked expansion of the tubes within the tube sheet [5]. IGSCC of steam generator tubing became prevalent in the 1980s, leading to steam generator retirement and replacement. PWSCC of pressurizer nozzles and control rod drive mechanism (CRDM) nozzles in the upper heads of PWR RPVs was observed in the late 1980s and has continued for more than two decades [6, 7].

SCC exhibits an intergranular morphology (Figure 3.3), both in base metal and weld metals. The cracking morphology in weld metals is often referred to as interdendritic, but it occurs primarily along the grain boundaries of packets of dendrites and not necessarily along all dendritic boundaries. The IGSCC susceptibility of these alloys was recognized in laboratory testing more than 50 years ago [3]. Important variables that affect SCC include stress intensity factors (Figure 3.4), corrosion potential (Figures 3.5–3.7), water purity, temperature, cold work, composition [especially chromium (Cr) content] (Figures 3.8 and 3.9), and microstructure (including grain boundary carbides and other particles) [1, 7–17].

The historical incidence of SCC is not always a good predictor of future problems, partly because inspections are incomplete and detection is insensitive to incipient cracking, and partly because aging and its synergy with degradation phenomena can lead to unexpected cracking. For Ni alloy base metals, the opportunity for aging is small, but for Alloy 182 and 82 weld metals, some microstructural evolution may occur. This may produce an increase in yield strength, changes in grain boundary composition and structure, and other factors that could alter susceptibility to SCC and environmentally assisted fracture.

The historical incidence of SCC is also dependent on various operational factors, including low leakage core operation (where cooler and hotter water mix and can produce thermal fluctuations and cyclic thermal fatigue loading on surface of the component). Also, the increasing use of non-deaerated make-up water might expose components to high corrosion potential conditions that can greatly increase crack growth rates (Figures 3.5, 3.6, and 3.10).

Most of this section will address SCC vulnerabilities, but there is growing concern for environmentally assisted fracture, a reduction in J-R tearing resistance [18, 19], and sudden fracture [20, 21]. The reduction in J-R tearing resistance can be very high under certain conditions of temperature or environment (Figure 3.11). In the high-temperature BWR and PWR environments, sudden fracture (Figure 3.12) has been observed in Ni alloy weld metals at stress intensity factors as low as 86 MPa$\sqrt{m}$ (78 ksi$\sqrt{in}$). In many but not all cases, the sudden fracture is consistent with plastic instability.

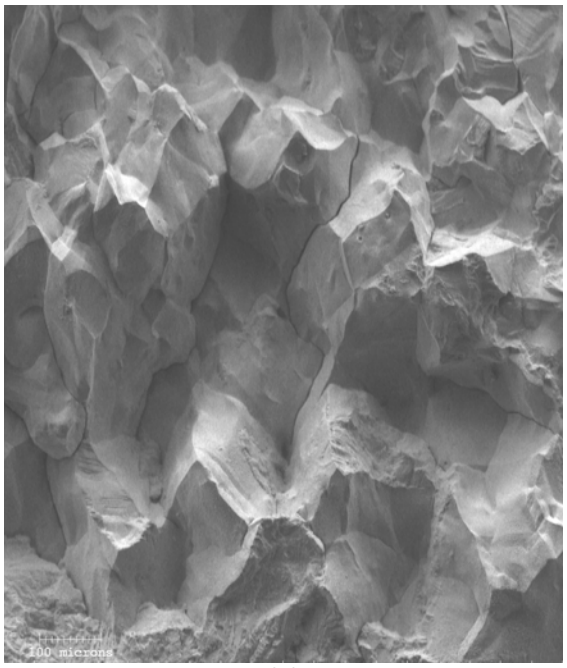

(a)

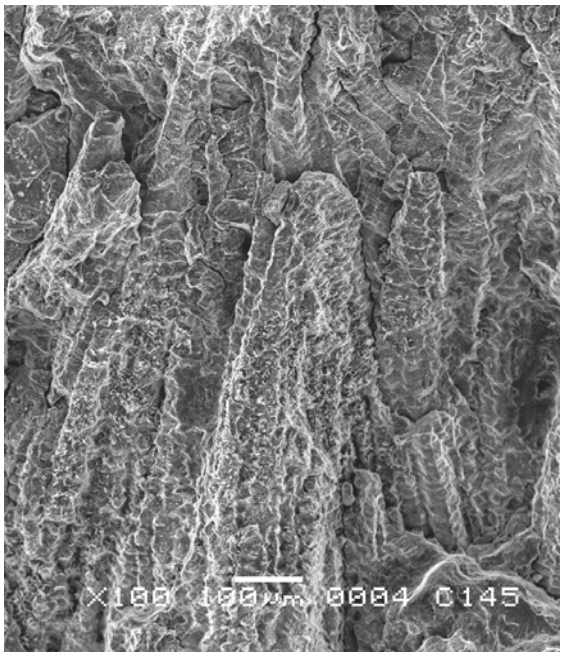

(b)

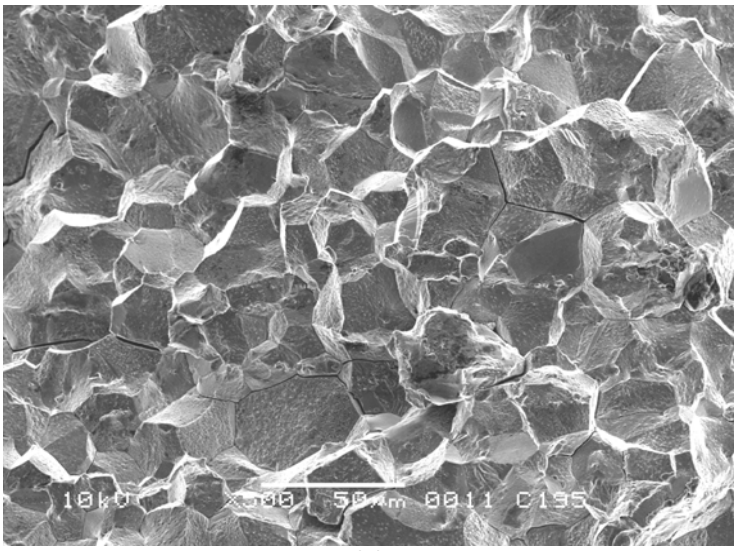

(c)

Figure 3.3. Scanning electron micrographs showing the intergranular fracture morphology of (a) Alloy 600, (b) Alloy 182 weld metal, and (c) alloy X-750 when tested in high-temperature water.

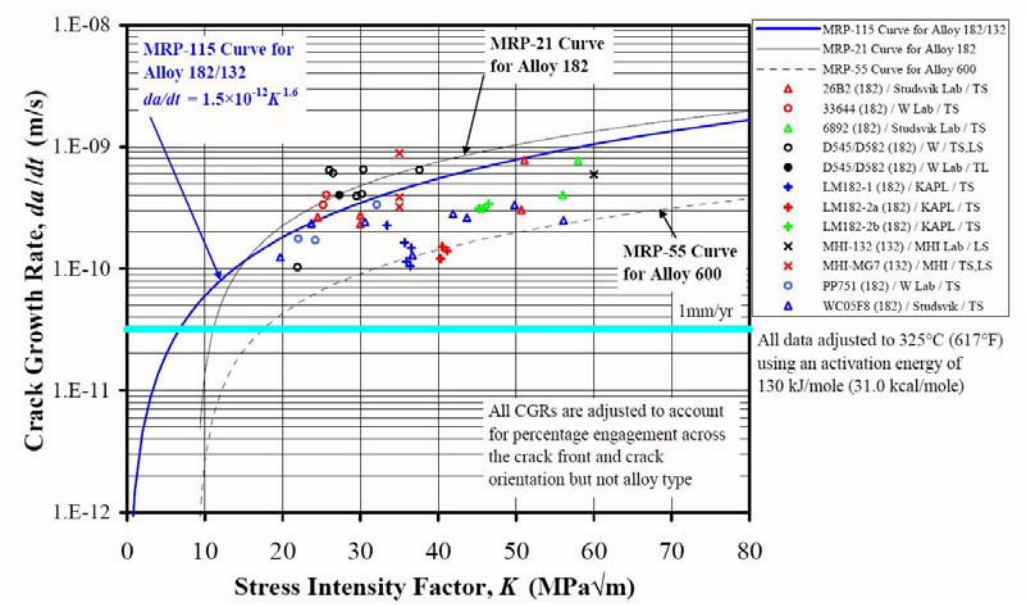

Figure 3.4. Crack growth rate of Alloy 182 and 132 weld metals in PWR primary water along with disposition curves for Alloy 182 weld metal (MRP-115 [22]) and Alloy 600 (MRP-55 [23]). Cold work and temperature cause an increase in crack growth rate.

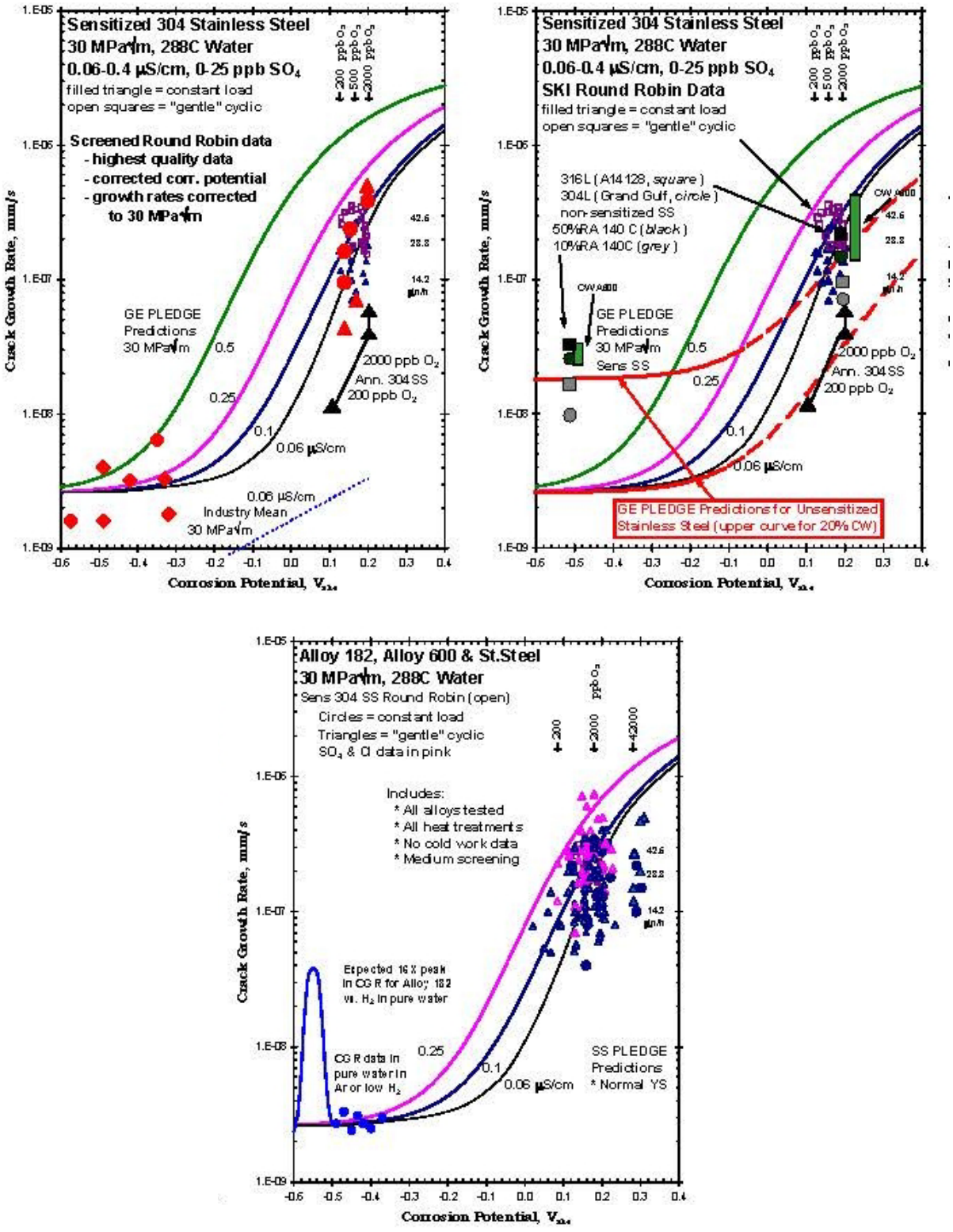

Figure 3.5. SCC growth rate vs. corrosion potential for stainless steels *(top)* and Ni alloys *(bottom)* tested in 288 °C (550 °F) high-purity water containing 2,000 ppb O_2 and 95–3,000 ppb H_2.

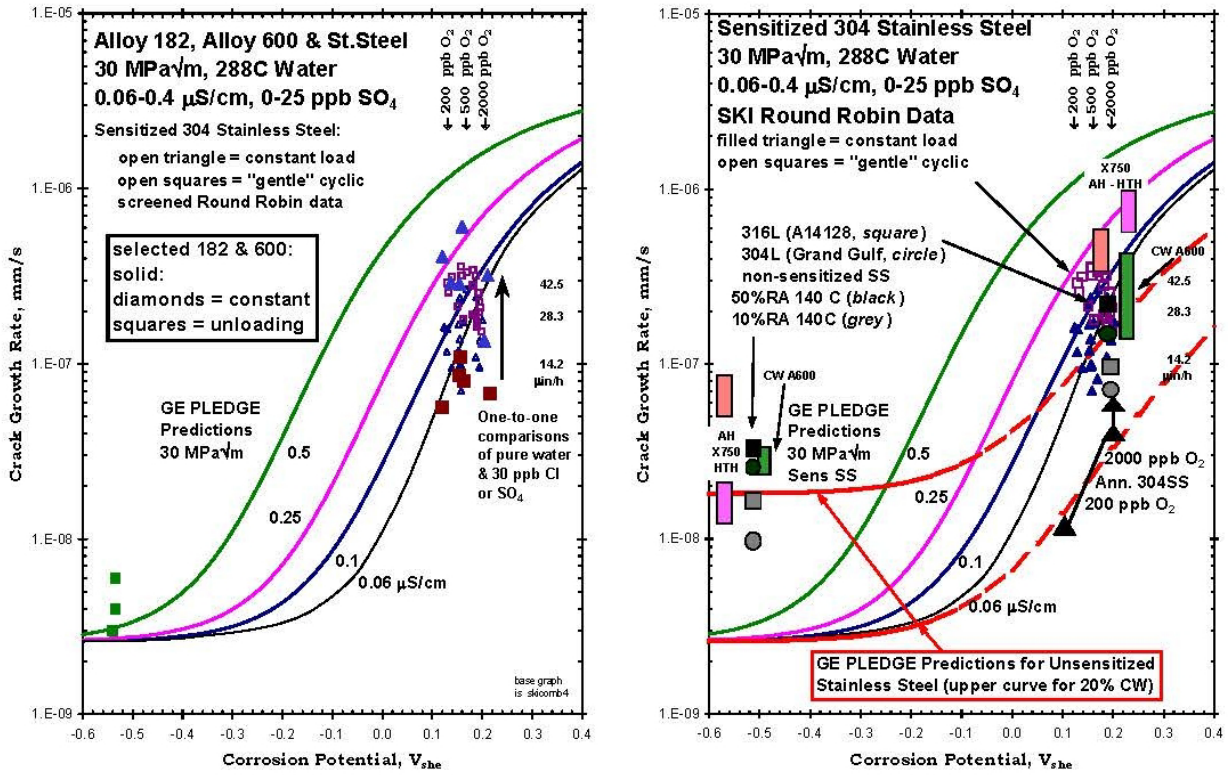

Figure 3.6. ***(Left)*** **The growth rates in high purity water at high corrosion potential fall within the observations for sensitized stainless steel (open symbols), and the effect of low potential or additions of 6 × 10^{-7} N SO_4 or Cl are consistent with the SCC behavior of sensitized stainless steel.** ***(Right)*** **SCC growth rate vs. corrosion potential for stainless steels in various conditions, 20% cold-worked alloys 600 and X-750 tested in 288 °C (550 °F) high-purity water containing 2 ppm O_2 and 95–3,000 ppb H_2 [24].**

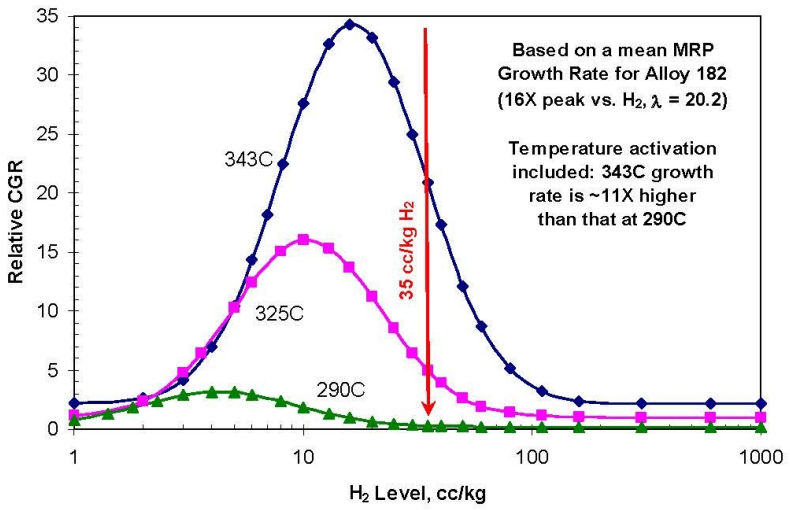

Figure 3.7. Predicted effect of H_2 on the relative crack growth rate of Ni alloy weld metals based on a 16× crack growth rate peak height at 290 °C, 325 °C, or 343 °C, (554 °F, 617 °F, or 650 °F) with the effect of temperature activation on crack growth rate factored in. From a H_2 level of 35 cc/kg, shifting to higher H_2 will monotonically decrease crack growth rate. For lower H_2, no benefit will occur until the H_2 level is below about 0.52, 3.1 and 7.7 cc/kg H_2 for 290 °C, 325 °C, and 343 °C, respectively. While the peak height is 16× at all temperatures, the crack growth rate is much higher at 343 °C.

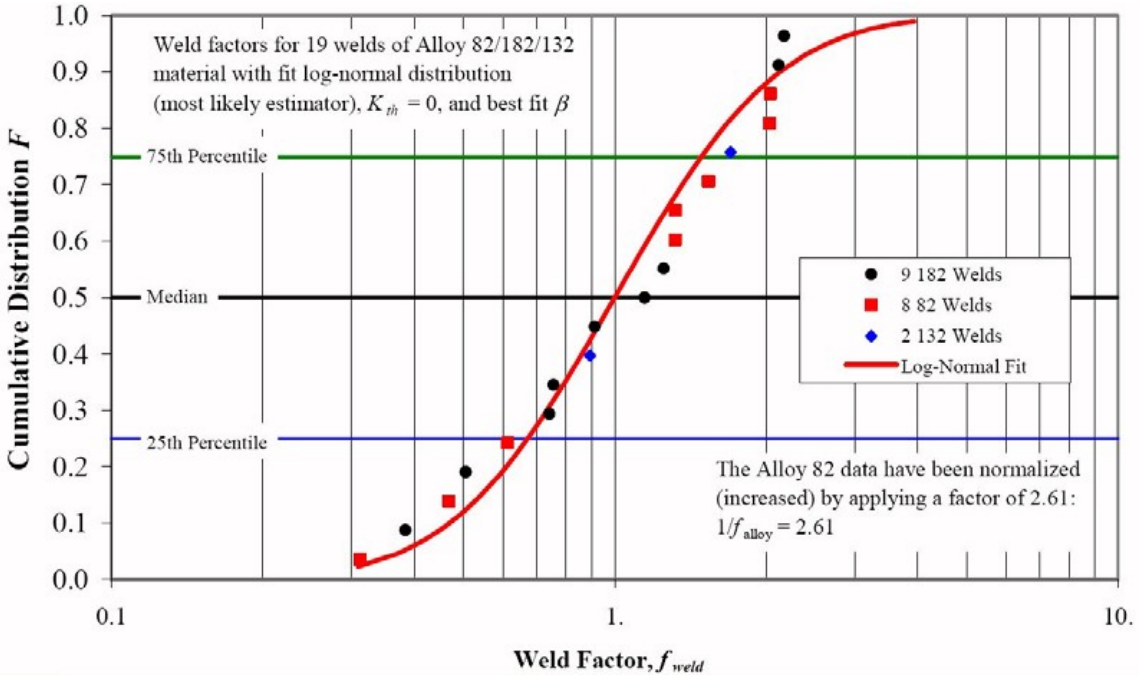

Figure 3.8. Analysis of the crack growth rate response in PWR primary water for alloys 182 and 132 and Alloy 82 weld metals. Recognizing that the Alloy 82 data have been increased by 2.6×, the cumulative distributions for these materials are intertwined, indicating identical response. Note that the Alloy 82 data in the plot indicate somewhat better SCC resistance [22].

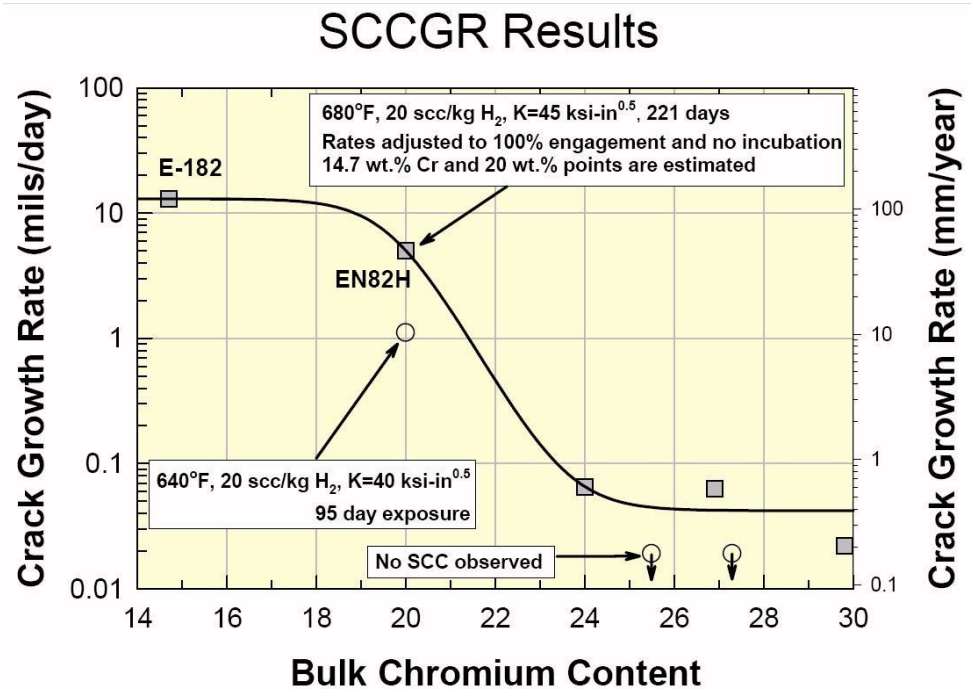

Figure 3.9. SCC growth rate vs. bulk Cr content of Ni alloy weld metals tested in 360 °C (680 °F) hydrogenated water [25–28].

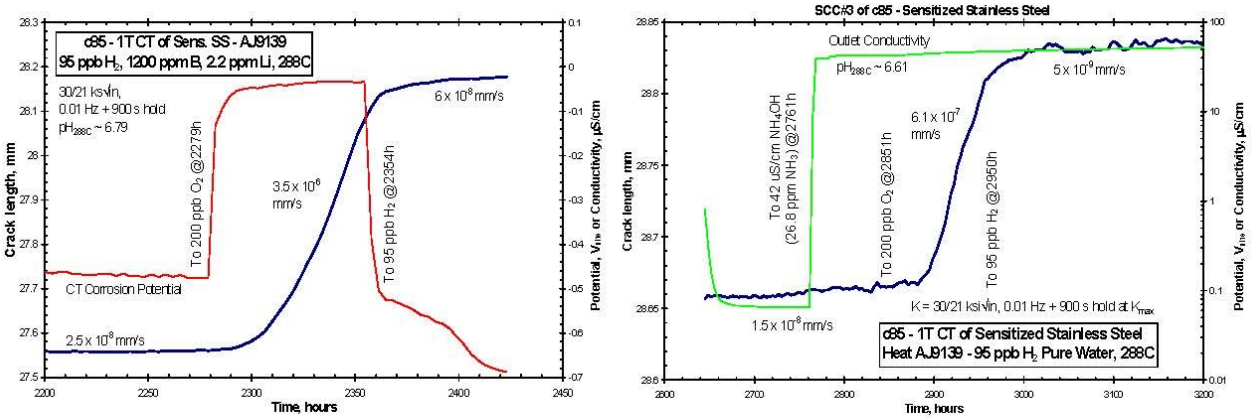

(a) (b)

Figure 3.10. SCC crack length vs. time of sensitized stainless steel in 288 °C (550 °F) showing that the presence of (a) 1,200 ppm B as H_3BO_3 and 2.2 ppm Li as LiOH, or (b) 26.8 ppm NH_3, results in a low growth rate until the corrosion potential becomes elevated at 2,279 h by the addition of 200 ppb O_2 [15, 16].

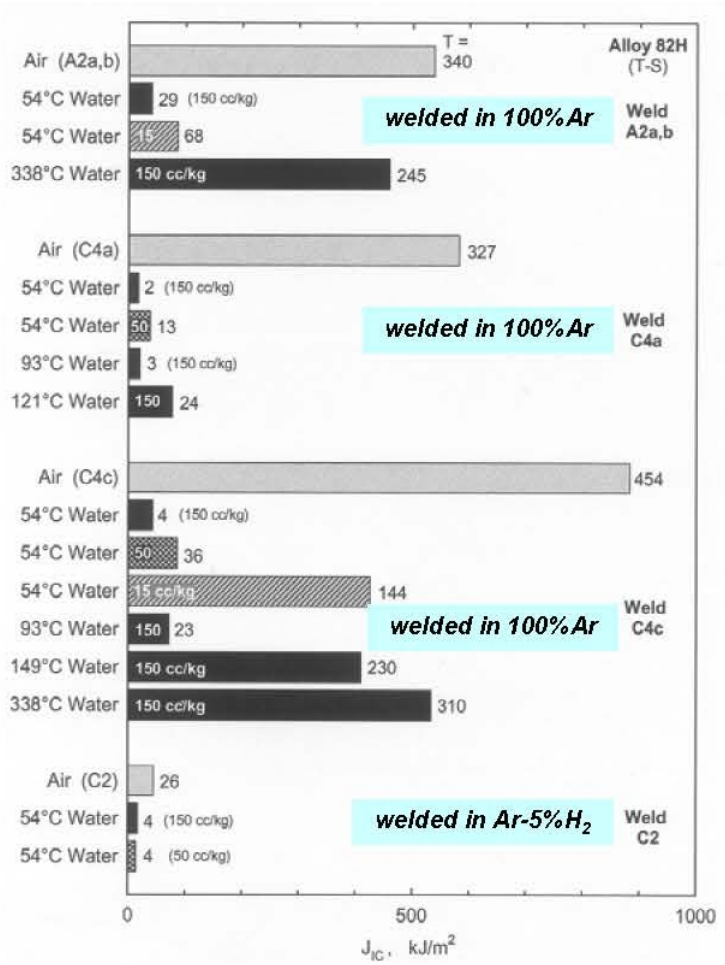

Figure 3.11. J-R data of Mills et al. on various Ni Alloy 82H weld metals showing a large reduction in fracture resistance in water versus air [18, 19]. Reprinted with permission of The Minerals, Metals & Materials Society.

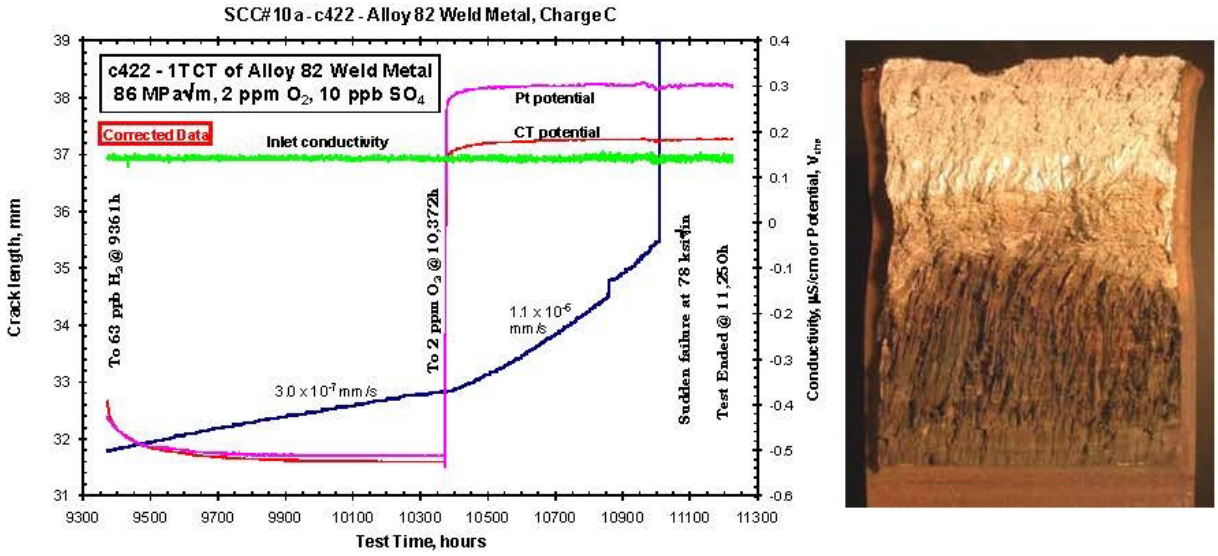

Figure 3.12. Examples of sudden failure of Alloy 182 weld metal tested in 288 °C (550 °F) water at increasing stress intensity factor (K) until failure occurred. The load and the crack depth at failure are very well defined, and the resulting "K_{IC}" is relatively low [20, 21]. Some of these rapid fracture events are consistent with plastic instability, others may not be.

3.2 PERSPECTIVE ON SCC DEPENDENCIES AND MECHANISMS

Until recently, the SCC of Ni alloys in PWRs has been considered a distinct and different phenomenon from SCC of nickel alloys in BWRs. However, there is increasing evidence that SCC follows a smooth transition between traditional BWR (most U.S. BWRs now operate at low corrosion potential using NobleChem™) and PWR primary water, with many common dependencies as a function of temperature, oxidant level, H_2 level, and water purity [8–17]. For example, as the corrosion potential is changed by varying the dissolved O_2 and H_2 level, a well-behaved transition in SCC growth rate is observed, both for Ni alloys and stainless steels (Figures 3.5 and 3.6).

Under deaerated conditions, the corrosion potential is controlled by the H_2–H_2O reaction, which is parallel to the Fe, Ni, and Cr metal-oxide phase boundaries in Pourbaix (pH-potential) diagrams (Figure 3.13). Changing pH in the mid-range of ~5–8 (pH at temperature) has little effect on SCC response, and more than three dozen on-the-fly chemistry changes (where the experimental conditions remain stable apart from the controlled change) were observed to have no effect on SCC growth rates in Ni alloys, even from pure water to elevated levels of H_3BO_3 and LiOH (Figure 3.14) [15]. Even the effect of H_2 on SCC is observed to be similar for BWR and PWR water [16, 17], which is unsurprising given the similarity between the two environments. The similarities in the two reactor types is more evident for BWRs that employ NobleChem™ to catalytically achieve low corrosion potentials that are very close to the H_2O/H_2 line (Figure 3.13).

This non-oxidizing condition is quite similar to the primary environment of PWRs, with three significant differences: solution pH, H_2 fugacity, and temperature.

Many of the factors used to distinguish SCC response in BWRs vs. PWRs have proven to be artificial [8, 10, 12, 24]. The positive experience of thermally treated Alloy 600 in PWRs was

considered to contradict the deleterious role of grain boundary carbides and Cr depletion in BWRs. However, grain boundary carbides are in fact beneficial in both environments, although when accompanied by Cr depletion at the grain boundary, SCC susceptibility increased in oxidizing environments. This is widely attributed to the slower repassivation rates at lower Cr concentrations in the pH-shifted chemistries that form when oxidants are present [8–10].

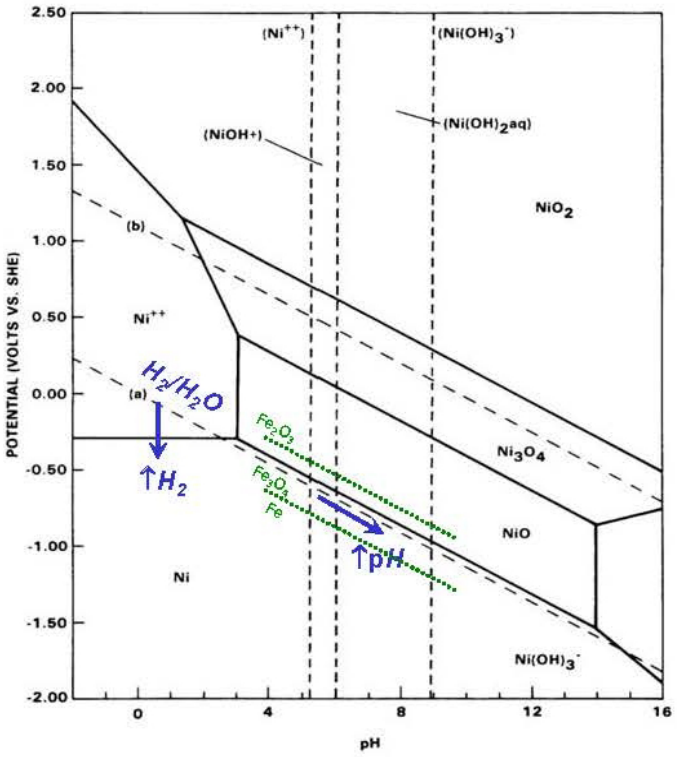

Figure 3.13. Ni–H_2O Pourbaix diagram at 300 °C (572 °F).

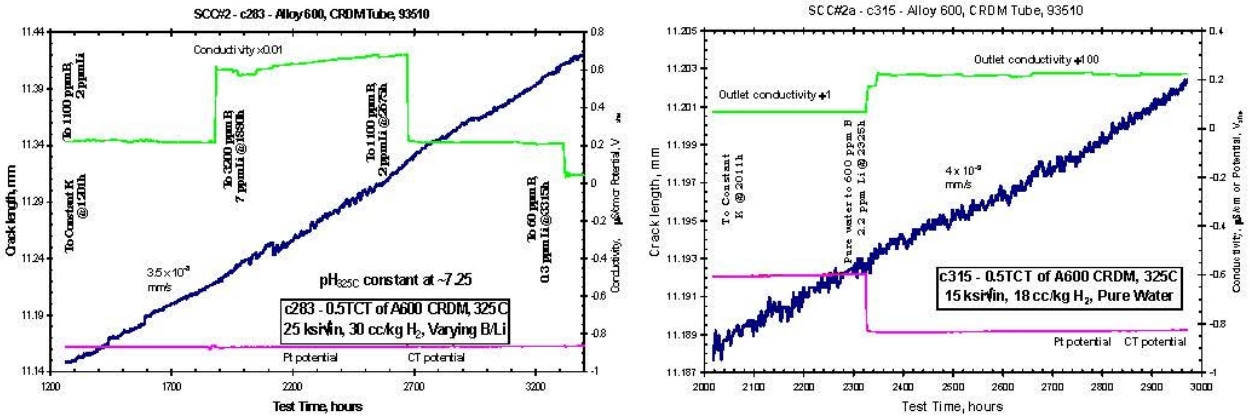

Figure 3.14. Crack length vs. time for Alloy 600 and tested in 325 °C water containing 30 cc/kg H_2 under constant K conditions showing that extensive variations in B and Li content in produced no change in crack growth rate [15].

Solution pH variations in the near-neutral regime have little effect on SCC in deaerated (e.g., PWR) water (Figure 3.14) [15], although they have some effect on the corrosion potential [112 mV / pH unit at 288 °C (550 °F)] because the corrosion potential under deaerated conditions is

controlled by the H_2O/H_2 reaction (this is the slope of the H_2O/H_2 line in Figure 3.13). Both pH and solution conductivity are higher in the PWRs as a result of H_3BO_3 and LiOH additions. The pH_{290C} is now typically in the range from 6.8 to 7.2 in PWRs (pH_{290C} represents 1,100 ppm B and 2 ppm Li, which gives a pH_{325C} = 7.25 and a pH_{340C} = 7.58) vs. 5.65 for pure (BWR) water, and the conductivity is 166 μS/cm vs. 5 μS/cm. There is a change in corrosion potential as a function of pH, but this difference is unimportant because there is no difference in potential relative to the metal – metal oxide phase transitions. Also, in the absence of oxidants, there is no potential gradient in the crack and therefore no aggressive crack chemistry develops.

Second, the difference in H_2 fugacity is only ~70×, from ~40 ppb H_2 in BWRs to ~3,000 ppb in PWRs. This produces only a small change in corrosion potential of about 100 mV, which can nevertheless be important to SCC of Ni alloys. Its role is related to a shift in the stability of Ni vs. NiO, which is affected by both H_2 and temperature (Figure 3.15). No potential gradient forms in the crack because H_2 (unlike oxidants) is not consumed, so no aggressive crack chemistry forms whether the H_2 level is high or low.

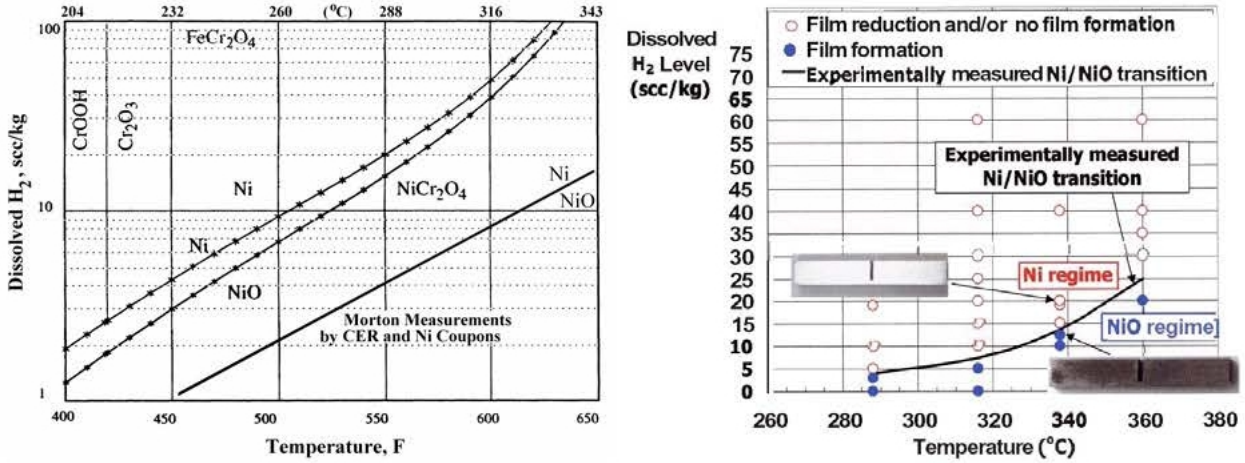

Figure 3.15. Ni/NiO phase boundary as a function of H_2 fugacity and temperature [29]. Copyright 2003 by the American Nuclear Society.

The third difference is temperature. The temperature of most structural components is 274 °C (525 °F) in a BWR [the feed water reduces the recirculating core outlet water from 288 °C (550 °F) to 274 °C]; thus, this is the temperature in the recirculation and cleanup piping, the annulus between the shroud and the pressure vessel, and the lower plenum region. In a PWR, the core inlet temperature is about 286 °C (547 °F), core outlet temperature is typically 323 °C [ranging from ~316 °C to 323 °C (601 °F to 613 °F)], and the pressurizer is ~343 °C (650 °F), nearly 70 °C (158 °F) hotter than most structural components in a BWR. For Ni alloys, this difference (323 vs. 274 °C) leads to a significant increase in crack growth rate of about 14× [23, 24, 30, 31]; compared to the 343 °C PWR pressurizer, the difference is about 40×.

Both crack initiation and crack growth rate are important factors in the emergence of SCC in plant components. Crack initiation can be viewed as dominant for non-structural components, such as the thin-walled steam generator tubing, and crack growth can account for a significant fraction of life in larger structural components. Crack growth can be quantified with greater precision, and the bulk characteristics of components are much better known than the highly variable surface characteristics, although modern steam generator fabrication can produce very well controlled surfaces. For structural components, there are many examples of *claims* of excellent surface

fabrication controls in components that were later proven to possess severely cold-worked and defected surfaces from which extensive cracking nucleated and grew.

Because there are many possible mechanisms of crack initiation (e.g., intergranular corrosion, pitting, pre-existing defects, mechanical cracks, and severely cold-worked/damaged surfaces), it can be very difficult to identify what initiated cracking. Even without visible problems, after extended service (e.g., a license extension of > 20 years), components that were viewed as not susceptible to SCC have experienced cracking. Thus, the evolving perspective is that it is necessary not only for component design and surface characteristics to be optimized to minimize the probability of crack initiation, but to also be inherently resistant to crack growth to ensure plant lifetimes commensurate with the desired 60–80+ year range.

3.3 NICKEL ALLOY COMPONENTS AND WELDS IN BWRS

Nickel-base weld materials are used extensively in BWRs [32] and are more prevalent than wrought Ni alloy components (Table 3.1). Alloy 182 and 82 weld metals are used to join the low alloy steel pressure vessel and pressure vessel nozzles to wrought Ni alloys and austenitic stainless steel components. Alloy 182 is typically used as a coated stick electrode designed for manual welding, whereas Alloy 82 is typically used in wire form for automated tungsten inert gas or metal inert gas welding. Figures 3.1 and 3.16 show the key components and their locations in GE BWRs, and Figures 3.17–3.20 show the configurations of some locations where Alloy 182 and 82 welds exist.

Different vessel fabricators used different nozzle-to-safe-end weld configurations, but Alloy 182 weld metal was used for the nozzle butter and/or the weld joint. These include the recirculation inlet and outlet nozzles, core spray nozzles, jet pump instrumentation nozzles, and feed water nozzles. Figures 3.17 and 3.18 show the details typical of the weld buildup with alloys 182 and 82 common in many BWRs. Alloy 182 was often used to butter the safe end, after which the vessel was heat treated (tempered) to restore its properties. Following this post-weld heat treatment (PWHT), the subsequent weld to the safe end was typically made with an Alloy 82 root pass then completed with Alloy 182. The dendritic structure shown in Figure 3.3 develops during weld solidification of both Alloy 182 and 82 welds, with the dendrites growing toward the top of the weld (opposite the direction of heat flow). Even when the entire weld was nominally made with Alloy 82, weld repair records at some plants indicate manual welding using Alloy 182 because of the repair geometry or limited access. Weld repairs are suspected of being the origin of preferred crack initiation and faster crack growth. Unfortunately, many weld repairs were poorly documented. The start and end point of welds are also areas of concern, especially for manual welds.

Essentially all internal attachments to the pressure vessel are made using Alloy 182 pads that are welded directly onto the pressure vessel after the 308/L SS cladding is applied and before the PWHT. Stainless steel weld metal has proved to be more resistant to SCC than Alloy 182 weld metal. The Alloy 182 attachments include the steam dryer hold down brackets, core spray brackets, and shroud support structures. The latter were typically constructed of wrought Alloy 600, with Alloy 182 welds used for its construction and attachment to the vessel (Figure 3.19). This represents the largest circumference of Ni base weld. Legs welded to the bottom head of the RPV support the structure in many cases. Alloy 182 and 82 welds were used for many of the penetrations through the bottom of the pressure vessel—the most numerous welds being in the control rod drive (CRD) housings (Figure 3.20). Finally, in most BWRs, water is pumped through the core using jet pumps, which require circular openings in the Alloy 600 support ledge and are attached using Alloy 182 and 82 welds.

In the standard BWR environment (normal water chemistry, or NWC), the water chemistry is oxidizing and Alloy 182 is susceptible to SCC. Alloy 182 cracking was first discovered during replacement of weld sensitized stainless steel recirculation piping. Since then, there have been continuing instances of cracking in Alloy 182. This section discusses the field cracking characteristics of Alloy 182, SCC dependencies, mitigation techniques, and improved materials.

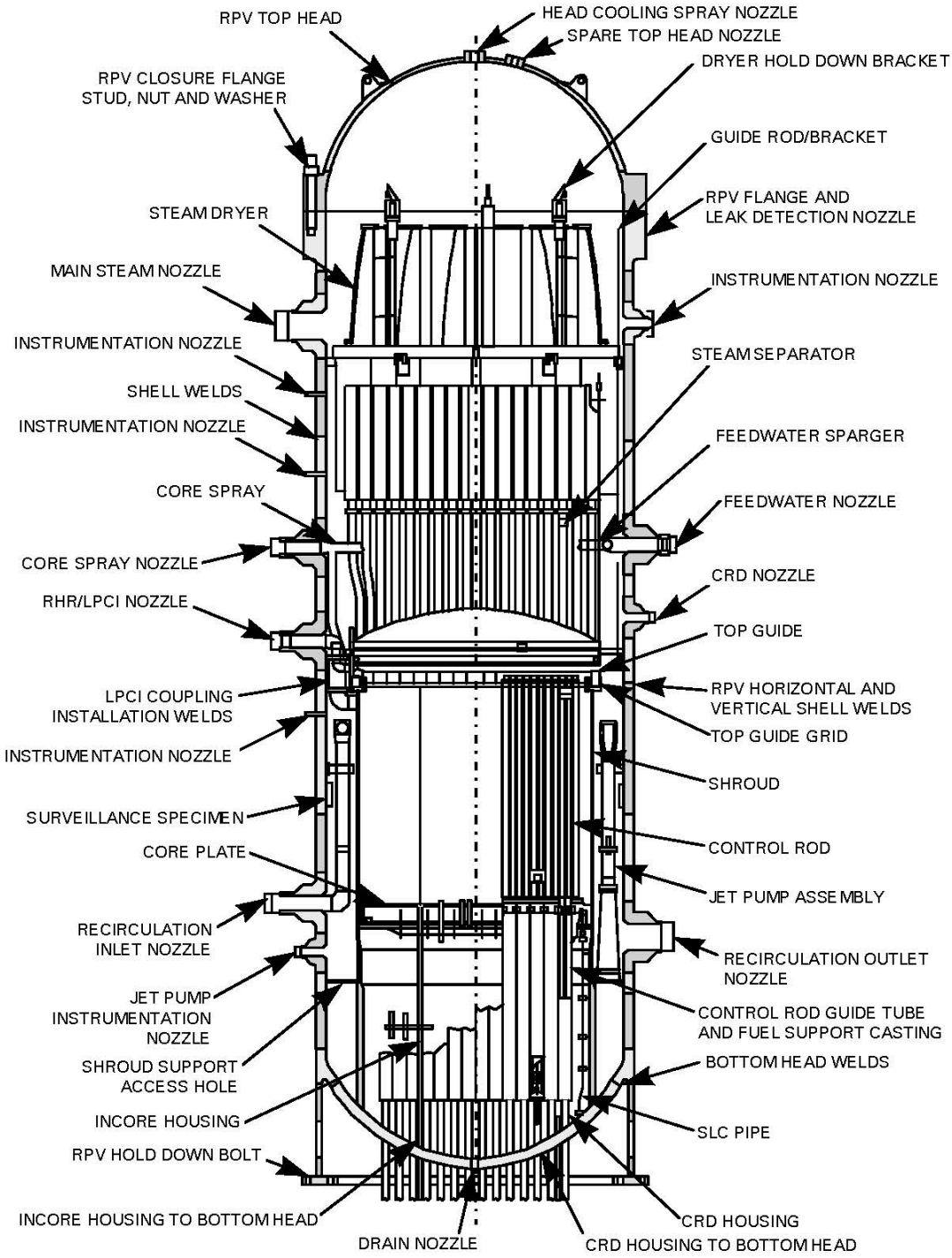

Figure 3.16. Schematic of typical BWR RPV, nozzles, and attachments.

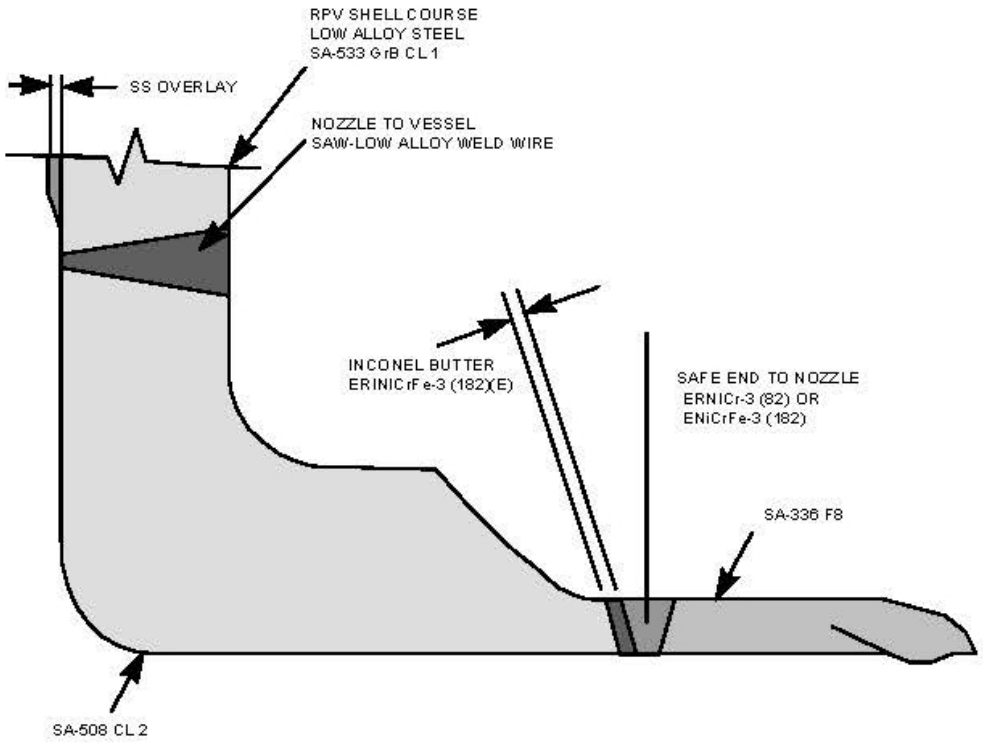

Figure 3.17. Typical BWR recirculation outlet nozzle, nozzle butter, weld, and safe end.

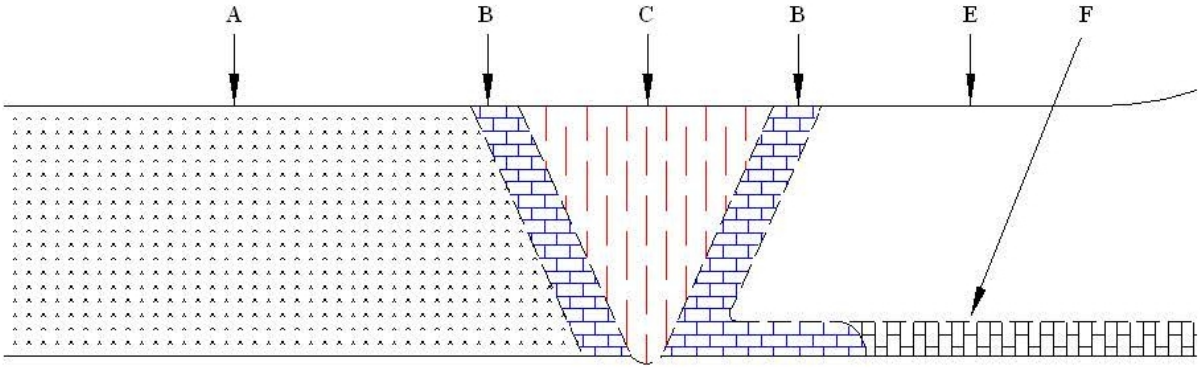

A) Stainless Steel Safe End
B) Alloy 182 Weld Butter
C) Alloy 182 or Alloy 82 Weld Metal
B) Alloy 182 Weld Butter
D) Low Alloy Steel Nozzle
E)··Low·Alloy·Steel¶
F)··Stainless·Steel·Cladding¶

Figure 3.18. Enlargement of safe end to nozzle weld region in BWRs using Alloy 182 and 82 weld metals.

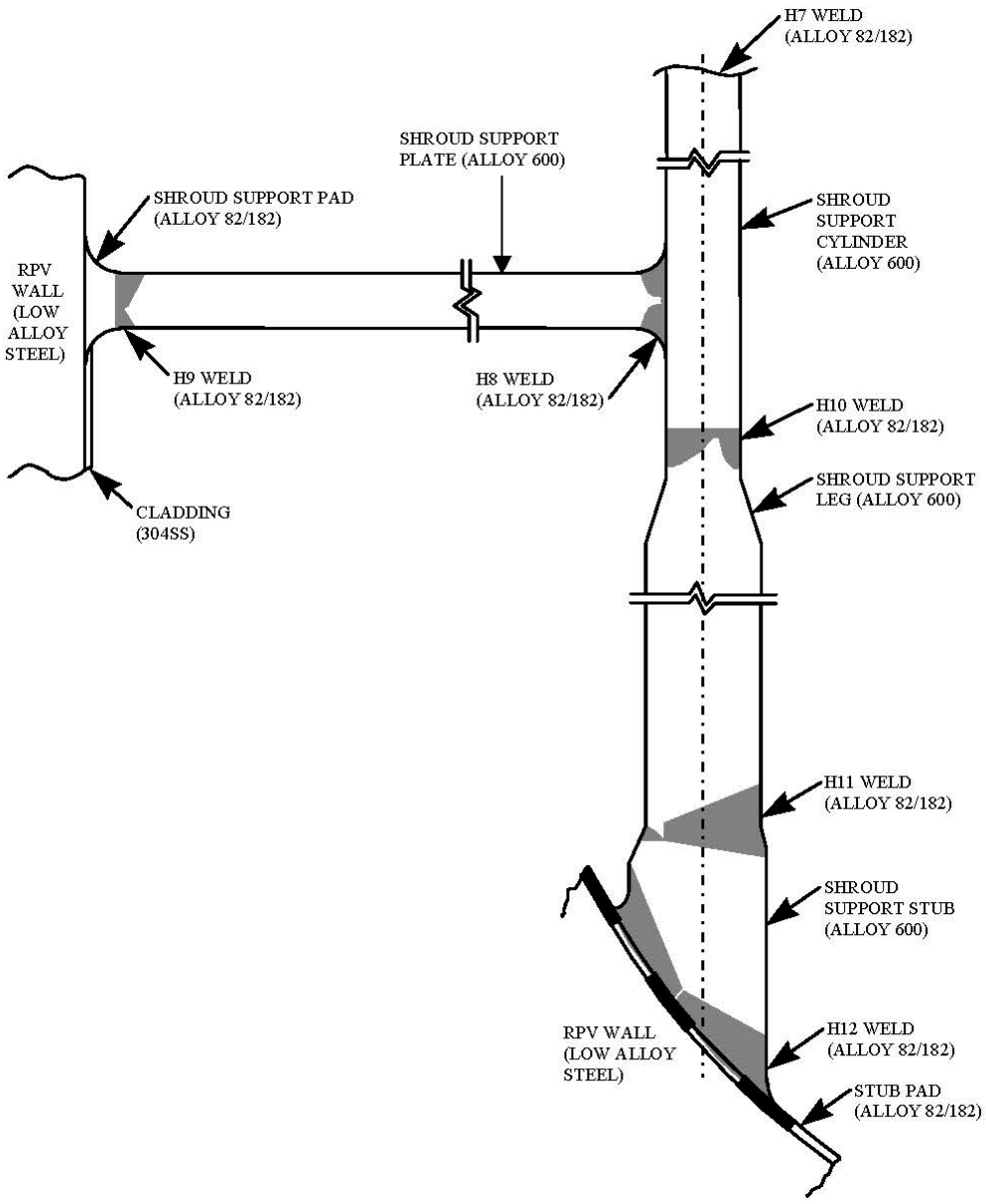

Figure 3.19. Typical BWR shroud support structure of the leg design with Alloy 182 used throughout. Also shown are the H9 and H12 welds that join the component to the RPV.

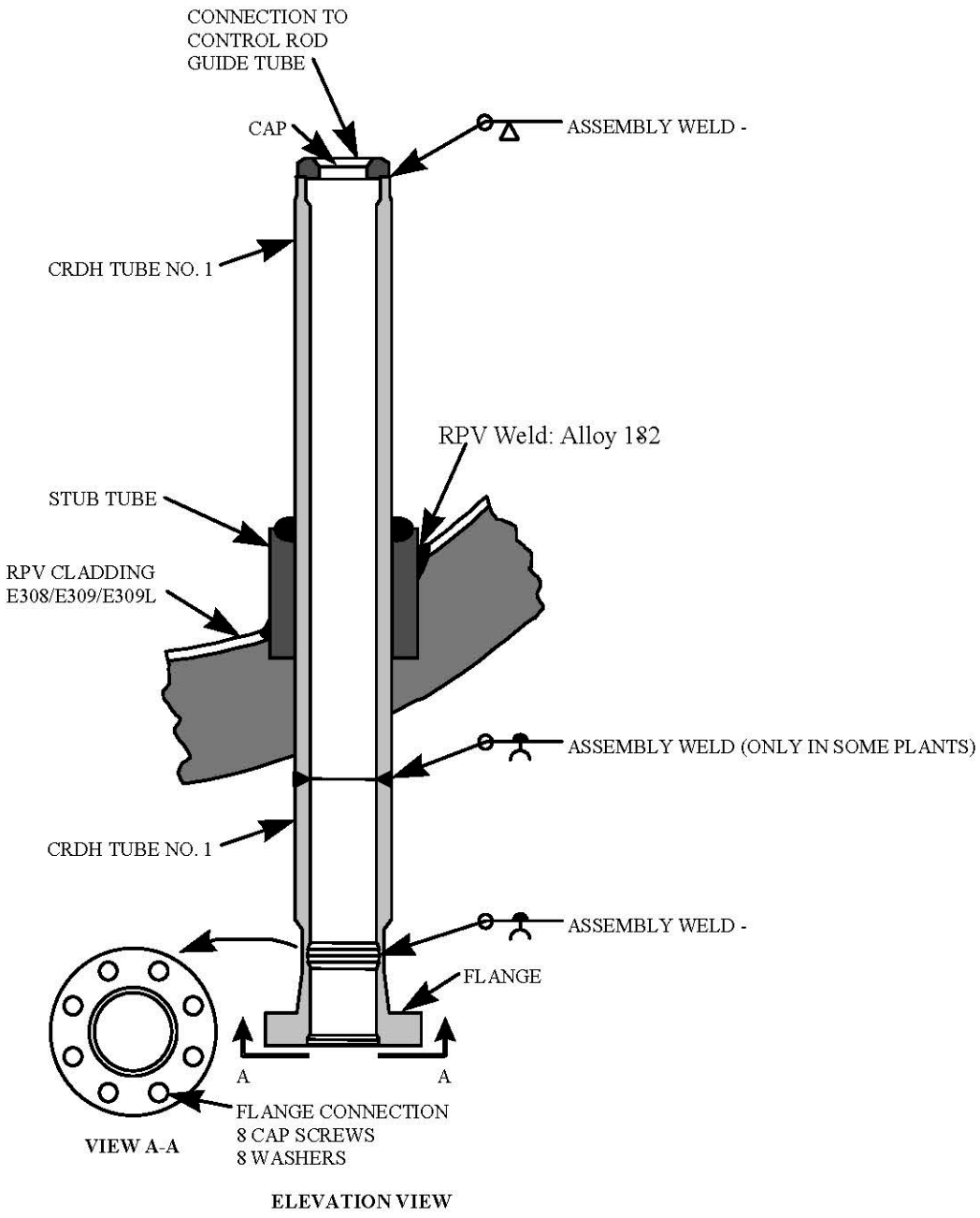

Figure 3.20. Typical CRD stub tube and CRD housing configurations. Alloy 182 used in stub tube to RPV weld.

3.4 SCC OPERATING EXPERIENCE OF NICKEL ALLOYS IN BWRS

The BWR Ni alloy components and welds listed in Tables 3.1, 3.4, and 3.5 have experienced SCC. There has also been extensive cracking of creviced Alloy 600, primarily in components, such as shroud head bolts, safe ends, and ledge and access hole covers. For Ni alloys and stainless steels, a high initial incidence of cracking occurred, primarily due to poor water chemistry management during the early operation of most BWRs (Figure 3.21). While dramatic

improvements were made in water purity, once cracks nucleated, growth was readily sustained even with good water chemistry. Figure 3.21 shows the correlation between BWR water purity and incidence of cracking in Alloy 600 shroud head bolts. In addition to the important effect of *average* water purity, both prediction and plant data show that very high conductivity early in life produced a different population of more severe cracking than is reflected by the plant *average* conductivity.

The overall experience with wrought Ni alloys in BWRs has been better than with welded austenitic stainless steels, where IGSCC has been widely observed in the heat affected zone of types 304 SS and 316 SS (but rarely in type 308L SS weld metal). This is especially true for furnace or weld-sensitized stainless steels, but unsensitized stainless steel has also cracked extensively, primarily due to the combination of weld residual stresses and weld shrinkage strains. Residual strains peak at the weld fusion line and are generally equivalent to 15–20% room temperature tensile strain [33, 34].

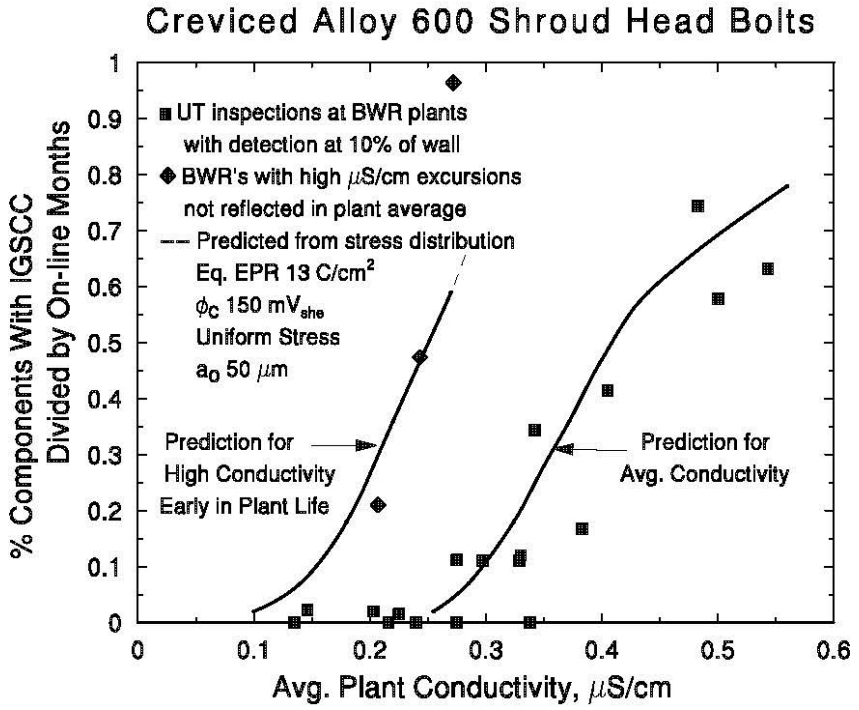

Figure 3.21. Observation and prediction of the incidence of SCC in Alloy 600 shroud head bolts as a function of average plant conductivity. An unusual population of bolts from three plants showed a much greater incidence of SCC because these plants had poor water chemistry early in their life, typical of most BWRs.

Table 3.4. Alloy 82 and 182 field cracking in one set of BWRs

Material	Component	Part	BWR Type	First Synch	Find Date	Cause
Alloy 182	Feed water sparger	End bracket	2	Sep-69	Oct-2000	IGSCC
Alloys 82 and 182	In-core monitor	Penetration		May-84	Aug-97	Most likely original fabrication weld defects (possible exception on 08-41)
Alloy 182	RPV head	Bracket	Non-GE BWR	Jan-81	Jan-95	IGSCC
Alloy 182	RPV head	Bracket	Non-GE BWR	Jun-80	Jan-95	IGSCC
Alloy 182	Shroud support	Leg	3	Mar-71	Dec-99	Probable IGSCC

Table 3.5. Alloy 182 field cracking in a second set of BWRs

Plant	System	Year of Detection	Location of Indication
E-1	Recirc	1990	Main loop
E-2	Recirc	1985	Flange
E-2	Core spray	1999	Brackets
E-3	Recirc	1996	Pipe weld
E-4	Recirc	1997	Pipe weld
E-4	Core spray	1999	Brackets
E-5	Core spray	1999	Brackets
E-6	Feed water	1985	Nozzle
E-6	RPV	1986	Head spring beams
E-6	RPV	1986	Flange
E-6	Feed water	1997	Nozzle
E-6	RHR	1997	Safe end
E-7	RPV	1985	Head spring beams
E-7	RPV	1990	Flange
E-7	Feed water	1995	Nozzle
E-8	RPV	1994	Head spring beams
E-8	Core cooling	1991	Nozzle
E-8	RPV	1995	Head spring beams

While extensive SCC of Alloy 600 has occurred in the crevices of components, there has been very good experience with Alloy 600 in the welded, non-crevice regions, particularly in the bottom-head region. Alloy 182 weld metal has not performed nearly as well. Initial concerns for the high probability of SCC for Alloy 182 were initially raised because of the laboratory test data from the United States [35] and subsequently confirmed internationally [11, 13, 14, 36]. This led to recommendations to inspect weld metal butters during the replacement of recirculation piping

that was necessitated by the IGSCC occurrence in weld sensitized, large diameter Type 304 SS pipes. The first inspection, performed at a BWR/3 around 1984, revealed cracking in several welds. Inspections were performed in the recirculation inlet and outlet safe ends during the piping replacement [37]. Cracking was detected using dye penetrant testing in 3 of 10 inlet nozzles and 1 of 2 outlet nozzles. The cracking was axial in all nozzle butters, with a maximum depth of about 70% of wall thickness. Boat samples were removed from one weld that attached the stainless steel safe end to the outlet nozzle. Metallography examination verified that the cracking was confined to the Alloy 182 weld and did not extend into the low alloy steel; it also established that cracking was interdendritic along intergranular dendrite grain boundaries and did not penetrate into the Alloy 82 root pass (corroborating the higher SCC resistance of Alloy 82 weld metal shown in laboratory data). Many axial segments initiated in the Alloy 182, with several circumferential segments that followed the fusion line.

Subsequently, cracking was detected in other BWRs. The number of affected nozzle-to-safe end welds varied from plant to plant, with one plant having six cracked nozzles. The frequency of cracking has now decreased, but leakage has occurred in some smaller diameter pipes. Some observations were associated with weld repair locations and the improper classification of inspection findings as weld geometry or internal weld defects. The cracked nozzles included recirculation inlet and outlet, core spray, and feed water nozzles. The cracking has remained primarily axial in nature, although there are some instances of circumferential cracking. Many of these cracked welds have been overlay repaired with a structural build-up of SCC resistant material to restore structural margin/integrity.

Knowledge of cracking in BWR core internal structures was very limited until the late 1990s, primarily because only a limited number of inspections were performed. The first components to be evaluated were the access hole covers, which were welded during plant construction after access was no longer needed to the lower plenum region. These welds were particularly susceptible because crevices existed where the cover recessed into the ledge. While cracking occurred in the creviced wrought Alloy 600 in many plants, it also initiated and/or propagated in the Alloy 182 weld metal. This heightened the concern for the occurrence of SCC for Alloy 182 in other locations.

The first instances of SCC in non-creviced attachment welds were found in hold-down brackets on the reactor vessel head that restrained the dryer assembly. These locations were inspected soon after SCC was first observed, and subsequent metallurgical evaluations confirmed the extent and morphology of cracking. The extent of cracking could not be accurately detected visually; only a penetration test (PT) examination or proper ultrasonic test (UT) interrogation could accurately characterize the extent of the tight weld cracks. While the cracked areas could be removed or repaired, their proximity to the RPV material heightened the need for periodic inspection of Alloy 182 welds in the reactor. Improved inspection approaches were developed by the EPRI's BWR Vessel and Internals Project between 1995 and 1998.

Subsequently, extensive SCC was discovered in Alloy 182 welds in the shroud support structure of a BWR/2 during a core shroud replacement in 1999. Visual inspections and liquid penetrant examinations were performed on the shroud support structure, revealing cracks in the attachment welds joining the conical support structure to the reactor vessel wall (Figure 3.22). This cracking was found in the weld build-up pad on the vessel wall (designated the H9 weld), as well as in other Alloy 182 welds and adjacent Alloy 600 in the lower conical section. Of greatest interest was the cracking found on the inside part (the lower bottom side) of the H9 weld, where nearly 300 individual cracks were found in 34 locations. These cracks were largely axial in nature (~90%); however, none entered the RPV low alloy steel. Since cracking was associated solely

with the underside of the actual core support structure, it was not detected during routine visual in-service inspection from the top surface. This led to inspections at other BWRs, and similar cracking was detected in another BWR/2 at the same H9 weld [38]. While the inspection technique was focused on circumferentially oriented cracking because the UT system was deployed from inside the vessel, the cracking appeared to be primarily axial.

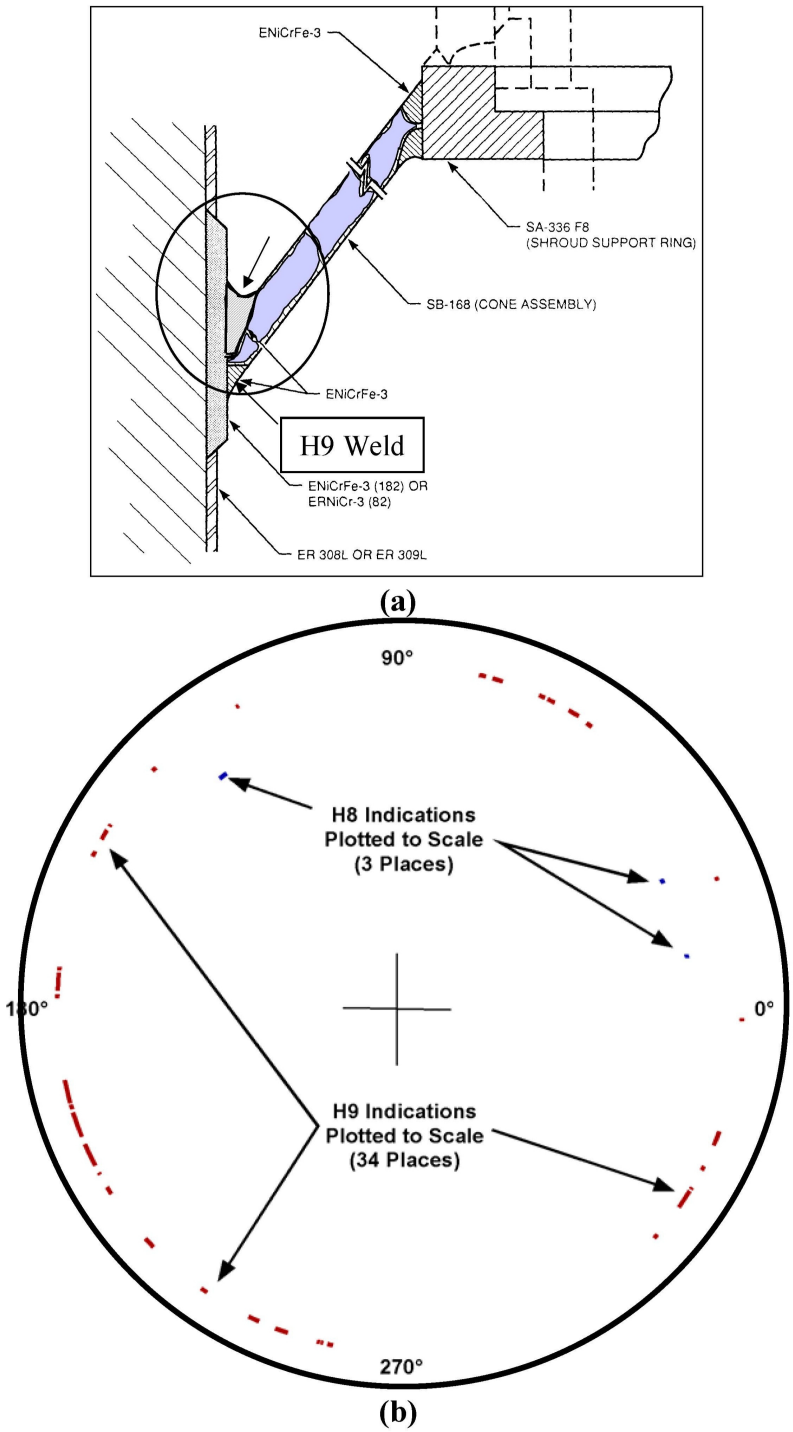

Figure 3.22. (a) Cross section of BWR/2 H9 weld and (b) schematic of the azimuthal orientation and length of the H8 and H9 indications (around vessel circumference) as determined by UT inspection.

3.5 OPERATING EXPERIENCE IN PWR PRIMARY SYSTEMS

Cracking was identified in thick section, forged, Alloy 600 components beginning in the mid-1980s with cracking first detected in the hottest components, i.e., pressurizer nozzles (Figure 3.2) [1, 2]. At all French PWRs, Alloy 600 pressurizer nozzles were replaced with stainless steel. In 1989, the first cracking of Alloy 600 upper head CRDM nozzles (Figures 3.23 and 3.24) occurred at Bugey 2, a first-generation French plant. Initially considered an isolated incident, this cracking was attributed to a stress concentration from a counter bore in the nozzles just below the level of the J-groove seal weld with the upper head combined with a relatively high operating temperature that was believed to be closer to that of the hot leg. However, CRDM nozzles at other plants in France exhibited the same type of cracking; however, in these subsequent episodes, the nozzles had no counter bores and their design was different (no tapered lower section). Furthermore, the upper head temperatures were the same as the inlet cold leg temperatures [39, 40].

These incidents of cracking in upper head CRDM nozzles shared three common features: (1) the presence of a significant cold-worked layer due to machining or grinding on the internal bore, (2) some distortion or ovalization (out-of-roundness) induced by the fabrication of the J-groove seal welds, and (3) a tendency to occur much more frequently in the outer set-up circles where the angles between the vertical CRDM nozzle and the domed upper head were greatest. The combination of these three features plus the fact that the upper head is stress relieved before the CRDM nozzles are welded in place pointed to high residual stresses being responsible for these premature failures.

Although the generic problem of Alloy 600 CRDM nozzle cracking first appeared in France, only sporadic instances of similar cracking were observed in other countries until the beginning of the 21st century, when numerous other incidents began to be reported. In some cases, where cracking was allowed to develop to the point of leaking primary water into the crevice between the CRDM nozzle and the upper head, circumferential cracks initiated on the outer surface of the CRDM nozzle at the root of the J-groove seal weld (U.S. experience, Davis Besse Nuclear Plant) [41]. This latter instance was also observed in 1989 at Bugey 2 but only to a minor extent. No further leaks of primary water due to CRDM nozzle cracking have occurred in France because of an inspection regime adopted to avoid them and a decision to replace all upper heads using thermally treated Alloy 690 CRDM nozzles [39, 40]. This same strategy, more economical than the cost of repairs and repeat inspections, has often been adopted elsewhere. The dangers of allowing primary water leaks to continue over several years so that extensive boric acid deposits accumulate was amply demonstrated by the discovery of very severe corrosion (wastage) of the low alloy steel of the upper head at the Davis Besse Nuclear Plant in Ohio in 2002 [7, 41].

The history of PWSCC in Alloy 600 and similar Ni base alloys has continued in recent years with the discovery of cracked Alloy 182 welds in several PWRs around the world (Figure 3.25) [41, 42]. This has occurred on the primary water side of the J-groove welds that seal the CRDM nozzles in the upper head and also in a few cases in the safe end welds of the RPV or pressurizer (Figure 3.26). One case has also occurred in the J-weld of a lower head instrumentation penetration [43]. Cracking seems to be significantly exacerbated by the presence of weld defects and weld repairs made during fabrication, usually to eliminate indications due to hot cracking, or slag inclusions, thus again implicating high residual stress in the failures observed to date. The cracking has often been described as interdendritic, but recent work shows that it is in fact intergranular. Incubation periods before detectable cracking seem to be on the order of twenty years.

It should be noted that all the Ni base weld metal cracking observed to date has involved welds that have not experienced the stress relief given to adjacent low alloy steel pressure vessel components [42]. Although the stress relief temperature is clearly not optimized for Ni base alloys (or stainless steels), it has been shown on mockups that such the surface residual stress of the welds is very significantly reduced and doubtless imparts greater resistance to PWSCC in PWR primary water.

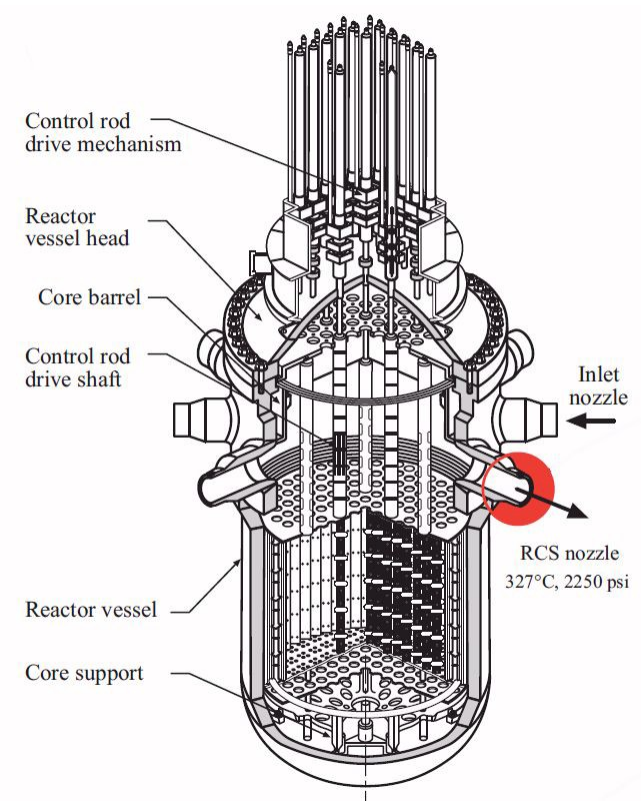

Figure 3.23. Schematic of a PWR pressure vessel and related structures.

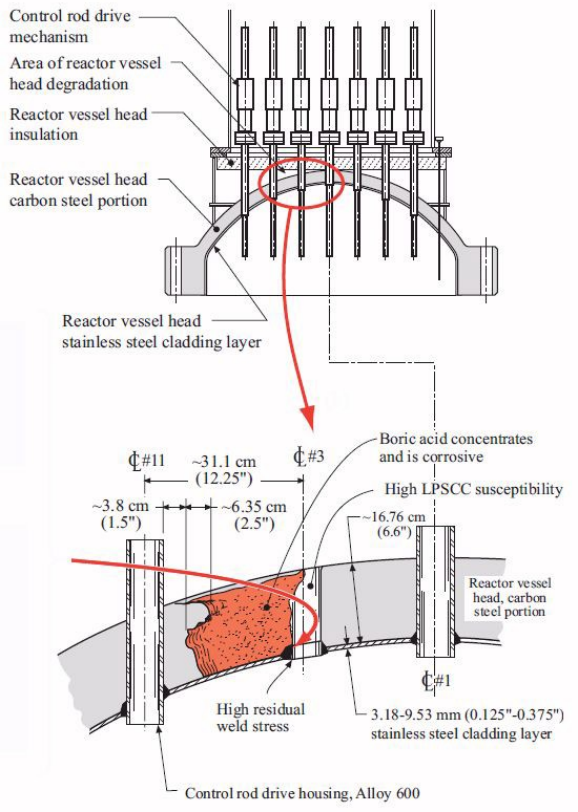

Figure 3.24. Schematic of the PWR CRDM penetrations.

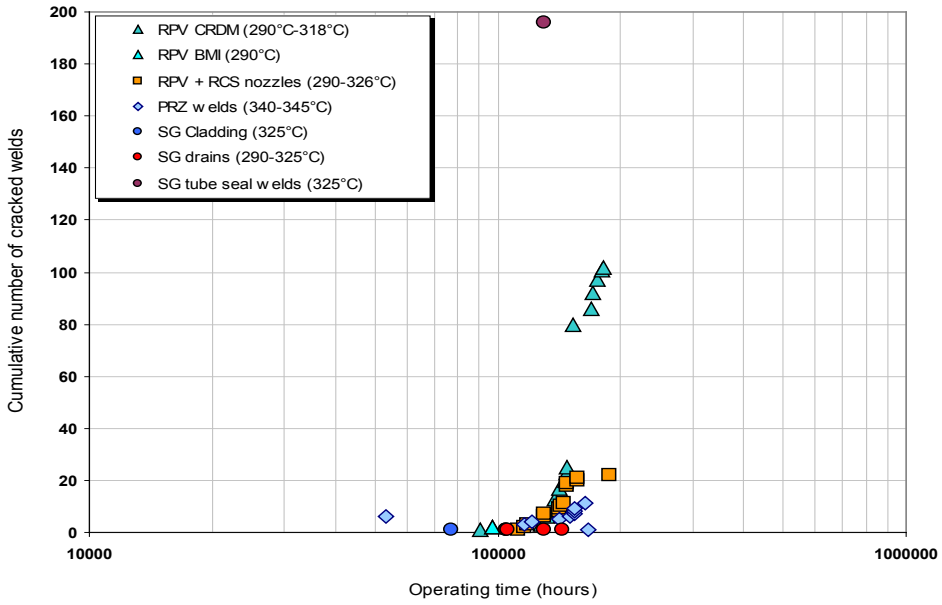

Figure 3.25. Time of detection of SCC in Alloy 182 welds in PWRs [41, 42].

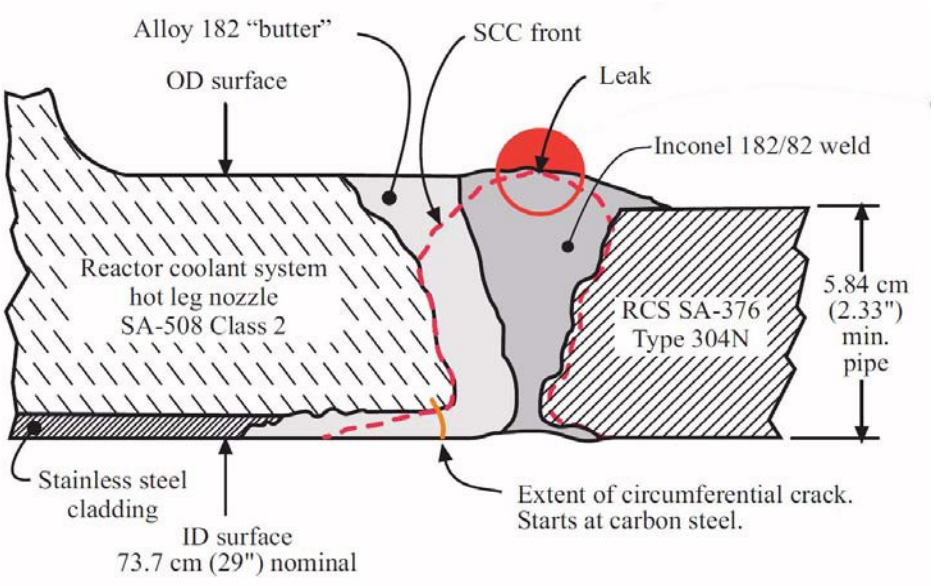

Figure 3.26. Schematic of the Alloy 182 weld used to join stainless steel piping to the RPV nozzle.

3.6 OPERATING EXPERIENCE OF PWR SECONDARY SYSTEMS

Most PWR steam generators are recirculating designs, although some are once-through designs where all of the secondary water entering the steam generator is transformed into steam. Most in-service PWSCC has occurred in recirculating steam generators (Figures 3.27 and 3.28). An important difference between the two with respect to the occurrence of PWSCC is that the once-through steam generators were subjected to a pre-service stress relief of the whole steam

generator at a temperature of about 610 °C (1,130 °F). In addition to contributing to grain boundary carbide precipitation in Alloy 600, some grain boundary Cr depletion (sensitization) also occurred. The lower strength and grain boundary carbide precipitation in once-through steam generators tubes has been beneficial to resist PWSCC on the primary side, despite the sensitization; however, even these steam generators are now being steadily replaced after typically 20 to 25 years of service [44]. In one case, an unintended ingress of thiosulfate into the once-through steam generators led (predictably) to extensive intergranular attack of the sensitized tubes.

PWSCC of Alloy 600 steam generator tubing in the mill-annealed condition became a major degradation mechanism from the 1970s onward for recirculating steam generators [45]. In 1971, the first confirmed primary side cracking of mill annealed Alloy 600 tubes of recirculating steam generators occurred when leakage at U-bends occurred in the Obrigheim, Germany after only two years of operation [4]. Cracking occurred in the tight U-bends, mainly on the inner two rows at the apex and at the tangent points and in the tube sheet at the transition expansion or roll expansion tube regions. This latter occurrence has been responsible for premature steam generator replacement at numerous plants.

The first roll transitions experiencing PWSCC were located on the hot leg side, where the temperature is typically around 320 °C and is 30 to 40 °C hotter than the cold leg inlet at 280 °C (536 °F). Thus, it was clear that temperature had a significant influence on PWSCC, indicating a thermally activated mechanism. The apparent activation energy, calculated from fitting the temperature dependence to the Arrhenius equation is rather high (~180 kJ/mole) so that a typical temperature difference of 30 °C (54 °F) between hot and cold legs could easily account for a factor of four to five increase in the time to the onset of detectable cracking. Thus, a reduction of hot leg temperature was employed for mitigation. Hot leg temperature reductions from 4 °C (7.2 °F) to even 10 °C (18 °F) have been applied.

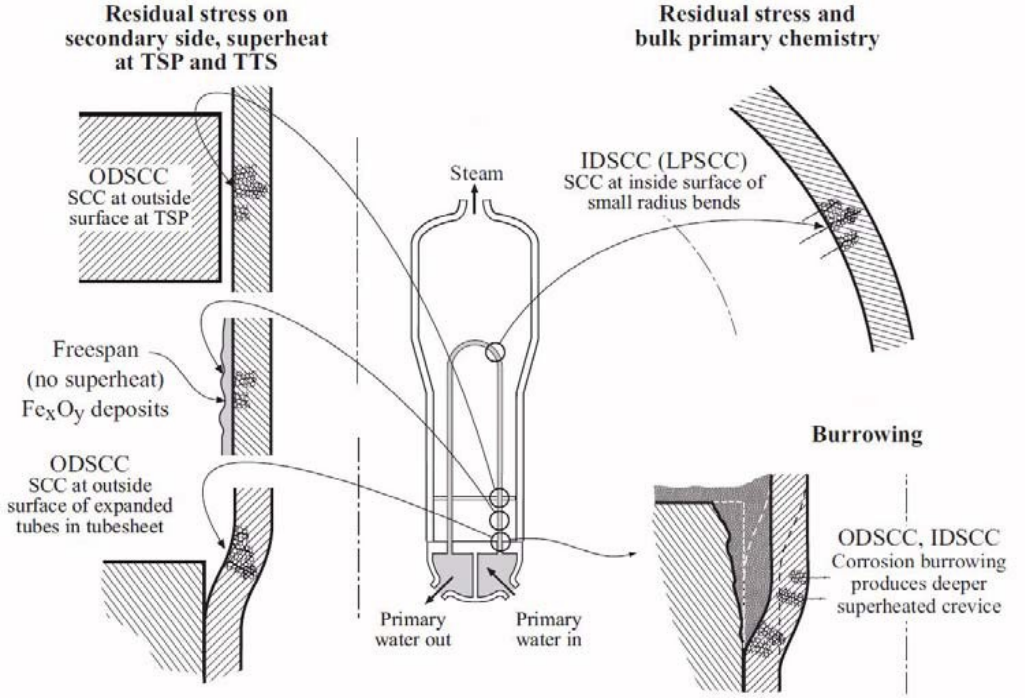

Figure 3.27. Schematic of locations where SCC most often occurs in Alloy 600 steam generator tubing.

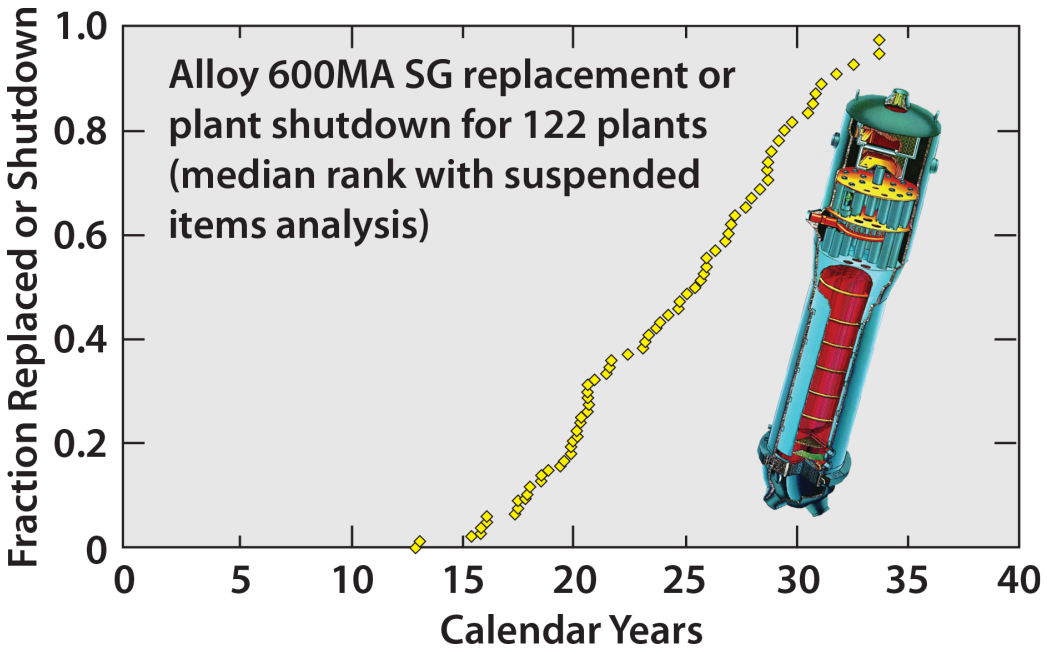

Figure 3.28. Fraction of Alloy 600 steam generators replaced per calendar years of operation.

The magnitude of the tensile residual stress from fabrication has also had a major impact on the time for detectable PWSCC to develop; only the most highly strained regions of steam generator tubing (i.e., first and second row U-bends, roll transition regions, expanded regions, and dented areas) have exhibited PWSCC. Consequently, several stress mitigation techniques have been developed, such as local stress relief of first and second row U-bends by resistance or induction heating, and shot peening or roto-peening to induce compressive stresses on the internal surface of roll transitions [46, 47]. While peening helps to prevent initiation of new cracks, it cannot prevent the growth of existing cracks whose depth is greater than that of the induced compressive layer, typically 100 to 200 μm (approximately 0.004 to 0.008 in.). Thus, peening has been most effective when most tubes have either no cracks or only very shallow ones (i.e., when practiced before service or very early in life) [47, 48].

Material susceptibility, in combination with the factors mentioned above, is also a major factor affecting the occurrence of PWSCC in service. Most PWSCC has occurred in mill-annealed tubing. However, it is important to emphasize that there is not a single product called “mill-annealed” Alloy 600 tubing since each tubing manufacturer has different production processes. Whereas some mill-annealed tubing has never experienced PWSCC over many years, other mill-annealed tubing has undergone PWSCC after only 1 to 2 years of service, particularly at roll transitions. This variability of PWSCC susceptibility can be seen even between heats from the same manufacturer in the same steam generator [1]. The variation in susceptibility to PWSCC of the heats of Alloy 600 typically fits approximately a lognormal distribution, perhaps indicating that a rather small fraction of Alloy 600 heats may be responsible for a disproportionately high number of tubes affected by primary side PWSCC. The reasons for this variability are only partly understood, as explained below.

This microstructural aspect of susceptibility to PWSCC is strongly affected by the final mill annealing temperature, which determines whether carbide precipitation occurs predominantly on grain boundaries or within the grains (intragranular). The most susceptible microstructures are those produced by low mill annealing temperatures, typically around 980 °C (1,796 °F) that

develop fine grain sizes (ASTM 9 to 11), copious quantities of intragranular carbides, and, usually, few to no grain boundary carbides [49, 50]. Higher mill annealing temperatures in the range of 1,040 °C (1,904 °F) to 1,070 °C (1,958 °F) avoid undue grain growth and leave enough dissolved carbon (C) so that intergranular carbide precipitation occurs more readily during cooling.

A further development to exploit the apparent advantages of grain boundary carbides for PWSCC resistance was to thermally treat the tubing for ~15 h at 705 °C (1,301 °F) after mill annealing. This heat treatment increases the density of intergranular carbides and provides enough time so that most of the C in solution is consumed and the Cr can diffuse to grain boundaries, thus eliminating depletion of carbide avoiding sensitization [50]. The beneficial influence of grain boundary Cr carbides on primary side PWSCC resistance has been extensively evaluated in laboratory studies; the results showed an improvement in life of thermally treated tubing of between 2 and 5 times relative to the mill annealed condition. In fact, primary side PWSCC resistance is improved with or without grain boundary Cr depletion, as also deduced from the generally much better operating experience of Alloy 600 tubing of once-through steam generators [44, 49, 50]. However, even thermally treated Alloy 600 tubing has cracked in service, but much less frequently than mill annealed Alloy 600. This has usually been attributed to a failure of the thermal treatment to produce the desired intergranular carbide microstructure either due to insufficient C or factors such as tube straightening prior to thermal treatment, which favors carbide precipitation on dislocations instead of grain boundaries.

Steam generator tubes with PWSCC detectable by non-destructive testing have usually been preventively plugged either to avoid leakage or before the crack length reaches some predefined conservative fraction of the critical size for ductile rupture. Sleeving has sometimes been deployed as a repair method in operating PWRs to avoid plugging and maintain the affected tubes in service. The sleeves bridge the damaged area and are welded to material ground beyond the damage. The ends of the sleeves may be expanded hydraulically or explosively and are in most cases sealed by rolling, welding, or brazing [5].

Modern (usually replacement) steam generators have been fabricated using Alloy 690 tubes thermally treated for 5 hours at 715 °C. As well as being highly resistant in severe laboratory tests to PWSCC in PWR primary water compared to either mill annealed or thermally treated Alloy 600, the lead steam generators with thermally treated Alloy 690 tube bundles have to date passed about 16 years of service with no known tube failures, related to PWSCC.

3.7 IMPROVED NICKEL ALLOYS AND WELD METALS

Efforts to improve Ni alloy resistance to SCC have focused on *incremental* improvements and *major* improvements. Incremental tuning includes additions of stabilizing elements [such as niobium (Nb), tantalum (Ta), and titanium (Ti)] and control of C levels, which minimizes the likelihood of grain boundary Cr depletion and creates a dispersion of MC-type carbides, where M represents the alloying element. An empirically-derived N-bar parameter has been used to assess the SCC susceptibility for Alloy 182 [51], represented by: N-bar = 0.13×(Nb+Ti)/(2×C) (in weight percent), with values below 12 indicating moderate susceptibility. A more recent measure is the stress corrosion resistance index, which includes Cr level in the assessment [52].

$$SCRI = Cr + (Nb+Ta)\times 5 + Ti\times 10 - 116.5\times C \quad \text{(in weight percent)} \qquad (1)$$

A value below 30 represents susceptibility. Higher crack growth rates have also been measured in tests performed to evaluate SCC susceptibility due to other alloying impurities, such as

phosphorous (P), sulfur (S), and silicon (Si), but this may be due to synergistic effects with Cr-depleted boundaries. These elements, especially elevated Si and lower manganese (Mn), adversely affect weldability by leading to a higher propensity for hot cracking that could accelerate crack advance. Vendor specifications have been adapted to account for these factors.

More significant improvements have been achieved by markedly increasing the Cr content, e.g., from 15–20% Cr to 27–30% Cr. Examples are Alloy 690 base metal (~30% Cr), Alloy 152/52 weld metals (~30% Cr), and Alloy 52i weld metal (~27% Cr). The higher Cr content imparts greater resistance to SCC (Figures 3.9, 3.29, and 3.30), but also brings some challenges. The higher Cr content of Alloy 690 makes it more prone to segregation and banding, thus requiring controlled processing. Alloy 152 and 52 weld metals are more prone to hot cracking and ductility dip cracking, and the very extensive efforts to improve their weldability have only been partly successful.

The PWR industry has shifted to Alloy 52 and 152 weld metal, and Alloy 600 has been replaced with Alloy 690. In general, the SCC susceptibility is significantly reduced. However, many Alloy 690 heats have exhibited high SCC growth rates when cold worked in laboratory experiments, and welds—especially if they have been repaired—can have residual strains greater than 25%. Issues with Alloy 690, and Alloy 152/52 materials will be discussed in the following Chapter. Some in the BWR industry still consider Alloy 82 an adequate choice when fabrication concerns are included in the decision process. But both PWR and BWR data (Figures 3.8 and 3.31) [25–28] indicate that the distinction between Alloy 182 and 82 weld metals is not very significant in laboratory experiments involving crack growth studies.

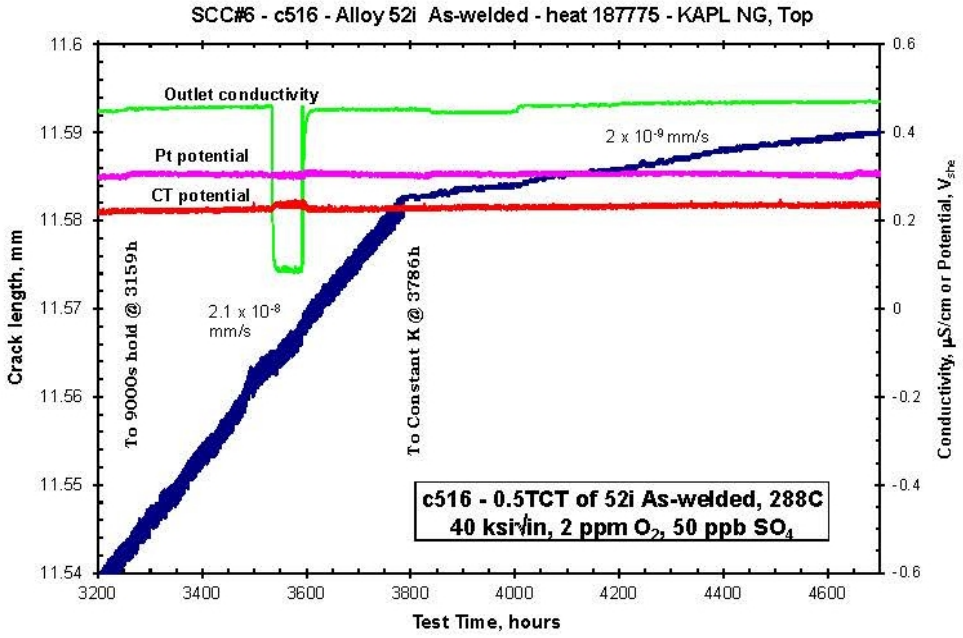

Figure 3.29. SCC response of 27% Cr, Alloy 52i weld metal in BWR water chemistry with 2 ppm O_2 and high levels of acid sulfate.

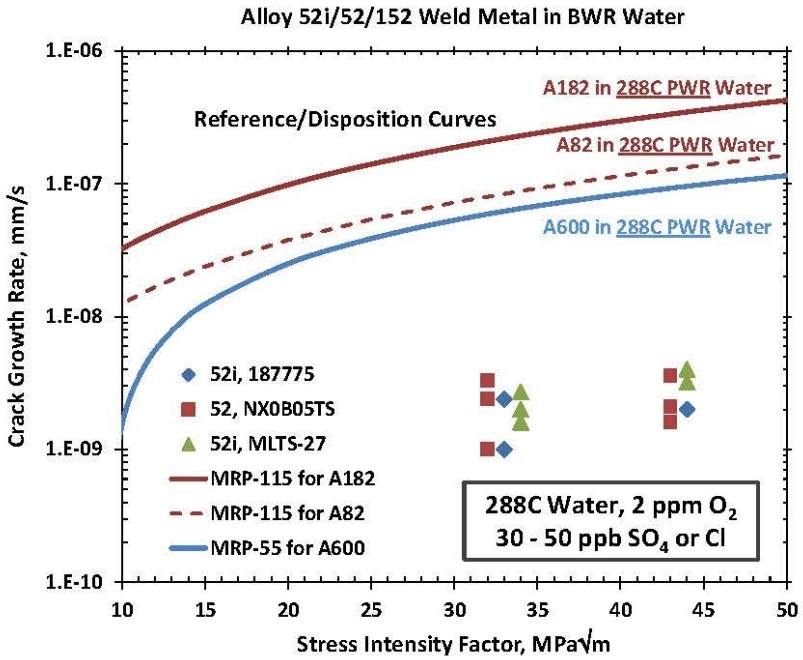

Figure 3.30. Summary of crack growth rates on Alloy 52 and 152 weld metals in BWR water with 2 ppm O_2 and high levels of acid sulfate or chloride. The growth rates in BWR water are ~50× lower than the disposition curve for Alloy 82 weld metal in PWR primary water (low corrosion potential) at 288ºC (550 °F) (dashed curve).

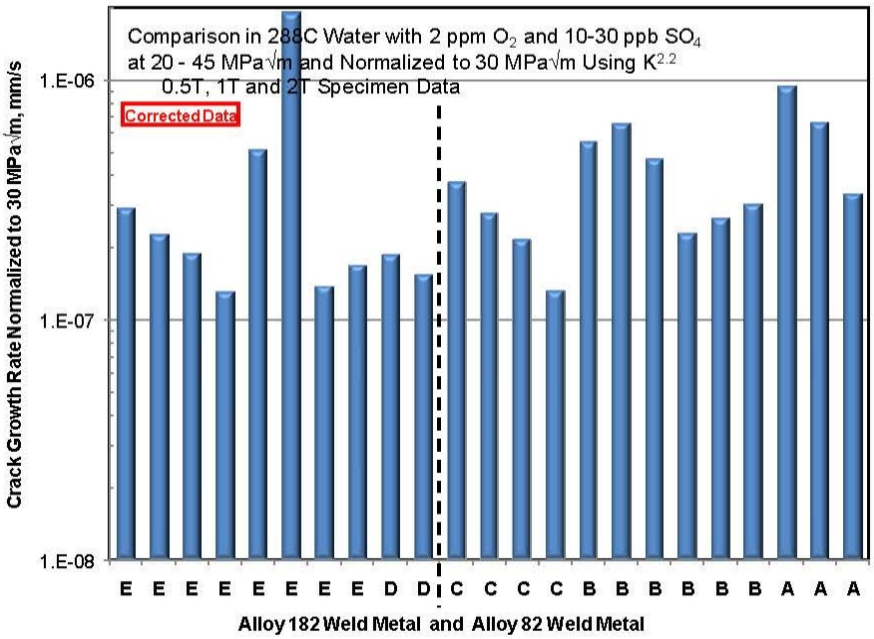

Figure 3.31. Overview of SCC growth rate data on five heats of Alloy 182 and 82 weld metal in 288 °C BWR water showing the lack of a distinctive difference between them, as well as their fairly high crack growth rates [25–28].

3.8 REFERENCES*

1. P. M. Scott, “Stress Corrosion Cracking in Pressurized Water Reactors—Interpretation, Modeling and Remedies,” *Corrosion* **56**(8), 771–782 (2000).
2. Ph. Berge, “Importance of Surface Preparation for Corrosion Control in Nuclear Power Stations,” *Materials Performance* **36**(11), 56 (1997).
3. J. Blanchet, H. Coriou, L. Grall, C. Mahieu, C. Otter, G. Turluer, “Historical Review of the Principal Research Concerning the Phenomena of Cracking of Nickel Base Austenitic Alloys,” pp. 1149–1160 in *Proc. NACE-5 Stress Corrosion Cracking and Hydrogen Embrittlement of Iron Base Alloys,* National Association of Corrosion Engineers, 1977.
4. H. J. Schenk, “Investigation of Tube Failures in Inconel 600 Steam Generator Tubing at KWO Obrigheim,” *Materials Performance* **15**(3), 25–33 (1976).
5. S. J. Green, “Steam Generator Failure or Degradation,” pp. 937–945 in “Corrosion in the Nuclear Power Industry,” *ASM Handbook, Vol. 13, Corrosion,* 1987.
6. W. Bamford and J. Hall, “A Review of Alloy 600 Cracking in Operating Nuclear Plants: Historical Experience and Future Trends,” pp. 1071–1079 in *Proc. 11th Int. Conf. Environmental Degradation of Materials in Nuclear Power Systems—Water Reactors,* Stevenson, Aug. 10–14, 2003, G. Was and L. Nelson (eds.), American Nuclear Society, 2003.
7. W. H. Cullen, Jr., and T. S. Mintz, *A Survey of Worldwide Experience with the Cracking Susceptibility of Alloy 600 and Associated Welds,* ADAMS ML040910354, Office of Nuclear Regulatory Research, U.S. Nuclear Regulatory Commission, Washington, DC, March 2004.
8. F. P. Ford and P. L. Andresen, “Development and Use of a Predictive Model of Crack Propagation in 304/316L, A533B/A508 and Inconel 600/182 in 288 °C Water,” pp. 789–800 in *3rd Int. Symp. Degradation of Materials in Nuclear Power Industry,* The Minerals, Metals &Materials Society, 1988.
9. P. L. Andresen and F. P. Ford, “Life Prediction by Mechanistic Modeling and System Monitoring of Environmental Cracking of Fe and Ni Alloys in Aqueous Systems,” *Materials Science and Engineering* **A103,** 167–183 (1988).
10. F. P. Ford and P. L. Andresen, “Corrosion in Nuclear Systems: Environmentally Assisted Cracking in Light Water Reactors,” pp. 501–546 in *Corrosion Mechanisms,* P. Marcus and J. Ouder (eds.), Marcel Dekker, 1994.
11. P. L. Andresen, “Fracture Mechanics Data and Modeling of Environmental Cracking of Nickel-Base Alloys in High Temperature Water,” *Corrosion* **47,** 917–938 (December 1991).
12. P. L. Andresen, “Conceptual Similarities and Common Predictive Approaches for SCC in High Temperature Water Systems,” Paper 96258, *Corrosion/96,* National Association of Corrosion Engineers, 1996.
13. P. L. Andresen, L. M. Young, P. W. Emigh, and R. M. Horn, “Stress Corrosion Crack Growth Rate Behavior of Ni Alloys 182 and 600 in High Temperature Water,” Paper 02510, *Corrosion/02,* National Association of Corrosion Engineers, 2002.

* Inclusion of references in this report does not necessarily constitute NRC approval or agreement with the referenced information.

14. P. L. Andresen, “SCC of Alloy 182 and 82 Weld Metals in BWR Water,” *Corrosion/10,* National Association of Corrosion Engineers, Houston, 2010.

15. P. L. Andresen, J. Hickling, K. S. Ahluwalia, and J. A. Wilson, “Effects of PWR Primary Water Chemistry on PWSCC of Ni Alloys,” *Proc. 13th Int. Symp. Environmental Degradation of Materials in Nuclear Power Systems,* Whistler, Aug. 19–23, 2007, P. King and T. Allen (eds.), The Canadian Nuclear Society, 2008.

16. P. L. Andresen, J. Hickling, K. S. Ahluwalia, and J. A. Wilson, “Effects of Hydrogen on SCC Growth Rate of Ni Alloys in High Temperature Water,” *Corrosion* **64**(9), 707 (2008).

17. P. L. Andresen and P. Chou, “Effects of Hydrogen on SCC Growth Rate of Ni Alloys in BWR Water,” *Proc. 15th Int. Symp. Environmental Degradation of Materials in Nuclear Power Systems—Water Reactors,* Colorado Springs, Aug. 7–11, 2011, J. Busby and G. Ilevbare (eds.), The Minerals, Metals & Materials Society, 2012.

18. C. M. Brown and W. J. Mills, “Load Path Effects on the Fracture Toughness of Alloy 82H and 52 Welds in Low Temperature Water,” *Proc. 12th Int. Symp. on Environmental Degradation of Materials in Nuclear Power Systems—Water Reactors*, Salt Lake City, Aug. 14–18, 2005, L. Nelson, P. King, and T. R. Allen (eds.), The Minerals, Metals &Materials Society, 2007.

19. C. M. Brown and W. J. Mills, “Fracture Toughness of Alloy 690 and EN52 Welds in Air and Water,” *Metallurgical Transactions A* **33A,** 1725 (June 2002).

20. P. L. Andresen and M. M. Morra, “Emerging Issues in Environmental Cracking in Hot Water,” *Proc. 13th Int. Symp. Environmental Degradation of Materials in Nuclear Power Systems,* Whistler, Aug. 19–23, 2007, P. King and T. Allen (eds.), The Canadian Nuclear Society, 2008.

21. P. L. Andresen, “Observations of Environmental Effects on Rapid Fracture,” unpublished data, GE Global Research Center, Schenectady, NY, 2010.

22. *Materials Reliability Program: Crack Growth Rates for Evaluating Primary Water Stress Corrosion Cracking (PWSCC) of Alloy 82, 182, and 132 Welds,* Report 1006696 (MRP-115), Electric Power Research Institute, 2004.

23. *Materials Reliability Program (MRP) Crack Growth Rates for Evaluating Primary Water Stress Corrosion Cracking (PWSCC) of Thick-Wall Alloy 600 Materials (MRP-55) Revision 1,* Final Report 1006695, Electric Power Research Institute, November 2002.

24. P. L. Andresen, P. W. Emigh, and M. M. Morra, “SCC of High Strength Ni-base Alloys in High Temperature Water,” Paper 04675, *Corrosion/04,* National Association of Corrosion Engineers, 2004.

25. G. A. Young, R. A. Etien, M. J. Hackett, J. D. Tucker, and T. E. Capobianco, “Physical Metallurgy, Weldability and In-Service Performance of Nickel-Chromium Filler Metals Used in Nuclear Power Systems,” *Proc. 14th Environmental Degradation of Materials in Nuclear Power Systems,* Virginia Beach, Aug. 23–27, 2009, T. Allen and J. Busby (eds.), American Nuclear Society, 2010.

26. R. A. Etien III, G. A. Young, T. E. Capobianco, J. V. Mullen, S. Leveillee, and P. C. Sander, “Development of a Corrosion Resistant and Highly Weldable Filler Metal For Use With Alloy 690,” Paper 08597, *Corrosion/2008,* National Association of Corrosion Engineers, Houston, TX, 2008.

27. G. A. Young, T. E. Capobianco, R. Etien III, J. V. Mullen, L. L. D’Amore, and S. Leveillee, “Development of a Highly Weldable and Corrosion Resistant Ni-Cr Filler Metal,” *Proc. 11th Environmental Degradation of Materials in Nuclear Power Systems—Water Reactors,*

Stevenson, Aug. 10–14, 2003, G. Was and L. Nelson (eds.), American Nuclear Society, 2003.

28. P. L. Andresen, "SCC of High Cr Alloys in BWR Environments," *Proc. 15th Int. Symp. Environmental Degradation of Materials in Nuclear Power Systems—Water Reactors,* Colorado Springs, Aug. 7–11, 2011, J. Busby and G. Ilevbare (eds.), The Minerals, Metals & Materials Society, 2012.
29. S. A. Attanasio and D. S. Morton, "Measurement of the Ni/NiO Transition in Ni-Cr-Fe Alloys and Updated Data and Correlation to Quantify the Effect of Aqueous Hydrogen on Primary Water SCC," *Proc. 11th Int. Symp. Environmental Degradation of Materials in Nuclear Power Systems—Water Reactors,* Stevenson, Aug. 10–14, 2003, G. Was and L. Nelson (eds.), American Nuclear Society, 2003.
30. D. S. Morton, S. A. Attanasio, and G. A. Young, "Primary Water SCC Understanding and Characterization Through Fundamental Understanding in the Vicinity of the Ni/NiO Phase Transition," *Proc. 10th Int. Symp. Environmental Degradation of Materials in Nuclear Power Systems—Water Reactors,* Lake Tahoe, Aug. 5–9, 2001, F. P. Ford and G. Was (eds.), National Association of Corrosion Engineers, 2002.
31. D. Morton, S. Attanasio, E. Richey, G. Young, and R. Etien, "Updated Data and Correlation to Quantify the Effect of Aqueous Hydrogen and Low Temperature on the SCC Growth Rate of Nickel-base Alloys in Primary Water," *Proc. Alloy 600 Conference,* Atlanta, June 2007, Electric Power Research Institute, 2007.
32. *BWR RPV License Renewal Industry Report, Revision 1,* Report TR-103836, Electric Power Research Institute, July 1994.
33. T. M. Angeliu, P. L. Andresen, E. Hall, J. A. Sutliff, and S. Sitzman, "Strain and Microstructure Characterization of Austenitic Stainless Steel Weld HAZs," Paper 00186, *Corrosion/2000,* National Association of Corrosion Engineers, 2000.
34. P. L. Andresen, T. M. Angeliu, L. M. Young, W. R. Catlin, and R. M. Horn, "Mechanisms and Kinetics of SCC in Stainless Steels," *Proc. 10th Int. Symp. Environmental Degradation of Materials in Nuclear Power Systems—Water Reactors,* Lake Tahoe, Aug. 5–9, 2001, F.P. Ford and G. Was (eds.), National Association of Corrosion Engineers, 2002.
35. A. Page, *Stress Corrosion Cracking of Alloys 600 and 690 and Weld Metals No. 82 and 182 in High Temperature Water,* EPRI NP-2617, Electric Power Research Institute, September 1982.
36. L. G. Ljungberg, *Stress Corrosion Cracking of Alloys 600 and 182 in BWRs,* EPRI/SKI Research Project 2293-1, interim reports, Electric Power Research Institute, 1991–1994.
37. *Reactor Pressure Vessel Attachment Welds: Degradation Assessment,* EPRI-NP-7139-D, Final Report, Electric Power Research Institute, May 1991.
38. H. S. Mehta, R. M. Horn, and G. B. Inch, "A Fracture Mechanics Evaluation of Observed Cracking at a BWR-2 Reactor Pressure Vessel Weld," *2002 ASME PVP Conference,* Aug. 4–8, 2002, Vancouver, B.C., Canada.
39. F. Champigny, F. Chapelier, and C. Amzallag, "Maintenance Strategy of Inconel Components in PWR Primary Systems in France," *Proc. Conf. Vessel Penetration Inspection, Cracking and Repairs,* Gaithersburg, MD, Sept. 29–Oct. 2, 2003, U.S. Nuclear Regulatory Commission, 2004.
40. P. Chartier, D. Edmond, and G. Turluer, "The French Regulatory Experience and Views on Nickel-base Alloy PWSCC Prevention," *Proc. Conf. Vessel Penetration Inspection, Cracking*

and Repairs, Gaithersburg, MD, Sep. 29–Oct. 2, 2003, U.S. Nuclear Regulatory Commission, 2004.

41. A. Hiser, "US Regulatory Experience and Prognosis with RPV Head Degradation and VHP Nozzle Cracking," *Proc. Conf. Vessel Penetration Inspection, Cracking and Repairs,* Gaithersburg, MD, Sept. 29–Oct. 2, 2003, U.S. Nuclear Regulatory Commission, 2004.
42. C. Amzallag, J-M. Boursier, C. Pagès, and C. Gimond, "Stress Corrosion Life Assessment of 182 and 82 Welds Used in PWR Components," *Proc. 10th Int. Conf. Environmental Degradation of Materials in Nuclear Power Systems—Water Reactors,* Lake Tahoe, Aug. 5–9, 2001, F. P. Ford and G. Was (eds.), National Association of Corrosion Engineers, 2002.
43. S. Thomas, "Bottom Mounted Instrumentation Penetration Condition Resolution," *Proc. Conf. Vessel Penetration Inspection, Cracking and Repairs,* Gaithersburg, MD, Sept. 29–Oct. 2, 2003, U.S. Nuclear Regulatory Commission, 2004.
44. P. A. Sherburne, "OTSG Materials Performance—25 Years Later," pp. 529–540 in *Proc. Fontevraud 4 Int. Symp.,* Société Française d'Energie Nucléaire, 1998.
45. D. R. Diercks, W. J. Shack, and J. Muscara, "Overview of Steam Generator Tube Degradation and Integrity Issues," *Nuclear Engineering and Design* **194,** 19–30 (1999).
46. G. Frederick and P. Hernalsteen, "Generic Preventive Actions for Mitigating MA Inconel 600 Susceptibility to Pure Water Stress Corrosion Cracking," presented at The Specialist Meeting on Steam Generators, Stockholm, Sweden, NEA/CSNI-UNIPEDE, October 1984.
47. P. Saint-Paul and G. Slama, "Steam Generator Materials Degradation," pp. 39–49 in *Proc. 5th Int. Symp. Environmental Degradation of Materials in Nuclear Power Systems—Water Reactors,* Monterey, Aug. 25–29, 1991, D. Cubicciotti and E. Simonen (eds.), American Nuclear Society, 1992.
48. P. Pitner and T. Riffard, "Statistical Evaluation of the Effects of Shot-Peening on Stress Corrosion of Alloy 600 in PWR Steam Generators," pp. 707–712 in *Proc. 6th Int. Symp. Environmental Degradation of Materials in Nuclear Power Systems–Water Reactors,* San Diego, Aug. 1–5, 1993, E. Simonen and R. Gold (eds.), The Minerals, Metals & Materials Society, 1993.
49. G. P. Airey, "The Stress Corrosion Cracking (SCC) Performance of Inconel Alloy 600 in Pure and Primary Water Environments," pp. 462–476 in *Proc. 1st Int. Symp. Environmental Degradation of Materials in Nuclear Power Systems—Water Reactors,* Myrtle Beach, Aug. 22–25, 1983, J. Roberts and W. Berry (eds.), National Association of Corrosion Engineers, 1984.
50. A. A. Stein and A. R. McIlree, "Relationship of Annealing Temperature and Microstructure to Primary Side Cracking of Alloy 600 Steam Generator Tubing and the Prediction of Stress Corrosion Cracking in Primary Water," pp. 47–51 in *Proc. of 2nd Int. Symp. Environmental Degradation of Materials in Nuclear Power Systems—Water Reactors,* Monterey, Sept. 9–12, 1985, J. Roberts and J. Weeks (eds.), American Nuclear Society, 1986.
51. M. Akashi, "Effects of Cr and Nb Contents on the Susceptibility of Alloy 600 Type Ni-base Alloys to Stress Corrosion Cracking in a Simulated BWR Environment," *Corrosion/95,* Orlando, FL, March 1995, National Association of Corrosion Engineers.
52. D. Sandusky, T. Okada, and T. Saito, "Advanced Boiling Water Reactor Materials Technology," *Materials Performance* **29**(1), 66–71 (1990).

4. POTENTIAL VULNERABILITIES OF ALLOY 690 AND ALLOY 152/52 WELD METALS IN PRESSURIZED WATER REACTORS

Steve Bruemmer
Pacific Northwest National Laboratory, Richland, Washington

4.1 INTRODUCTION

Wrought Alloy 690 and its associated weld metals (Alloys 152, 52, 52M, and other variants) have become the common replacement and repair materials for Alloy 600 and Alloy 182/82 weld metals with lower chromium content in PWRs, primarily due to their superior resistance to primary side SCC. Although SCC susceptibility of Alloy 600 in hydrogenated water at high-temperature was identified by laboratory testing in 1959, its significance on PWR components performance was not fully recognized until the 1980s, when cracking of Alloy 600 tubing prompted the need to replace or retire steam generators. In addition to primary-side and secondary-side steam generator tubing degradation, cracking of other Alloy 600 PWR components has been documented, including pressurizer heater sleeves and welds, pressurizer instrument nozzles, reactor vessel closure head nozzles and welds, reactor vessel outlet nozzle welds, and reactor vessel head instrumentation nozzle and welds. Pressurizer nozzles operating at the highest temperature were the first thick-section Alloy 600 component identified to crack in service and were typically replaced with austenitic stainless steels. More serious concerns emerged when through-wall SCC was found in control rod drive mechanism (CRDM) nozzles in the upper head of the PWR pressure vessels. Following the practice for steam generator tubing, Alloy 690 was selected as the replacement material for the nozzles; Alloys 152, 52, and 52M were used as associated welds.

This chapter is different from others in the compendium of LWR materials issues because Alloy 690 and its weld metals have not experienced significant degradation in service. On the contrary, successful performance of these alloys in PWRs has been noticed for about two decades as effective replacement materials for Alloys 600, 182, and 82 in PWRs. In addition, the high-Cr weld metals have also been used extensively and without incident as a corrosion-resistant overlay for component repair. In general, potential degradation modes of concern for Alloy 690 are similar to Alloy 600, including SCC, corrosion fatigue, and environment-induced fracture at high and low temperatures. The high-Cr weld metals encounter similar issues along with a susceptibility to ductility dip and hot cracking during welding plus significant dilution effects for dissimilar metal welds. Vulnerabilities to corrosion and cracking have only been identified in laboratory experiments, and typically during testing in off-normal material conditions and/or in severe environments. Many of these observations will be summarized here with a focus on SCC in PWR primary water environment along with a discussion of technical issues where the available knowledge is insufficient to properly confirm the extent of degradation resistance for Alloy 690 and its weld metals at this time.

4.2 COMPOSITION, PROPERTIES, AND METALLURGY OF ALLOY 690 AND ITS WELD METALS

4.2.1 Alloy 690 Material Specifications

Inco Alloys International originally developed Alloy 690 under the trade name Inconel Alloy 690; it is now owned by Special Metals Corporation [1]. Although this alloy is listed under the Unified Numbering System (UNS) designation in American Society for Testing and Materials (ASTM) and in American Society of Mechanical Engineers (ASME) standards, it is generically referred to as Alloy 690 in the nuclear power industry, as is Alloy 600. The most commonly used product forms in the *ASME Boiler and Pressure Vessel Code* for wrought Alloy 690 materials are seamless pipe, tubing, rod, bar, wire, plate, sheet, and strip. Because Alloy 690 was developed to replace Alloy 600 for light water nuclear power reactors, both are listed in the same ASME Code material specification.

The ASME Code chemical composition requirements (given in weight percent) for Alloy 690 are: 58.0 Ni (min), 27.0–31.0 Cr, 7.0–11.0 Fe, 0.05 C (max), 0.5 Mn (max), 0.5 Si (max), 0.015 S (max), and 0.5 Nb+Ta (max). However, more conservative requirements on chemical composition, processing, mechanical properties, and heat treatment are imposed on Alloy 690 by utilities and vendors for PWR applications. For example, the Electric Power Research Institute (EPRI) guidelines [2] require the carbon content to be between 0.015 and 0.025 wt % for Alloy 690 steam generator tubing in an attempt to optimize the distribution of carbide precipitates in the final microstructure. Slightly different carbon concentration ranges have been identified for thick-wall PWR components [3] with 0.015–0.035 wt % for Alloy 690 RPV head penetrations, whereas 0.01–0.04 wt % has been routinely specified for bars, plates, and heavy section tubing.

The most critical difference between Alloy 690 and Alloy 600 chemical requirements is for Cr; Alloy 600 requires a much lower concentration, 14–17 wt %. This change in Cr level in Alloy 690 is compensated for by a decrease in the Ni concentration. All other elements are similar in the basic ASME specification, although Fe is slightly higher and Mn and Si are slightly lower in Alloy 690 than in Alloy 600. Minimum ASTM specifications [4] for Alloy 690 mechanical properties at room temperature are yield strength, 205 MPa; tensile strength, 586 MPa; and total elongation, 35%.

4.2.2 Key Aspects of Alloy 690 Metallurgy and Microstructure

Alloy 690 is fully austenitic up to its melting temperature, which ranges from 1,343 °C (2,449 °F) to 1,377 °C (2,511 °F). The predominant second phase is a Cr-rich carbide that precipitates both at grain boundaries and in the matrix, depending on final processing and heat treatment. The type of Cr carbide that forms in Alloy 690 is $Cr_{23}C_6$, while Cr_7C_3 and $Cr_{23}C_6$ are common in Alloy 600. Grain boundary carbide precipitates typically form as discrete particles during cooling from the mill-anneal (MA) temperature or during thermal treatment (TT) from the solution-anneal (SA) temperature. The much higher Cr concentration in Alloy 690 promotes carbide nucleation at higher temperatures and during more rapid cooling rates than Alloy 600 [5, 6]. Carbide precipitate distributions can be quite variable in MA materials but should be semi-continuous to continuous along grain boundaries in an alloy given a proper SA and TT, as illustrated in Figure 4.1. Significant Cr depletion develops during the growth of intergranular (IG) Cr carbides, but minimum Cr concentrations in Alloy 690 tend to be 20 wt % or greater for TT temperatures and treatment durations [7–13]. Several corrosion studies have been performed documenting the

excellent resistance of Alloy 690 to IG corrosion (due to sensitization) after heat treatments consistent with the TT condition.

Discontinuous, cellular precipitation of $Cr_{23}C_6$ also occurs in Alloy 690 due to grain boundary migration [9] (example shown in Figure 4.1b) and can produce local regions of more extensive Cr depletion. This has been identified in several Alloy 690TT extruded tubing heats produced for PWR upper head penetrations [12, 13], but it does not influence the minimum Cr level adjacent to the carbide.

Titanium nitride (TiN) and Ti carbo-nitrides are typically minor phases in Alloy 690, but their shape, size, and distribution can be highly variable, depending on processing history and heat chemistry. Certain Alloy 690 plate heats have exhibited large TiN particles in the matrix, often associated with compositional banding. Isolated, small TiN precipitates have also been discovered at grain boundaries [12] in both plate and extruded tubing heats. They are smaller and well spaced in comparison to Cr carbides formed during thermal treatment. Interestingly, these small IG TiN particles remained after solution annealing at 1,100 °C (2,012 °F) followed by water quenching while $Cr_{23}C_6$ precipitates were removed [12, 13].

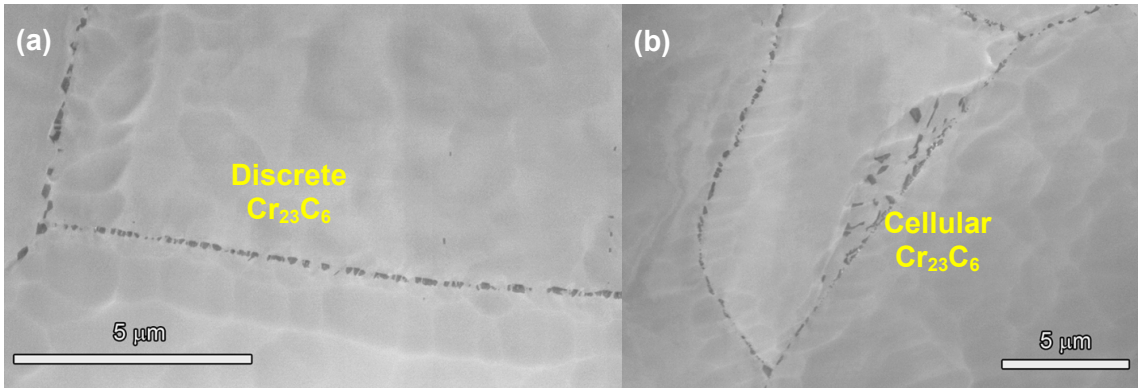

Figure 4.1. Scanning electron micrographs illustrating semi continuous Cr carbide precipitation in a thermally treated Alloy 690: (a) distribution of discrete IG $Cr_{23}C_6$ carbides and (b) distribution of discrete carbides along with a local region of boundary migration and cellular carbide growth [9]. Reprinted with permission of The Minerals, Metals & Materials Society.

Compositional banding can occur in this high Cr alloy [14] and can produce large variations in grain size and precipitate distributions. Banding can be present in the billet and can persist through very extensive processing steps (e.g., the steps required to produce plate and tubing products). Melting practice, homogenization, and critical strain during early working will affect the extent of banding. As a result, bands of fine grains with high densities of carbides and nitrides can exist within the microstructure along with areas of extremely large grains with few second phases. An example of this microstructural inhomogeneity in an Alloy 690 plate material is given in Figure 4.2.

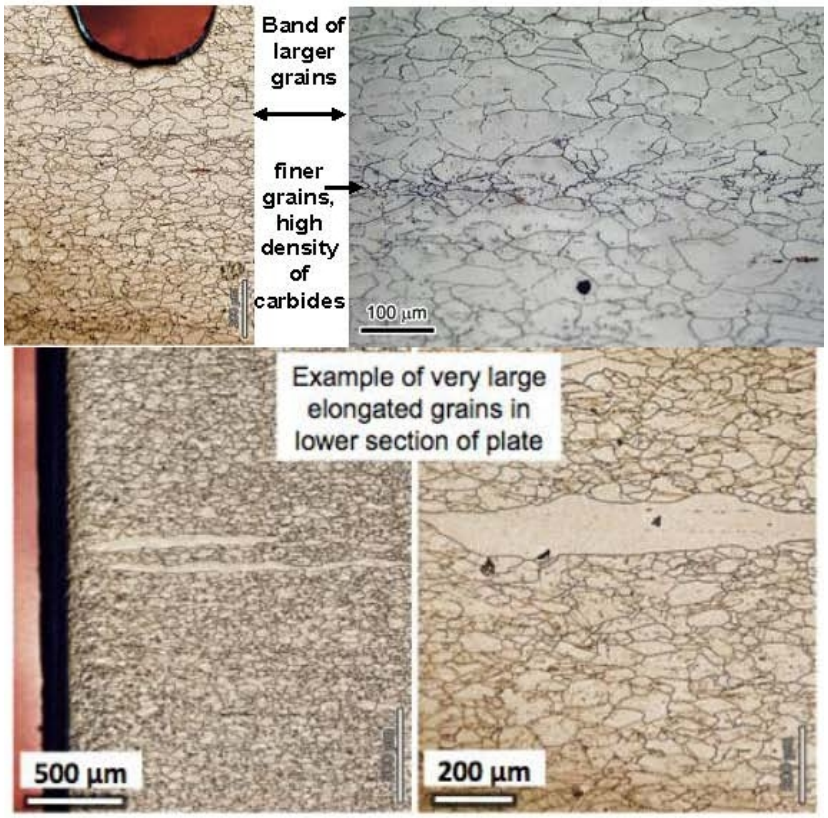

Figure 4.2. Optical micrographs illustrating microstructural variations due to compositional banding in an Alloy 690 plate material [14].

Carbide and nitride precipitation distributions have been found to play an important role in the evolution of deformation microstructures in Alloy 690 during cold work. High-resolution scanning and transmission electron microscopy (TEM) characterizations of heavily deformed Alloy 690 materials [12, 15, 16] have revealed small IG voids and cracked precipitates (primarily carbides) at grain boundaries as well as cracked particles (primarily larger nitrides) in the matrix. So far, extensive permanent (sub-micron size) damage of this type has only been documented in tubing and plate heats unidirectionally cold rolled (CR) to reductions greater than ~20%. Comparisons among cold-rolled materials indicate that void formation and precipitate cracking at grain boundaries directly depend on the starting distribution of IG precipitates. As noted earlier, the predominant precipitate formed is $Cr_{23}C_6$ with semi-continuous carbide distributions commonly found in Alloy 690TT materials and in Alloy 690MA materials. An example of the permanent damage that forms during CR is presented in Figure 4.3 for a 26% cold-rolled Alloy 690MA plate. A regular distribution of cracked carbides and voids along grain boundaries can be seen in Figures 4.3(b–d). The typical permanent damage spacing on many boundaries was on the order of 1 µm. Larger TiN particles in the matrix, often present in clusters extending for >50 µm, were also extensively cracked [Figure 4.3(e)]. This plate also exhibited compositional banding where an even higher density of cracked IG carbides and IG/matrix nitrides was indicated. Very limited research has been done to assess the threshold level of deformation that promotes this permanent damage, nor has work been done to investigate heat-to-heat and the starting microstructure effects.

This high level of cold work represents an extreme condition that is not representative of any Alloy 690 in reactor operation. However, such studies identify the need to better quantify

microstructures resulting from variations in processing and component fabrication procedures, including welding, straightening, and surface grinding. This research should be performed in tandem with the improved understanding of Alloy 690 processing and fabrication practices [17]. Key areas of study include: the mapping of precipitation, deformation structures, and damage in Alloy 690 weldments. Weld metal, fusion line, and heat affected zone (HAZ) regions exposed to complex temperature and strain cycles need to be better characterized. These regions develop low-to-moderate tensile strains from warm/cold work [18], and comparisons need to be made to the cold-work damage in Alloy 690 base metal described above. Electron backscatter diffraction (EBSD) has shown great promise in documenting general and local plastic strain distributions [19]. The degree of plastic strain can be indicated through characterization of local grain misorientations, and comparisons can be made among different materials, deformation levels, and microstructural regions such as a banded region or the HAZ. Although limited, EBSD has been applied effectively to assess the influence of thermomechanical treatments on microstructures of Alloy 690 materials and welds and SCC [12, 18, 20].

Another second phase in Alloy 690 worth identifying is the ordered intermetallic Ni_2Cr. It was hypothesized that formation of this phase is possible during extended reactor operation. The possibility that Ni_2Cr could form raised concerns that it might produce significant matrix hardening and embrittlement. Several extensive studies [21–24] have been conducted with the general conclusion that long-range ordering and Ni_2Cr formation can occur in a Ni-30%Cr alloy, but a minimum of 7 wt % Fe is sufficient to inhibit formation of this NiCr phase in Alloy 690. However, the EPRI guidelines for steam generator tubing [2] and pressure vessel nozzles [3] require a higher minimum content of 9 wt % Fe for a greater safety margin. Additional research on long-range ordering in Alloy 690 is still needed to verify and confirm that Ni_2Cr will not form during extended reactor operation (60–80 years), with potential adverse effects on reactor component performance.

There are other aspects of Alloy 690 microstructure and metallurgy, but these are not believed to be needed to underpin the key issues for the long-term degradation resistance in LWR service and so are not reviewed here. More detailed background information on Alloy 690 is given in reviews in EPRI Materials Reliability Program documents [25, 26].

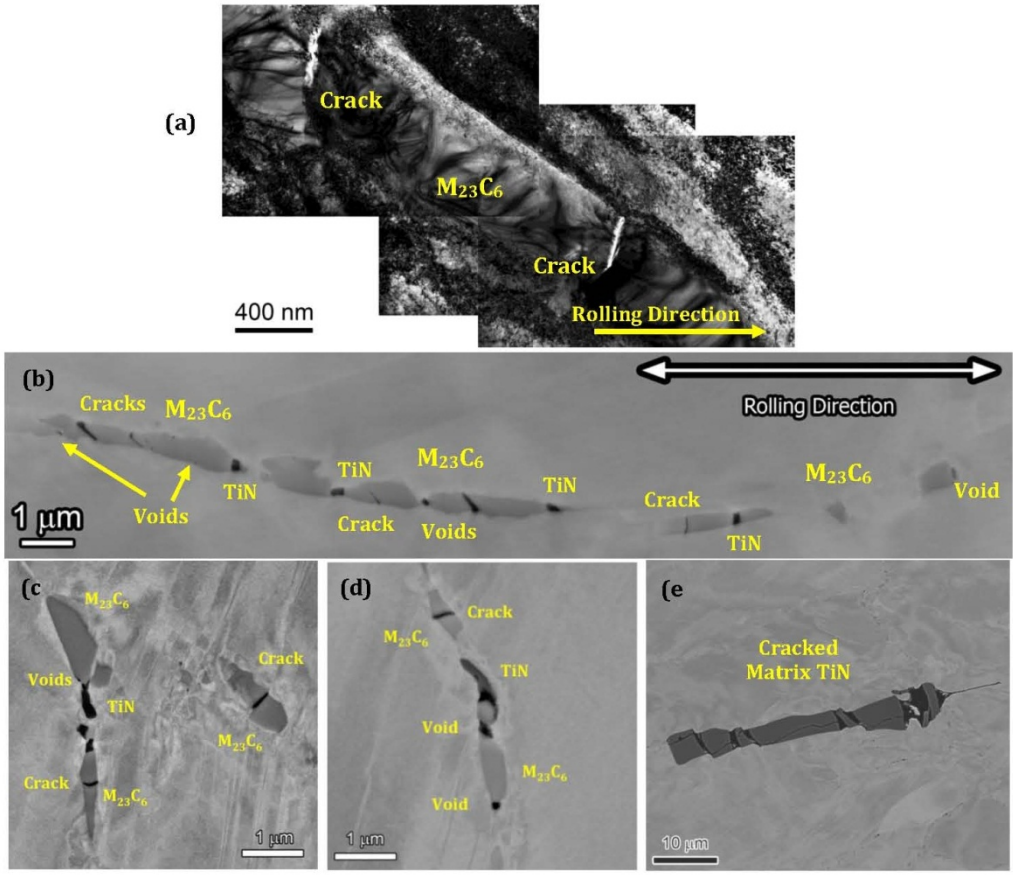

Figure 4.3. Transmission electron brightfield micrograph (a) showing a cracked IG carbide and high strain contrast in the adjacent matrix along with scanning electron micrographs illustrating grain boundary damage (voids and cracks) associated with carbide precipitates (b, c, and d) in a 26% CR Alloy 690 plate material. Cracking of larger matrix TiN particles (e) was also common in this plate material [12, 15, 16].
Reprinted with permission of The Minerals, Metals & Materials Society.

4.2.3 Material Specifications, Metallurgy, and Microstructure for Alloy 690 Weld Metals

The replacement of Alloy 600 with Alloy 690 prompted a change in welding products from Alloy 182 and 82 to higher chromium versions, Alloy 152 (shielded metal arc welding electrode) and Alloy 52 (gas tungsten and gas-metal welding filler metal). Based on specification sheets from Special Metals Corporation [27], several compositional differences can be seen among the three primary weld filler metals. Chemical composition requirements (weight percentages) for Alloy 152 are 28.0–31.5 Cr, 7.0–12.0 Fe, 0.05 C (max), 5.0 Mn (max), 0.50 Si (max), 0.015 S (max), 0.50 Mo (max), 0.50 Cu (max), 0.50 Ti (max), 0.50 Al (max), 0.03 P (max), and 1.0–2.5 Nb+Ta. Slightly different composition requirements (weight percentages) were established for Alloy 52: 28.0–31.5 Cr, 7.0–11.0 Fe, 0.04 C (max), 1.0 Mn (max), 0.75 Si (max), 0.015 S (max), 0.50 Mo (max), 0.30 Cu (max), 1.0 Ti (max), 1.10 Al (max), 1.5 Al+Ti (max), 0.02 P (max), and 0.1 Nb+Ta. Somewhat later, a modified Alloy 52 weld metal was developed and was identified as Alloy 52M. The overall composition is very similar to Alloy 52 except for the addition of B and Zr to improve

resistance to ductility dip cracking and to reduce inclusions. The Alloy 52M composition requirements (weight percentages) are 28.0–31.5 Cr, 7.0–11.0 Fe, 0.04 C (max), 1.0 Mn (max), 0.50 Si (max), 0.015 S (max), 0.50 Mo (max), 0.30 Cu (max), 1.0 Ti (max), 1.10 Al (max), 0.02 P (max), 0.5–1.0 Nb, 0.02 Zr (max), and 0.005 B (max). It is interesting that only maximum and no minimum concentrations are identified for the key additions of B and Zr. In addition, a few other differences in composition requirements can be identified for Ti, Al, and Nb.

Much less metallurgical and microstructural detail is available for the various Alloy 690 weld metals. Additional characterization is needed to better understand variability among the different weld metals and among welding practices. An important concern for welding of these high chromium, nickel alloys has been the formation of weld cracks [27–38].

Plant experience has shown that Alloys 152, 52, and 52M can be difficult to weld and are susceptible to weld cracking. Welding problems and cracking that occurred during manufacture and repair of PWR components have prompted considerable effort to develop specialized welding equipment and to optimize welding process parameters along with minor modifications to the base weld metal composition. Overall, these changes have significantly improved weldability of these high chromium nickel alloys; however, technical issues remain with the formation of weld defects, particularly with respect to ductility dip cracking in Alloy 52 and 52M welds.

Examples of ductility dip cracks discovered in an Alloy 52 mockup weld [29] are shown in Figure 4.4. The EBSD image enables a better visual image of the individual weld metal grains and highlights areas of plastic deformation. The typical large, elongated grains can be seen along with a collection of very fine grains along certain grain boundaries. The fine grains associated with the IG cracks suggest that local recrystallization may play some role in the cracking process. High strains depicted by large changes in crystal orientation within a grain are found at many of the high-angle grain boundaries and within the interior of many of the grains. Other regions examined also showed a mixture of large, elongated grains and local regions of very fine, recrystallized grains. As expected, high strains were found associated with cracks and grain boundaries in this entire region. Although some fundamental research has been performed [32–34, 38], there is no agreement on the root cause for cracking in these complex weld metals.

The microstructures and microchemistries developed within Alloy 152/52/52M welds that are representative of PWR plant components can be quite variable across the weld, and certainly at interfaces with base metals such as Alloy 690, low alloy steel, and stainless steel. In the weld metal, large, elongated grains containing a cellular dendritic solidification substructure are present along with areas of finer grains, often at weld pass boundaries and near the weld metal to base metal fusion lines. An example of the microstructural distribution across an Alloy 152 weld is presented in Figure 4.5. The orientation and size of the Alloy 152 grains can be seen to change as the fusion line with the Alloy 690 base metal is approached. Some degree of macro-segregation of Nb and Mn is typically seen [12, 29, 35–37 with the Nb-rich carbides forming at interdendritic sites. High-energy grain boundaries do not appear to exhibit strong segregation but often have a distribution of Nb (Ti) and Cr-rich $M_{23}C_6$ carbides. In many areas, the small Nb-rich carbides appear to locally pin the grain boundaries and promote a wavy morphology that has been suggested to improve resistance to the initiation of weld cracks [32–34]. The EBSD examinations have indicated that plastic strain is associated with high-energy grain boundaries and with some low-energy interdendritic boundaries; however much higher strains can be present at weld pass boundaries and near dissimilar metal interfaces [12, 18, 20, 35–37]. Recent work by Morra [20] has indicated the presence of relatively high strain in the weld metal transition region (partially melted and unmixed zones) adjacent to the fusion line with the

base metal. In nearly all cases, additional characterization and analyses are needed to better understand microstructures and microchemistries throughout those welds and to relate the analyses to degradation susceptibility.

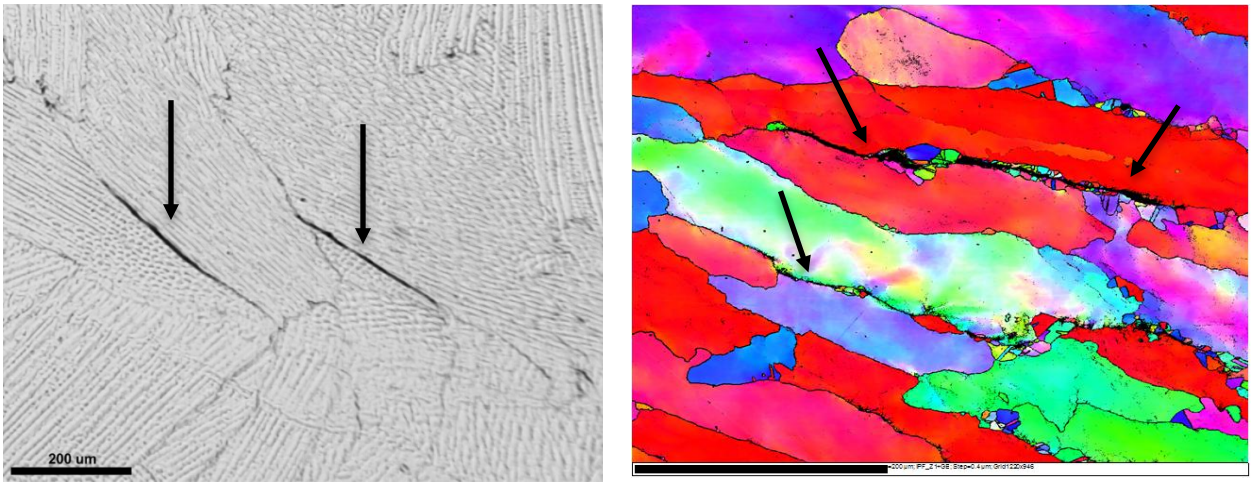

Figure 4.4. SEM (a) and EBSD inverse pole (b). Images showing ductility dip microcracks (locations are indicated by arrows) in an Alloy 52 mockup weld [29]. Fine grains can be seen associated with the cracks in the EBSD image.

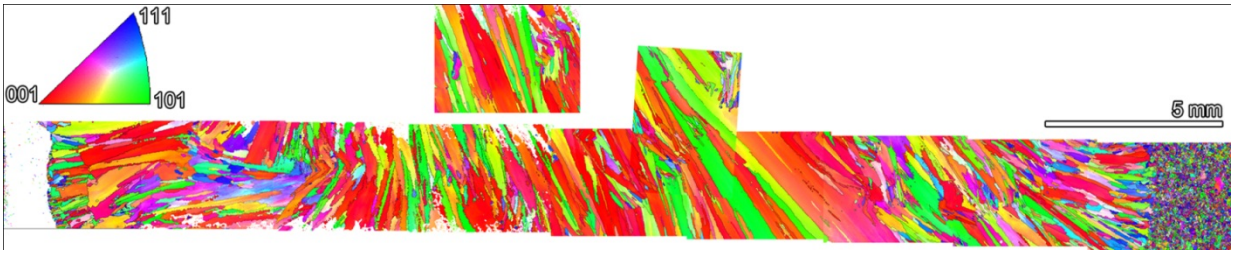

Figure 4.5. Montage of EBSD inverse pole. Images illustrate the grain microstructure changes across an Alloy 152 weld. The transition from Alloy 152 weld metal to Alloy 690 base metal is on the far right of the montage.

4.3 CORROSION, STRESS CORROSION, AND CORROSION FATIGUE OF ALLOY 690 AND ITS WELD METALS IN PWR PRIMARY WATER

4.3.1 Service Experience

The primary applications of Alloy 690 in PWRs have been as thin-wall (steam generators) or thick-wall (reactor pressure vessel head penetrations) tubing components to replace Alloy 600. PWR steam generator tubing is exposed to a challenging environment, including high temperatures, high stresses/strains, and a primary water environment that produced extensive IGSCC in Alloy 600 materials. The large number of tubes in each steam generator provides many different conditions to exist and/or develop promoting SCC initiation and growth.

Eighty-nine steam generators manufactured with Alloy 690TT tubing material were in international service as of 2008 with no reported primary-water SCC indications [26]. This excellent performance has now continued for more than 20 years in a few generators and for more than 15 years in approximately 40 generators. Although important improvements have been made to steam generator design and fabrication, service experience for Alloy 690 steam generator tubing confirms the considerable SCC resistance in PWR primary water.

The second major PWR component where SCC of Alloy 600 prompted replacement by Alloy 690 was for reactor pressure vessel head penetrations. The initial observation of primary water SCC was in the early 1990s and led to the replacement of 33 vessel heads in France by 2000 and nearly 30 vessel heads in the United States by 2008 [26]. Consistent with steam generator tube experience, no cracking has been identified for the Alloy 690 penetration nozzles or associated Alloy 152/52 welds after more than a decade of service. Alloy 690 has also been used in several other Alloy 600 component replacements in U.S. plants (e.g., pressurizer heater sleeve) without reported service failures.

4.3.2 Corrosion and Surface Oxidation Issues

Alloy 690 exhibits excellent resistance to both general and IG corrosion in PWR primary water environments. Many investigators have examined oxide film formation on Alloy 690 over the last decade and have compared it to that for Alloy 600. High-resolution characterizations have been limited [39–41] but suggest the formation of a continuous, high-Cr content protective film. The most comprehensive analysis on Alloy 690 has been conducted by Combrade and co-workers [39]. They concluded surface oxidation in PWR primary water occurs by this kinetic sequence:

1. selective oxidation of Cr and rapid initial growth of a thin Cr_2O_3 oxide layer,
2. restricted oxide growth due to near-surface Cr depletion allowing Ni and Fe transport through the film,
3. resumption of Cr-rich oxide growth with logarithmic kinetics, and
4. development of the bilayer oxide with Ni/Fe spinels forming on top of the Cr_2O_3 inner oxide layer.

Quite different corrosion/oxidation structures have recently been discovered [42] to form at both Alloy 690 crack surfaces and on polished surfaces during exposure to 360 °C (680 °F) PWR primary water. Nanoscale localized oxidation occurs from the surface and appears to follow dislocation substructures into the alloy matrix. Penetrative oxidation starts as shallow, well-spaced, small diameter (<5 nm), filaments after short exposure time and evolves to dense filaments that consume most of the remaining metallic matrix to a depth of several hundred nanometers. The oxide filaments have been characterized at near-atomic resolution by TEM and atom probe tomography to reveal a core structure of small chromia platelets surrounded by a nanocrystalline MO-structure oxide.

Alloy 690 grain boundaries intersecting the surface show no sign of localized oxidation; degradation appears to be limited to the dislocation structures [42]. Moreover, significant depletion of Cr is observed at grain boundaries to several micrometers below the surface along with evidence of boundary migration during the exposure to PWR primary water. A detailed understanding of surface oxidation processes and the stability of corrosion layer is expected to enable informed assessment of the long-term stability of the protective oxide film and the resistance of Alloy 690 to localized corrosion, SCC initiation, and SCC growth. This includes

corrosion and oxidation reactions with, and degradation of, the preexisting dislocation structures (due to both bulk deformation and surface preparation) and grain boundaries.

4.3.3 Stress Corrosion Crack Initiation

Laboratory SCC initiation testing for Alloy 690 has primarily focused on thin-wall tubing, typically reverse U-bend, double U-bend, constant load tensile, four-point bend, and steam generator tubing mock-up specimens. Investigations have been performed under a variety of environmental conditions described as simulated PWR primary water (often outside the normal operational range for temperature, Li, B, and dissolved hydrogen) along with some tests in higher-temperature doped-steam. The basic result from nearly all early Alloy 690 testing was the lack of any observable SCC. As more severe loading conditions and environments were applied, a few investigators reported limited IG cracking. Those results have been reviewed in some detail [25, 26] and have been linked to off-normal testing conditions not relevant to PWR service. Initiation testing on thick-walled tubing materials in simulated PWR primary water has been limited. The exception has been research [43] on Alloy 690 nozzle heats using uniaxial tensile specimens under constant, active load in primary water at 360 °C (680 °F) for duration approaching 10 years. The most recent report has indicated no cracking; however, results of high-resolution ex situ characterizations of these specimens have not been published to confirm whether finer cracks might be present.

Stress corrosion crack initiation remains one of the most significant unknowns for potential failure time range prediction in LWR structural alloys, including highly resistant Alloy 690 materials. As discussed in the previous section, surface corrosion/oxidation in PWR primary water is another key aspect but many other materials variables must be considered. It is pertinent to evaluate the influence of microstructure damage due to cold work or surface grinding on SCC nucleation. Carefully planned and conducted crack initiation tests on the same Alloy 690 heats and under conditions where SCC susceptibility has been seen in crack growth tests (described in the following section) may be of considerable value. Such tests have recently been started at General Electric Global Research [44] using blunt-notch specimens and at Pacific Northwest National Laboratory [45] using uniaxial tensile specimens under active constant load.

4.3.4 Stress Corrosion Crack Growth in Alloy 690

The early belief that Alloy 690 was essentially immune to SCC in representative PWR primary water was dispelled by crack-growth testing results [46] on cold-worked material about 10 years ago. The measured growth rates were quite low, but they identified the need for evaluations of heat-to-heat differences and the influence of thermo-mechanical processing. Quite a different concern was created when investigators at Bettis released data [47, 48] showing extremely high SCC growth rates in pertinent hydrogenated water environments on both cold-rolled and tensile-strained Alloy 690 plate materials when tested in the S-L or S-T orientation. For reference, the S-L orientation (or rolling direction) is parallel to the cold-rolling direction, while the S-T orientation (or transverse direction) is perpendicular to the cold-rolling direction. This information prompted considerable expansion of crack-growth testing on Alloy 690 and has led to an improved understanding of the influence of cold work.

Improvements in laboratory crack-growth testing and in-situ crack length detection have enabled remarkably low SCC rates to be measured in as-received, non-cold-worked Alloy 690. The approach for such tests is illustrated in Figure 4.6 for two extruded Alloy 690TT materials representative of CRDM tubing. Multiple evaluations of SCC response are made after a series of

transitioning steps resulting in long test times of a year or more. Maximum crack-growth rates under constant stress intensity (K) conditions for these materials was ~9 × 10^{-10} mm/s (3.5 × 10^{-11} in./s). Overall, the number of tests and measured SCC propagation rates at constant K or load on non-cold-worked Alloy 690 remain limited. A recent summary of published results includes data from tests on Alloy 690 HAZ specimens (Figure 4.7). In general, most crack growth rates at constant K are below 10^{-9} mm/s (4 × 10^{-11} in./s) for as-received materials and range from ~10^{-9} to 10^{-8} mm/s (4× 10^{-10} to 4 x0 10^{-9} in./s) for the HAZ specimens.

Research at many different laboratories [47–58] has clearly demonstrated the influence of cold work on SCC susceptibility in Alloy 690. A systematic evaluation has been conducted investigating the effects of the percentage of CR, specimen orientation, heat treatment condition, and microstructure on the SCC response for a single CRDM Alloy 690TT tubing heat [52–54, 57]. Cold rolling to 17% and 31% reductions and testing in the S-L orientation produced a consistent increase in measured SCC propagation rate to 3 × 10^{-9} mm/s (1.1 × 10^{-10} in./s) (Figure 4.8) and 1 × 10^{-7} mm/s (4× 10^{-9} in./s) (Figure 4.9), respectively. This change, (Figure 4.10), documents a 500× increase in the measured crack growth rate compared to non-cold-rolled material. Cold rolling promotes IGSCC with morphology of cracking completely IG for the 31% specimen, but only partial IG engagement is seen for the 17% specimen.

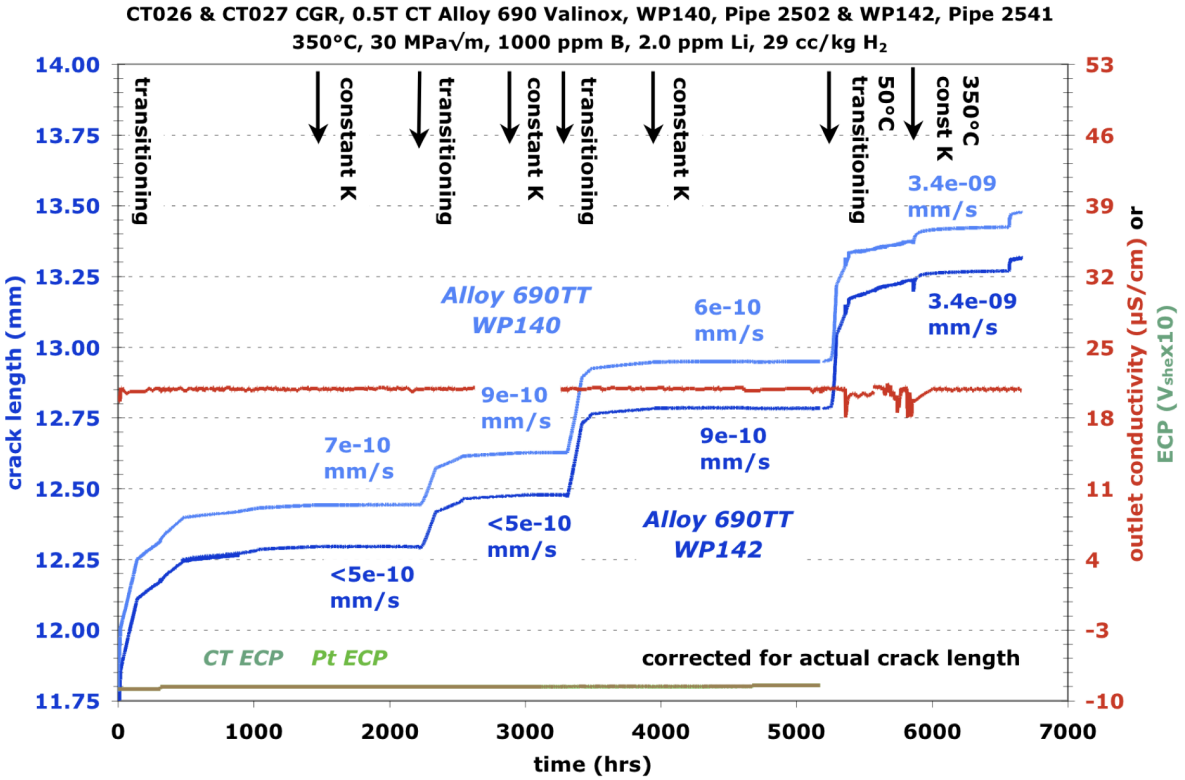

Figure 4.6. Overview of crack-growth test for two as-received Alloy 690TT materials in simulated PWR primary water at 350 °C (662 °F).

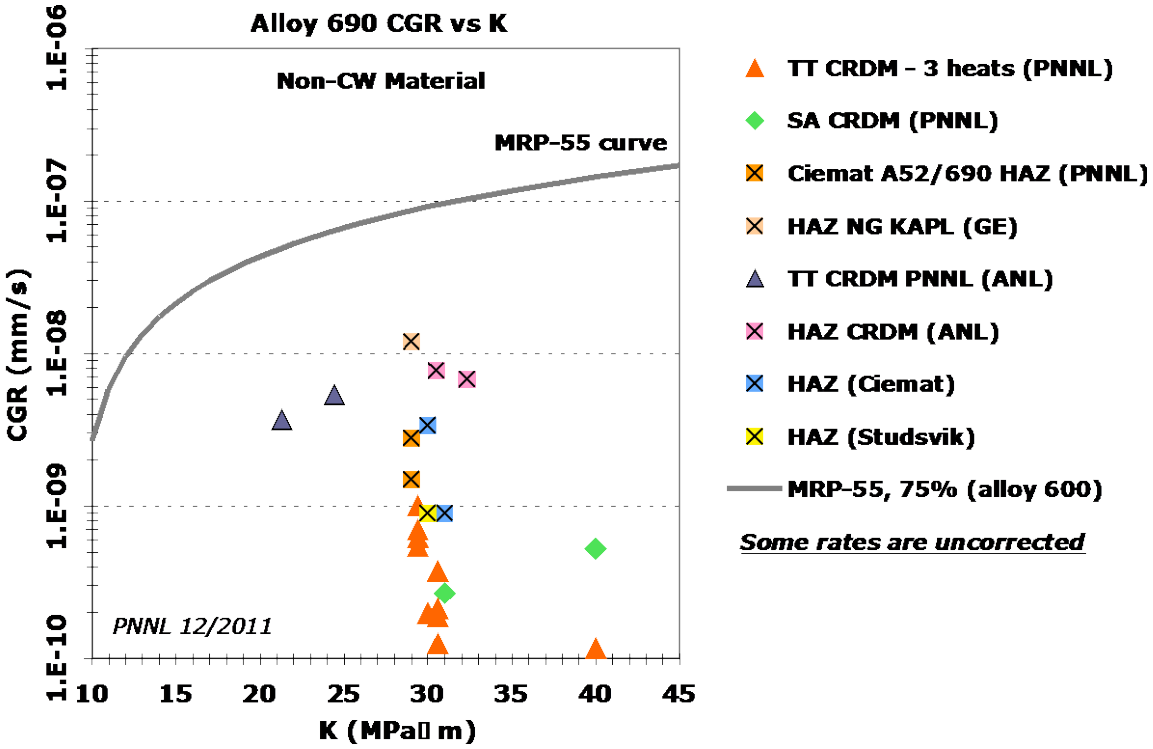

Figure 4.7. Summary of crack-growth test for as-received Alloy 690TT CRDM materials and Alloy 690 HAZ specimens in simulated PWR primary water.

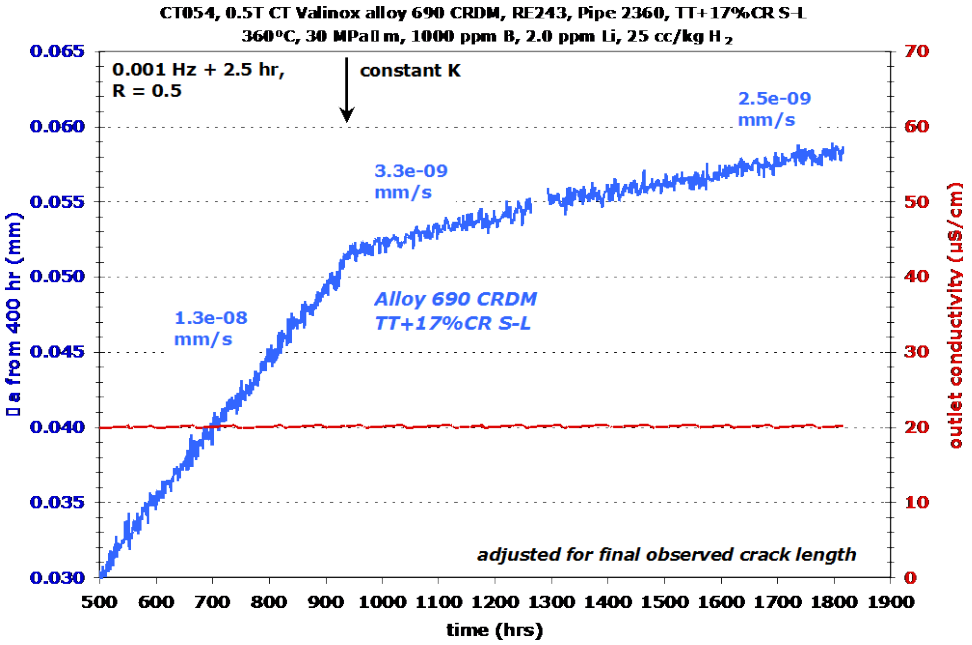

Figure 4.8. Crack growth response at 360 °C (680 °F) during cycle + hold and constant K of TT+17% CR S-L Alloy 690 CRDM.

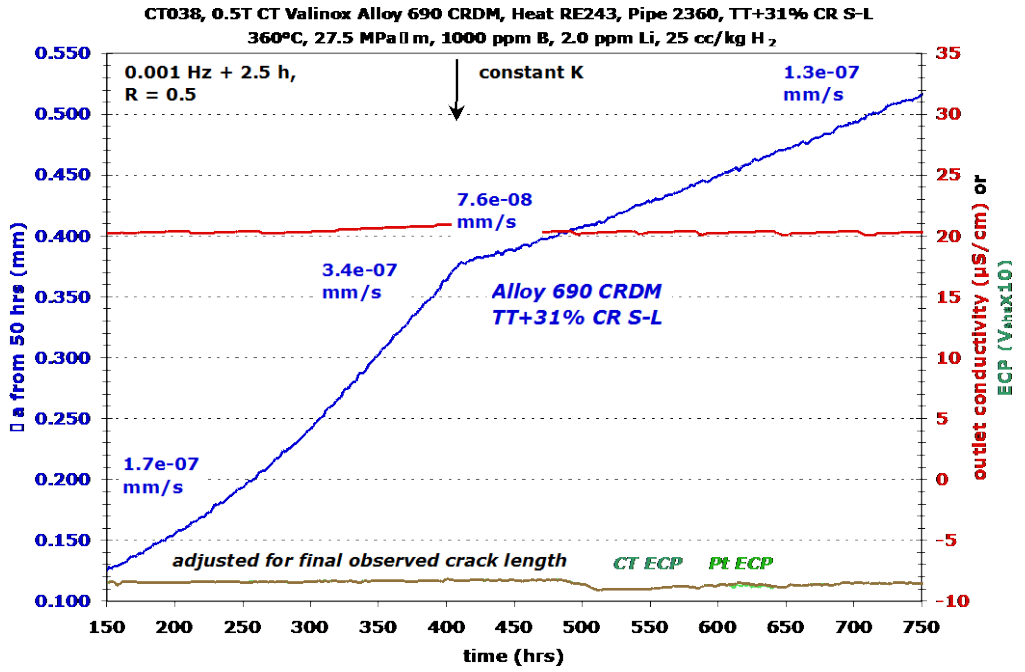

Figure 4.9. Crack growth response during cycle + hold and constant K of TT+31% CR S-L Alloy 690 CRDM.

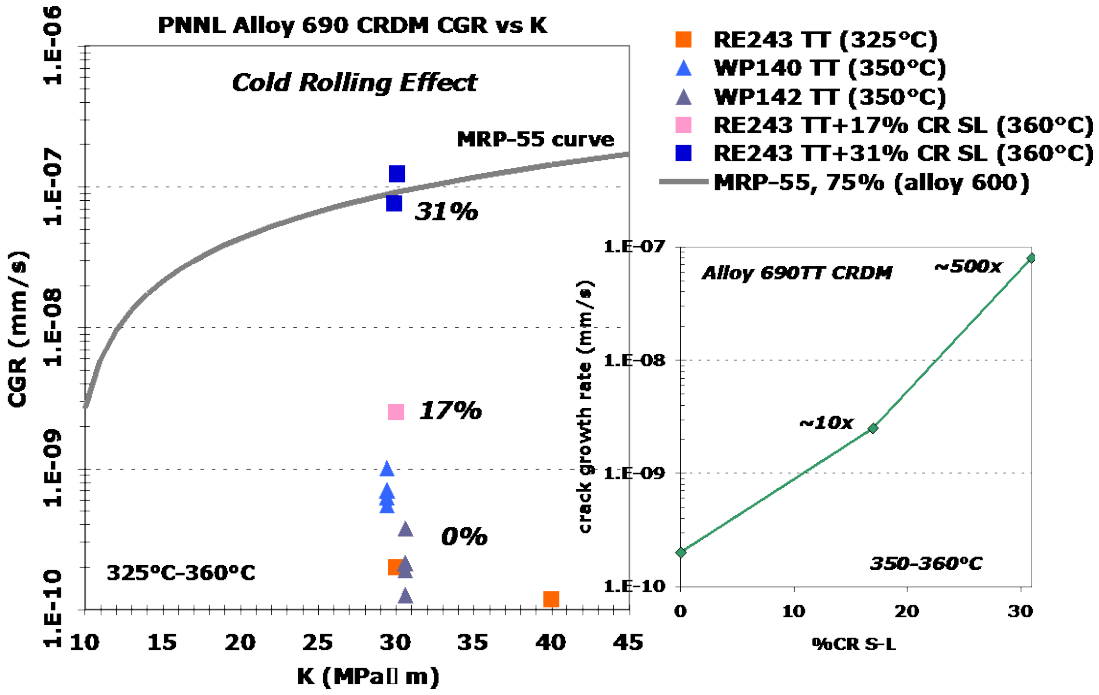

Figure 4.10. Crack growth response as a function of K level for the TT specimens and plotted as a function of the percentage of CR and testing in S-L orientation.

The most extensive crack-growth testing on cold-worked Alloy 690 materials has been performed at General Electric Global Research [49, 50, 55, 58] examining a wide range of tubing and plate heats in the cold-rolled and cold-forged condition. This research has substantiated that the primary factors controlling IGSCC susceptibility in PWR primary water are the degree and

nature of cold work along with the microstructural homogeneity of the alloy. In particular, extremely high SCC propagation rates (up to 10^{-6} mm/s, similar to those observed at Bettis Laboratory) were observed in a heavily banded Alloy 690 plate heat after significant cold work by rolling or forging. A summary of all Alloy 690 experimental data reported as of August 2011 is given in Figure 4.11 and illustrates a continuum of response from limited if any SCC growth at low levels of cold work to propagation rates more than a 1,000× higher in certain cold-worked heats.

A few recent tests have revealed very high crack growth rates. However, the earlier results from Bettis Laboratory investigation [47, 48] found these rates at lower levels of K and percentage of CR. In addition, they also measured high SCC propagation rates in tensile-strained Alloy 690 that is more relevant to a possible service condition (e.g., the Alloy 690 weld HAZ). Although it seems likely that a banded microstructure can be detrimental and increase SCC susceptibility, one of the Bettis Alloy 690 heats showing high growth rates was reported to have a homogeneous, non-banded microstructure, and several highly banded and cold-forged Alloy 690 heats have shown only moderate crack growth rates [55]. A final observation of importance for this issue is that the materials showing *very high* crack growth rates that do not change (remain very high) as a function of test temperature or hydrogen concentration [47, 48, 55]. By comparison, materials exhibiting low-to-high *SCC rates* in crack growth tests do show growth rates that depend directly on both test temperature (similar to Alloy 600 activation energy) and hydrogen concentration (rates decrease at dissolved hydrogen levels below the Ni/NiO stability line) [54]. Additional research is needed to assess the reasons why certain cold-worked heats exhibit very high versus moderate-to-high SCC rates, including the influence of compositional banding on Alloy 690 SCC susceptibility.

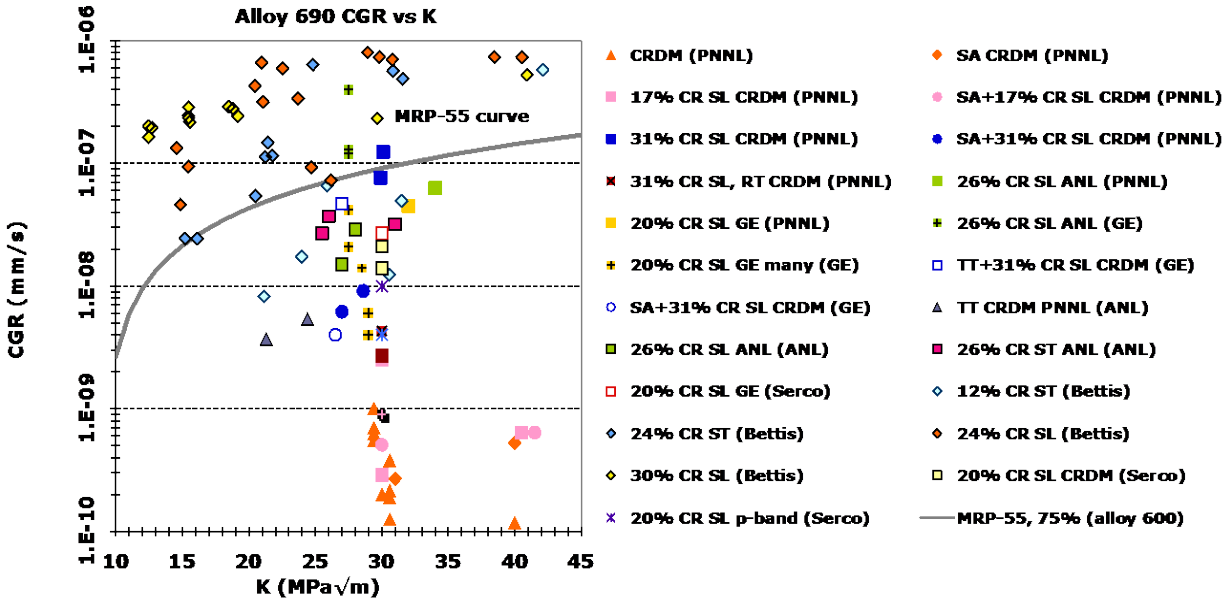

Figure 4.11. Summary of crack growth rate measurements [47–58] on Alloy 690 plate and tubing materials illustrating cold-rolling effects on SCC susceptibility.

The starting matrix and grain boundary microstructures will clearly influence the development of damage during cold working and IGSCC susceptibility. In order to evaluate the influence of IG carbides, the same Alloy 690TT tubing heat was solution annealed and water quenched to remove the semicontinuous $M_{23}C_6$ at grain boundaries. As discussed in the section on Alloy 690

metallurgy and microstructure, quite different IG permanent damage structures were observed between the TT and SA materials after CR. However, the average hardness and EBSD-measured average matrix strains (from misorientation) were nearly identical [49]. Crack-growth testing [54] revealed an order-of-magnitude lower SCC rate for the 30% to 31% cold-rolled SA materials than that measured for the TT materials. An example of this behavior is shown for the 30% cold-rolled materials tested in S-L orientation in Figure 4.12, while the SA and TT response for the different cold-rolled conditions are summarized in Figure 4.13. No influence of initial material condition is observed for the 0% and 17% cold-rolled materials, but a difference of ~10× is observed for the highly strained materials when tested in either the S-L or T-L orientations. This observation suggests that the TT condition may not be an optimal condition for Alloy 690 SCC resistance, at least in highly cold-worked materials. Additional research is needed to confirm SCC behavior as a function of heat treatment condition and to determine the role of grain boundary precipitates and their nature. One additional heat treatment condition was evaluated in this Alloy 690 CRDM tubing heat to modify the rolling-induced dislocation structure while leaving the permanent grain boundary damage (i.e., moderate density of IG voids and few cracked carbides). The 31% cold-rolled Alloy 690TT material was given a short duration (<5 hours) anneal at 700 ºC (1,292 ºF) that resulted in a 25× decrease in measured SCC propagation rate [53, 54].

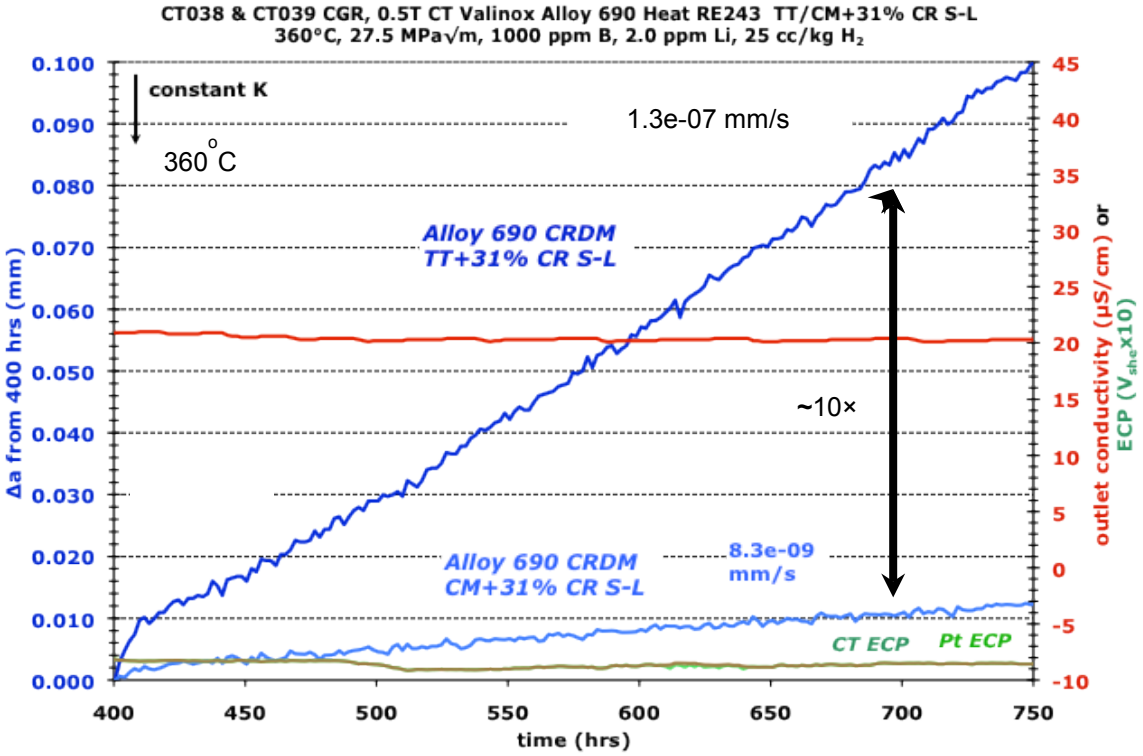

Figure 4.12. Crack growth response at constant K comparing the TT+31% CR S-L Alloy 690 CRDM to the SA+31% CR S-L Alloy 690 CRDM. These specimens were tested in series [54]. Reprinted with permission of The Minerals, Metals & Materials Society.

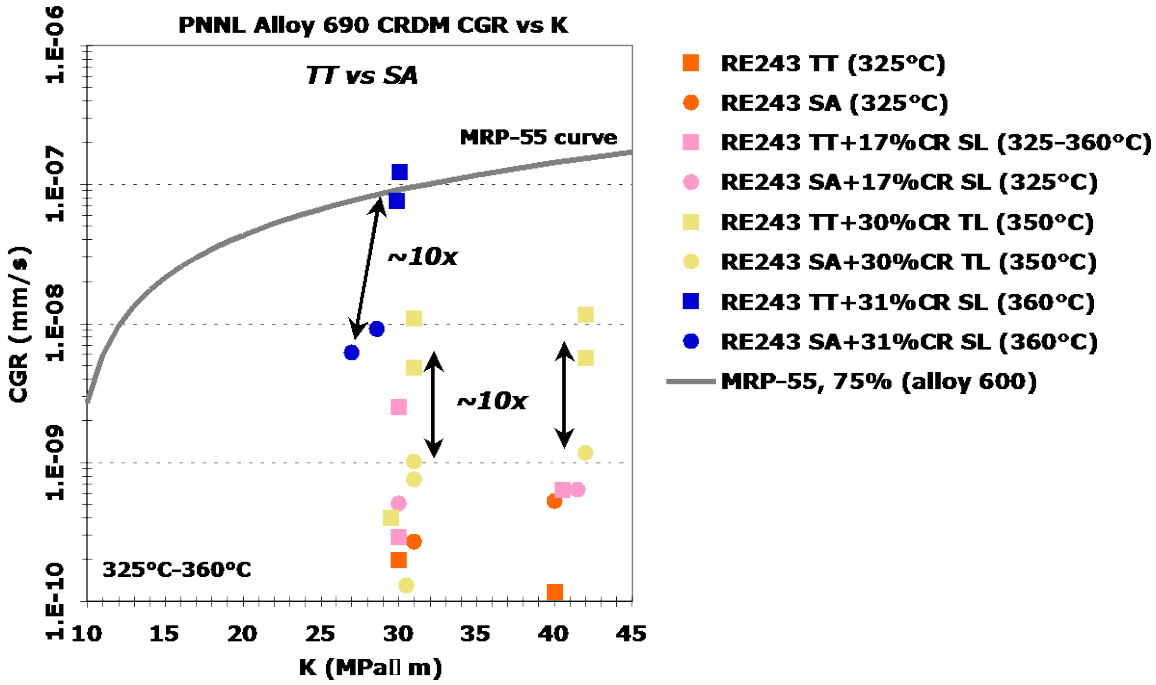

Figure 4.13. Crack growth rate of the thermally treated and solution annealed materials plotted as a function of stress intensity [54].
Reprinted with permission of The Minerals, Metals & Materials Society.

In order to provide insights on the influence of the rolling-induced permanent damage (grain boundary containing cracked carbides and voids) on IGSCC propagation, several high-resolution characterizations [53] have been performed on areas adjacent to cracks and crack tips produced in crack-growth test specimens. Several preliminary conclusions were made from the observations that are worth mentioning because of their implications on the mechanisms controlling SCC susceptibility in cold-worked Alloy 690 in PWR primary water environment. Scanning electron microscopy (SEM) observations indicated that the preexisting cracked carbides and voids at grain boundary did not accelerate environment-induced crack growth. The SCC path consistently follows the grain boundaries and did not "jump" between perpendicular cracks across carbides or between voids at carbide interfaces. The most significant observed interaction with the preexisting permanent damage is that many IGSCC cracks end at the cracked carbides. These crack-tip locations are often open and blunted as the SCC crack terminates at the crack across the carbide that is oriented perpendicular to the grain boundary propagation path. IG carbides clearly enhance localized grain boundary deformation during CR and produce permanent damage. Based on these limited observations and on the significant effect of the recovery anneal on the SCC crack growth response for the 31% cold-rolled Alloy 690TT material, it was suggested that localized grain boundary strains and stresses promote IGSCC susceptibility and not the cracked carbides and voids [53].

In addition to the crack examinations in the SEM, more detailed crack-tip characterizations were also performed on these same materials using TEM techniques [13, 53]. In general, the main observations were the presence of:

- loose crystallites of Ni/Fe-rich spinel in open cracks,
- fine polycrystalline Ni/Cr/Fe spinel and/or MO-structure oxide (not Cr rich) on the crack surfaces,

- penetrative oxidized filaments into the Alloy 690 matrix off crack surfaces, and
- very narrow (<10 nm) crack tips with oxide present.

No evidence for preferential grain boundary oxidation or enhanced void formation was found in regions beyond the open crack tips. Key differences for the Alloy 690 were identified versus prior examinations on Alloy 600 crack tips produced in PWR primary water [59–61] and on stainless steel tips produced in BWR or PWR environments [61–63]. No evidence for penetrative IG oxidation in the Alloy 690 samples has been found, while it is one of the defining crack-tip characteristics for Alloy 600. Grain boundaries do not appear to be an active path for oxidation in the 30% Cr Alloy 690 as they are in the 16% Cr Alloy 600 when exposed to PWR primary water environment. Surprisingly, penetrative oxidation was detected off the crack surfaces and into the matrix grains. Results indicate that the primary mechanism promoting IGSCC in PWR primary water for Alloy 690 is not a stress-assisted, grain boundary oxidation process as proposed for Alloy 600. Alloy 690 SCC cracks were open to their tips (similar to stainless steels) in both oxygenated and hydrogenated water, but a thin, protective, Cr-rich film is not found on the crack surfaces to the crack tips for Alloy 690. Therefore, preliminary observations are different from stainless steels that form Cr-rich spinel films to the tips consistent with a slip oxidation mechanism for SCC propagation. This brief description of the initial crack-tip characterizations illustrates the need for more detailed examinations on tailored materials to define important grain boundary microstructural/microchemical aspects and processes controlling IGSCC.

Even though SCC service failures have not been detected in Alloy 690 components, proactive confirmatory research is needed to understand underlying causes of IGSCC being seen in laboratory tests and to ensure the presence of adequate technical data supporting cracking resistance for long-term reactor operation. Additional materials testing and characterizations may permit parametric limits to be established for SCC susceptibility in PWR primary water environment and to determine material modifications that could ensure adequate performance.

Stress corrosion of Alloy 152/52/52M weld metals in PWR primary water

In nearly all cases, as-welded Alloy 152, 52, and 52M materials have exhibited excellent SCC resistance and low crack-growth rates in laboratory tests. Most crack-growth data have been generated at either General Electric [49, 55, 57, 64] or Pacific Northwest National Laboratory [65, 66]. Results for many different weld metals and more than 15 welds demonstrate that IGSCC occurs, but IG engagement is limited, resulting in propagation rates less than 5×10^{-9} mm/s (2×10^{-10} in./s). An example illustrating the range in observed SCC response is given in Figure 4.14 for two Alloy 52M welds. The Alloy 52M V-groove weld exhibits a constant K crack growth rate of 4×10^{-9} mm/s (1.6×10^{-10} in./s), while the Alloy 52M narrow groove weld shows very little crack growth with a rate of ~8×10^{-10} mm/s (3×10^{-11} in./s) Significant IG areas were observed ahead of and along the crack front of the V-groove specimen, providing confirmation for the higher measured SCC propagation rate. Several other weld metal specimens have shown slightly higher rates when switching from cycle + hold transitioning, but in these cases the measured rate decreases with time at constant K, reaching much lower stable values. Figure 4.15 summarizes the reported SCC measurements from various laboratories on Alloy 152 and 52 type welds and illustrates crack growth rates below 5×10^{-9} mm/s (2×10^{-10} in./s) for all but one Alloy 152 weld [45, 61] and an Alloy 52M overlay at a high K value [66]. The 1×10^{-8} mm/s (4×10^{-10} in./s) propagation rate measured in the Alloy 52M overlay was found to occur in a lower Cr (~24 wt %) weld layer, and rates measured in the Alloy 52M overlay layers with the proper 30 wt % Cr were ~3×10^{-9} mm/s (1×10^{-10} in./s). The one exception that has not been explained is the comparatively high constant load crack growth rates [up to ~6×10^{-8} mm/s (2.4×10^{-9} in./s)]

reported by Argonne National Laboratory on an Alloy 152 weld [51, 67]. Three specimens have now been tested and are reported to give consistent crack growth results and a high degree of IG engagement, suggesting that this weld is more susceptible to IGSCC.

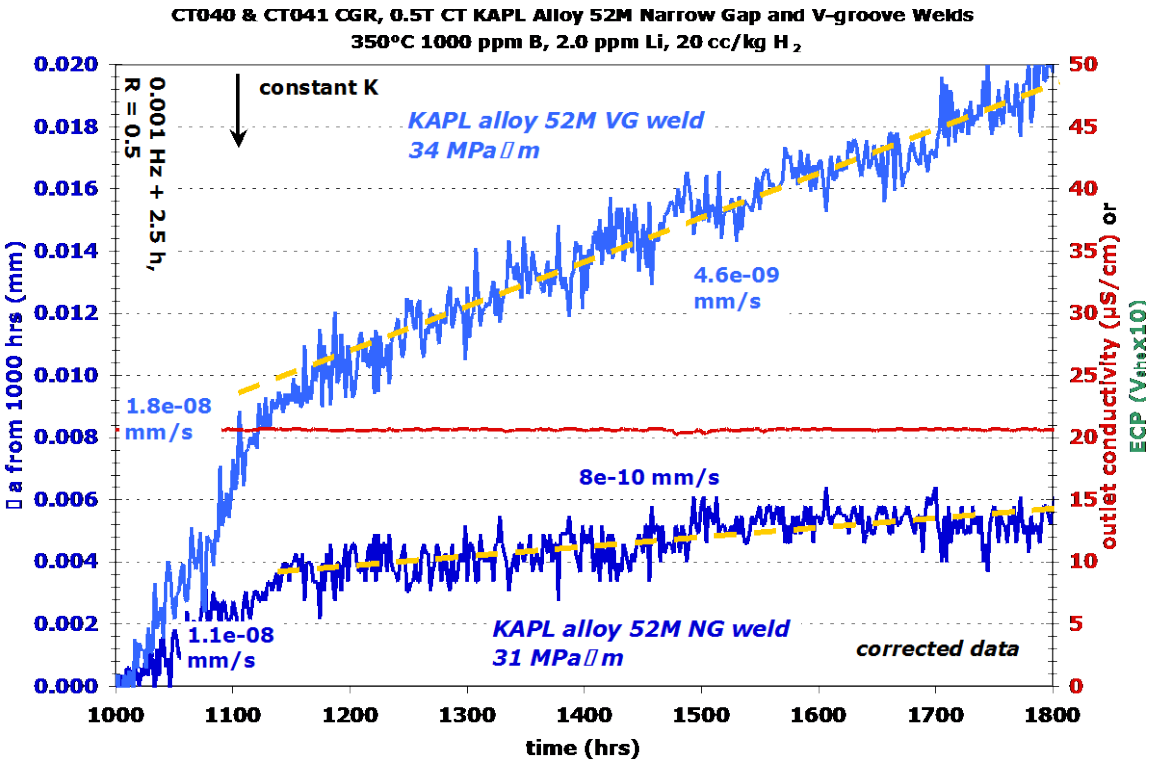

Figure 4.14. Measurements of constant K crack growth for two Alloy 52M welds showing low to very low propagation rates [64].

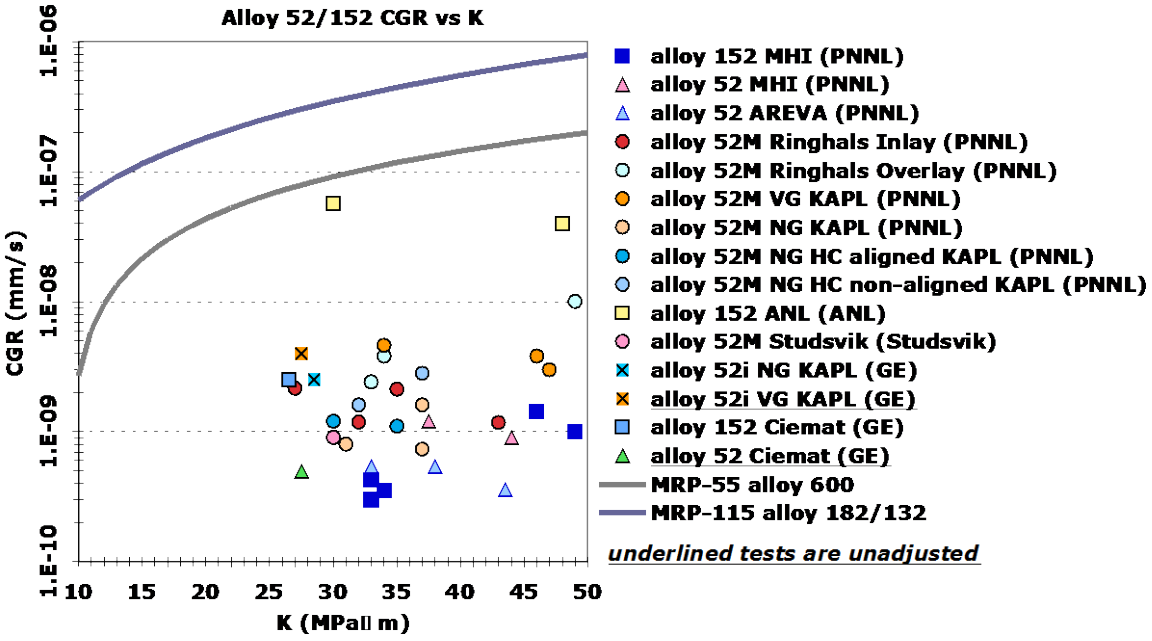

Figure 4.15. Summary of reported SCC propagation rates at constant K or constant load on alloy 152 and 52 type welds [64].

All but one of the welds were tested in the as-welded condition. One alloy 152 weld was evaluated at Pacific Northwest National Laboratory [65], both in the as-welded condition and after a low alloy steel stress relief annealing treatment. No influence on the SCC response was observed. Recently, General Electric also cold-forged an Alloy 152 weld in an attempt to simulate a high-strain condition. As might be expected from the results on cold-worked Alloy 690, preliminary results have indicated higher SCC growth rates. A key concern is the potential damage created during weld repairs, and this represents an essential need to be evaluated and characterized along with more diverse welds (e.g., heats, weld types, weld parameters, constraint) representing industry practice. It is also worthwhile to identify the potential effects of preexisting weld defects and cracks on subsequent SCC susceptibility. These flaws could create or enhance the opportunity for easier SCC initiation and growth due to the local microstructure and microchemistry plus its effect on the effective crack tip K level if the flaw is relatively deep. A few attempts have been made to evaluate the influence of weld cracks on SCC initiation [35–37] and propagation [66] with no indication of increased susceptibility. Although these limited studies have provided some initial information, additional experimentation is needed on well-controlled and characterized materials to properly assess the effects of weld defects on SCC response in PWR primary water environment.

4.3.5 Stress Corrosion of Weld Heat Affected and Dilution Zones in PWR Primary Water

The primary justification for the examination of cold-work effects on Alloy 690 microstructure evolution and SCC behavior is that weld shrinkage induces tensile plastic strain in the HAZ. As a result, crack growth along the HAZ is best represented by the S-L orientation with the plane of deformation that exhibits the highest SCC propagation rates. A few estimates of Alloy 690 HAZ plastic strain have been made based on EBSD measurements of misorientation [18, 46, 68]. These suggest that strains are somewhat lower than seen for stainless steel welds (less than ~15%) and are localized near the fusion line. As mentioned earlier, slightly higher strains have been identified in the partially melted zone.

A limited number of tests have been conducted to assess Alloy 690 HAZ SCC growth rates using compact tension (CT) specimens aligned with the weld fusion line and the HAZ. The best procedure seems to be carefully polish and etch the side surfaces of the CT specimen blank and to then to machine the notch and side grooves. Unfortunately, the weld fusion line typically meanders with depth through the specimen thickness, and the initial precrack during aggressive cycling can drive the crack outside the HAZ. These issues present challenges to a successful test in welds produced, particularly when the HAZ is not highly susceptible to SCC. In most cases, companion baseline tests have not been performed on the Alloy 690 base metal for a direct comparison to the HAZ results. Perhaps not surprisingly, crack-growth tests on Alloy 690 HAZs have not produced conclusive results. The limited data reveals low rates ($1–5 \times 10^{-9}$ mm/s ($0.4–2 \times 10^{-10}$ in./s) similar to that reported for base metal specimens, although isolated measurements [69, 70] have approached ~1×10^{-8} mm/s (4×10^{-10} in./s). The implications of these slightly higher rates are uncertain, especially considering the statistics in sampling, minor variations in test variables and the sparse data. It appears that additional testing and evaluation would better establish SCC behavior in the HAZ and adjacent areas of the weld fusion line. Integrated research is required that combines continued tests on representative mockup heats, tailored thermo-mechanical treatments to produce microstructures consistent with the HAZ, partially melted zone and the unmixed zone, and detailed characterizations of SCC interactions with these fusion line microstructures.

Dissimilar metal welds present an even more complicated fusion zone region, where unique microstructures and microchemistries are created between the alloy 152/52/52M weld metal and either low alloy steel or stainless steel. This reaction zone between the Ni-30%Cr alloy and the Fe-based steels produces significant dilution zone of complex composition along with the potential for new phase formation. Detailed characterizations and SCC evaluations of these dissimilar metal weld regions have not been reported. They represent another unknown for the long-term SCC resistance in PWR service, and research is needed to understand the characteristics of growing crack in the fusion zone region.

4.3.6 Corrosion Fatigue in PWR Primary Water

Just as SCC evaluations on Alloy 690 were concluded to be limited in the previous sections, it appears that focused corrosion fatigue testing has not been conducted on wide variety of materials and material conditions. Hickling [26], who reviewed several testing programs [71–74], concluded that sufficient data had been generated on prototypic reactor materials. Thick-walled Alloy 690 showed a reduction in fatigue life and an increase in cyclic crack-growth rates when tested in a simulated PWR primary water environment. However, this behavior was about the same as or somewhat better than that of other Ni-base alloys, such Alloy 600. All of these test results were obtained from Alloy 690, which is highly resistant to SCC. The limited testing that has been done on cold-worked materials as part of SCC crack-growth tests reveals accelerated cyclic crack growth, particularly under gentle cycling conditions. Of particular interest is the assessment of environmental enhancement (based on the comparison of crack-growth rates measured in PWR primary water versus estimated growth rates in air) routinely performed at Argonne National Laboratory [75, 76]. Results on as-received CRDM Alloy 690 materials showed little or no environmental enhancement, while significant enhancement, consistent with high SCC propagation rates, was observed in highly cold-rolled plate. Similar enhancements of cyclic crack growth rates have been seen at other laboratories during SCC tests on highly cold-worked Alloy 690 materials. Those materials that exhibit high SCC propagation rates also often show higher cyclic rates. Therefore, a similar issue exists for corrosion fatigue as discussed at some length in the previous section for SCC in PWR primary water.

4.4 CORROSION AND STRESS CORROSION CRACKING OF ALLOY 690 IN SECONDARY WATER

Research directed at providing information on the corrosion and SCC resistance of Alloy 690 in both nominal and faulted PWR secondary water chemistry has been significant due to the early use of Alloy 690 as steam generator tubing [28]. The water chemistry on the PWR secondary side is quite different from that on the primary side, including the chemical composition (with the absence of Li, B, and H_2 additions, and the presence of volatile alkalizing agents and possible impurities) and a higher, less-stable electrochemical potential. Gorman [77] has reviewed the international experience as of 2003 and examined probable causes for corrosion and cracking. The focus was on the degradation observed for mill-annealed Alloy 600 tubing, with some discussion addressing replacement tubing materials Alloy 600TT and Alloy 690TT. No known examples of degradation have been reported for Alloy 690TT, and, in general, laboratory tests have shown it to be highly resistant to corrosion and SCC in normal and most faulted secondary-side environments.

The most significant issue observed for Alloy 690TT has been the SCC in Pb-contaminated secondary water environments. Results show that the high-chromium Alloy 690 is susceptible to degradation in Pb-doped environments. Corrosion and transgranular SCC of Alloy 690TT

materials has been seen in the laboratory [78–86] for tests in neutral, acidic, caustic, and AVT (all-volatile-treated) water doped with Pb. Alloy 690 is most prone to PbSCC in high pH conditions (>9 at 330C), where it is more susceptible to cracking than Alloy 600.

It is important to note that even though the laboratory test results suggest SCC susceptibility, no secondary-side steam generator tube failures have been reported for Alloy 690TT, due to this cause. Considering the high number of corrosion and SCC failures in Alloy 600 tubing directly linked to Pb [78, 87, 88], service experience indicates that Alloy 690TT tubing has a significantly improved resistance to degradation. However, a recent review by Staehle [89] makes the case that Alloy 690TT tubing is likely to show secondary-side PbSCC during extended service. Pb greatly concentrates on surfaces of tubing in the superheated crevices either in drilled holes or in line contact geometries. High Pb concentrations (up to ~10%) have been observed even though trace Pb levels (parts per trillion) are present in the feedwater. These high surface Pb levels are expected in crevice regions of replacement Alloy 690 steam generators along with alkaline chemistries, creating conditions where severe PbSCC has been observed in laboratory tests. Staehle [89] also points out that Alloy 690 is prone to scale formation in the presence of Pb contamination, and local scale growth may accelerate SCC propagation.

Another secondary-side impurity of concern is the sulfur species on outer-diameter SCC of steam generator tubing [90, 91]. Alloy 690TT has been included in selected general corrosion and static SCC tests performed in complex sulfur-containing environments without any significant degradation reported. Limited evaluations of SCC propagation rates have also been performed [92, 93] in severely faulted secondary water (both highly acidic and highly alkaline), and again, no cracking was discovered for Alloy 690TT. More discerning crack-growth testing has not been conducted in secondary-side environments as has been done for primary-side environments. As a result, it seems likely that higher SCC susceptibility for cold-worked Alloy 690 would also be observed in AVT water and faulted secondary-side environments under similar test conditions. The most important impurity concern is Pb, and additional testing is needed to ensure long-term degradation resistance in service. If the opportunity occurs, it would be very useful to perform detailed examinations of corrosion and surface films in pulled tubes. Critical evaluations of secondary-side water chemistry on SCC behavior of Alloy 690TT using crack-growth testing techniques are also recommended, even though the PWR application is for thin-walled tubing. The direct measurement of corrosion products in secondary-side crevices will identify local impurity environments in the modern Alloy 690 steam generators and help specify conditions for laboratory tests to confirm long-term corrosion and SCC resistance.

Although not directly relevant to the PWR secondary-side environments, selected tests have been performed on Alloy 152 and 52 welds in oxidizing BWR water with impurities [94]. Crack-growth tests were performed at moderate-to-high K levels and very aggressive water chemistry conditions (2 ppm O_2 and 50 ppb SO_4 or Cl). In all cases, growth rates were low and the difference between 360 °C (680 °F) PWR primary water and BWR water at 288 °C (550 °F) was small. In any event, the BWR tests strongly support the excellent SCC resistance of the high-Cr weld metals in high-temperature water.

4.5 ENVIRONMENT-INDUCED FRACTURE AT LOW TEMPERATURES

Another potential issue of concern is a reduction in the fracture resistance of Alloy 690 and its weld metals during long-term exposure and dynamic straining in reactor water environments. This issue was first revealed by research of Mills [95–97] who observed large reductions in

fracture resistance in nickel-base alloys when tests were performed in low temperature water. Other researchers [98–101] have now confirmed this response in Alloy 690 and in alloy 152 and 52 weld metals. The phenomenon is often referred to as low-temperature crack propagation (LTCP), and it is not yet clear whether it represents a genuine reduction in fracture properties of the material or a form of rapid subcritical crack growth due to the environment. Both aspects may be involved. A typical feature of LTCP is the transition from ductile dimple fracture to brittle IG cracking; the alloy microstructure and probably grain boundary microchemistry have a crucial effect on susceptibility to SCC. The controlling mechanism of this "embrittlement" is clearly a form of hydrogen cracking with hydrogen ingress during prior exposure in high-temperature water and crack-tip corrosion during straining at lower temperature. Some data exist to characterize elements of the problem, but the detailed understanding to predict effects of material and environmental variables is lacking. It represents another area where additional research is needed, not only on the LTCP mechanisms, but also on interrelationships between IGSCC at high temperatures and IG crack extension at low temperatures during outages.

4.6 SUMMARY

Relevant properties and characteristics have been reviewed for Alloy 690 and its weld metals (Alloys 152, 52, and 52M) in relation to potential degradation issues for long-term LWR service. Alloy 690 and its associated weld metals have been effective replacement materials for Alloys 600, 182, and 82 in PWRs with no significant degradation identified (except tied to manufacturing or operation problems). Potential degradation modes of concern were evaluated, focusing on environment-assisted cracking, because SCC susceptibility has been identified in laboratory tests. For the most part, vulnerabilities have only been discovered during testing using off-normal material conditions (e.g., highly cold-worked Alloy 690) or in severe environments (e.g., Pb-containing secondary water). While these observations indicate the need for additional research to understand mechanisms promoting SCC and to establish limiting material–environmental conditions for susceptibility, excellent resistance has been documented for tests under representative service conditions. Recommended proactive research should include detailed evaluations of primary water SCC of cold-worked Alloy 690, as-welded alloy 152/52/52M, Alloy 690 HAZ (including the partially melted and unmixed zones), and dilution zone regions in dissimilar metal welds. Comprehensive characterizations are recommended in combination with SCC testing on multiple heats and welding conditions. Corrosion fatigue of Alloy 690 and its weld metals was not discussed in detail, but it presents many of the same questions as for SCC, and material effects on susceptibility are expected to be similar. While laboratory tests in PWR primary water only reveal SCC susceptibility under certain more-aggressive material conditions, Pb-containing secondary-side environments have been shown to produce extensive cracking of as-received Alloy 690. Steam generator experience with Alloy 690TT tubing has not yet identified this problem (as was found for Alloy 600 tubing); however, it represents a potential long-term vulnerability. Additional research is recommended, including secondary-side examinations of Alloy 690TT tubes removed from service. Several other material (e.g., weld cracking) and service degradation (e.g., LTCP) issues were also briefly discussed to identify aspects of the current understanding as well as interrelationships to other long-term degradation concerns.

The key concerns for Alloy 690 and its weld metals during extended PWR service to greater than 60 years discussed above are summarized here.

- Secondary-side SCC of Alloy 690TT steam generator tubing associated with Pb concentration particularly at line contact crevices. This issue may be observed much sooner

than 60 years, but has the potential to develop into a significant and widespread degradation mode during long-term operation.

- SCC of Alloy 690TT vessel penetrations and steam generator tubing in PWR primary water environments due to cold/warm work or mechanical damage. Deformation-induced high strength regions can exhibit significant SCC susceptibility with important heat-to-heat and microstructural effects. Even though such high strain regions do not appear to be likely in typical weld HAZs, the potential concern remains for off-normal microstructures including those created by compositional banding.

- SCC of alloy 152/52 welds and overlays particularly in high-strength regions created during welding and repair welding. Detailed understanding of strain and microstructural variability in service welds/overlays is limited, and direct assessment of effects on SCC susceptibility is needed.

- Weld defects, ductility dip, and hot cracking for alloy 152/52 weld metals and dissimilar metal dilution zones. A significant variability is expected for plant welds, and detailed characterizations are lacking. Evaluations of weld defect effects on SCC initiation and growth are needed.

- SCC of dissimilar metal welds of alloy 152/52 and LAS/SS, which represent an important issue for dilution zones (Cr depletion and Fe enrichment) and interface regions. Detailed understanding of strain and microstructural variability in limited and direct assessment of effects on SCC susceptibility is needed.

- Long-range ordering and Ni_2Cr precipitation. Although this does not appear to be an issue for service temperatures over 40 years, matrix strength increase, particularly for SCC susceptibility of Alloy 690 and weld metals, may be a potential long-term issue.

- While not discussed explicitly above, wear of steam generator tubing is a known operational issue and is typically a result of design issues rather than specific material conditions. However, if conditions for wear develop, this material will be susceptible to this form of degradation, although this is not unique to extended operating periods.

4.7 REFERENCES*

1. *INCONEL Alloy 690,* Publication SMC-079, Special Metals Corporation, 2002.
2. *Guidelines for PWR Steam Generator Tubing Specification and Repair," Vol. 2, Rev. 1: Guidelines for Procurement of Alloy 690 Steam Generator Tubing,* EPRI TR-016743-V2R1, Electric Power Research Institute, 1999.
3. A. McIlree and G. Ilevbare, *Materials Reliability Program: Guidelines for Thermally Treated Alloy 690 Pressure Vessel Nozzles (MRP-241),* 1015007, Electric Power Research Institute, 2008.

* Inclusion of references in this report does not necessarily constitute NRC approval or agreement with the referenced information.

4. ASME SB-167, “Specification for Nickel-Chromium-Iron Alloys (UNS N06600, N06601, N00690, N06025, and N06045) Seamless Pipe and Tube,” *ASME Boiler & Pressure Vessel Code,* Section II Material Specifications, Part B, 2001.

5. J. M. Sarver, J. R. Crum, and W. L. Mankins, “Carbide Precipitation and the Effect of Thermal Treatments on the SCC Behavior of Inconel Alloy 690,” p. 581 in *Proc. 3rd Int. Symp. Environmental Degradation of Materials in Nuclear Power Systems—Water Reactors,* Traverse City, Aug. 30–Sept. 3, 1987, G. J. Theus and J. Weeks (eds.), The Metallurgical Society, 1987.

6. T. Yonezawa et al., “Effect of Heat Treatment on Corrosion Resistance of Alloy 690,” p. 593 in *Proc. 2nd Int. Symp. Environmental Degradation of Materials in Nuclear Power Systems—Water Reactors,* Monterey, Sept. 9–12, 1985, J. Roberts and J. Weeks (eds.), American Nuclear Society, 1986.

7. K. Norring, K. Stiller, and J. Nilsson, “Grain Boundary Microstructure, Chemistry, and IGSCC in Alloy 600 and Alloy 690,” *Proc. 5th Int. Symp. Environmental Degradation of Materials in Nuclear Power Systems—Water Reactors,* Monterey, Aug. 25–29, 1991, D. Cubicciotti and E. Simonen (eds.), American Nuclear Society, 1992.

8. K. Stiller, J. Nilsson, and K. Norring, “Structure, Chemistry and Stress Corrosion Cracking of Grain Boundaries in Alloys 600 and 690,” *Metallurgical and Materials Transactions A* **27A**(2) (1996).

9. T. M. Angeliu and G. S. Was “Behavior of Grain Boundary Chemistry and Precipitates upon Thermal Treatment of Controlled Purity Alloy 690,” *Metallurgical Transactions A* **21,** 2097 (1990).

10. J. J. Kai, G. P. Yu, C. H. Tsai, M. N. Liu, and S. C. Yao, “The Effects of Heat Treatment on the Chromium Depletion, Precipitate Evolution and Corrosion Resistance of Inconel Alloy 690,” *Metallurgical Transactions A* **20A,** 2057 (1989).

11. R. S. Dutta, R. Tewari, and P. K. De, “Effects of heat-treatment on the extent of chromium depletion and caustic corrosion resistance of Alloy 690,” *Corrosion Science* **49,** 303 (2007).

12. S. M. Bruemmer and M. B. Toloczko, *Pacific Northwest National Laboratory Investigation of Stress Corrosion Cracking in Nickel-Base Alloys,* NUREG-CR-7103 Volume 2, U.S. Nuclear Regulatory Commission, January 2012.

13. S. M. Bruemmer, M. Olszta, L. E. Thomas, and M. B. Toloczko, “Linking Grain Boundary Microstructure to Stress Corrosion Cracking of Cold Rolled Alloy 690 in PWR Primary Water,” *Corrosion 2012,* National Association of Corrosion Engineers, 2012.

14. M. Morra, J. Grande, M. Othon, and E. Willis, “Quantification of Grain Size and Banding in Differently Thermo-Mechanical-Processed Heats of Alloy 690 Using Image Analysis,” *MRP Alloy 690/152/52 Research Collaboration Meeting,* Electric Power Research Institute, December 2010.

15. S. M. Bruemmer, M. J. Olszta, and M. B. Toloczko, “Cold Rolling Effects on Grain Boundary Damage and Stress Corrosion Crack Growth in Alloy 690,” Paper A062-T04, *Proc. Fontevraud 7 Int. Symp.: Contribution of Materials Investigation to Improve the Safety and Performance of LWRs,* Société Française d'Energie Nucléaire, Avignon, Sep. 26–30, 2010.

16. S. M. Bruemmer, M. J. Olszta, M. B. Toloczko, and L. E. Thomas, “High Resolution Characterization of Grain Boundary Damage and Stress Corrosion Cracks in Cold-Rolled Alloy 690,” p. 301 in *Proc. 15th Int. Conf. Environmental Degradation of Materials in*

Nuclear Power Systems—Water Reactors, Colorado Springs, Aug. 7–11, 2011, J. Busby and G. Ilevbare (eds.), The Minerals, Metals & Materials Society, 2012.

17. G. Theus et al., *Materials Reliability Program: Material Production and Component Fabrication and Installation Practices for Alloy 690 Replacement Components in Pressurized Water Reactor Plants (MRP-245),* 1016608, Electric Power Research Institute, 2008.
18. M. Morra, M. Othon, D. Wark, P. Chou, and E. Willis, "Characterization of Alloy 690 to 52-Type Welds, Weld Interfaces and Base Metal Interfaces," NRC–Industry 2011 Meeting on Alloy 690 Research, June 2011.
19. E. M. Lehockey, Y-P. Lin, and O. E. Lepik, "Mapping Residual Plastic Strain in Materials Using Electron Backscatter Diffraction," p. 247 in *Electron Backscatter Diffraction in Materials Science,* Schwartz et al. (eds.), Springer, 2000.
20. M. Morra, M. Othon, and D. Wark, "Macro and Microstructural Mapping and Residual Plastic Strains Analysis of Alloy 690 Base Metals and HAZ of Weldments," MRP Alloy 690/152/52 Research Collaboration Meeting, December 2010.
21. K. Smith, A. Klein, P. Saint-Paul, J. Blanchet, "Inconel 690, A Material with Improved Corrosion Resistance for PWR Steam Generator Tubes," p. 319 in *Proc. 2nd Int. Symp. Environmental Degradation of Materials in Nuclear Power Systems—Water Reactors,* Monterey, Sept. 9–12, 1985, J. Roberts and J. Weeks (eds.), American Nuclear Society, 1986.
22. A. Marucco, "Atomic Ordering in the Ni-Cr-Fe System," *Materials Science and Engineering* **A189,** 267 (1994).
23. T. Larsson, J. O. Nilsson, and J. Frodigh, "On the Possibility of Forming Ordered Ni2Cr in Alloy 690," p. 143 in *Proc. 9th Int. Symp. Environmental Degradation of Materials in Nuclear Power Systems—Water Reactors*, Newport Beach, Aug. 1–5, 1999, S. Bruemmer, F. P. Ford and G. Was (eds.), The Minerals, Metals & Materials Society, 1999.
24. F. Delabrouille et al., "Long range ordering in Ni Alloys containing 30% Cr," p. 888 in *Proc. 14th Int. Symp. Environmental Degradation of Materials in Nuclear Power Systems*, Virginia Beach, Aug. 23–27, 2009, T. Allen and J. Busby (eds.), American Nuclear Society, 2010.
25. H. Xu S. Fyfitch, P. Scott, M. Foucault, R. Killian, and M. Winters, *Materials Reliability Program, Resistance to Primary Water Stress Corrosion Cracking of Alloys 690, 52, and 152 in Pressurized Water Reactors (MRP-111),* 1009801, Electric Power Research Institute, 2004.
26. J. Hickling, *Materials Reliability Program, Resistance to Primary Water Stress Corrosion Cracking of Alloys 690 in Pressurized Water Reactors (MRP-258),* 1019086, Electric Power Research Institute, 2009.
27. S. D. Kiser, E. B. Hinshaw, J. R. Crum, and L. E. Shoemaker, "Nickel Alloy Welding Requirements for Nuclear Service," p. 21 in *Focus on Nuclear Power Generation* 2005, Special Metals Corporation.
28. Special Metals Corporation, *Product Datasheets for Inconel Alloy 152, 52 and 52M Weld Metals*, www.specialmetals.com/products.
29. S. M. Bruemmer, M .B. Toloczko, M. J. Olszta, R. J. Seffens, and P. G. Efsing, "Characterization of Defects in Alloy 152, 52 and 52M Welds," p. 319 in *Proc. 14th Int.*

Symp. Environmental Degradation of Materials in Nuclear Power Systems, Virginia Beach, Aug. 23–27, 2009, T. Allen and J. Busby (eds.), American Nuclear Society, 2010.

30. B. Hood and W. Lin, "Weldability Testing of Inconel Filler Materials," p. 69 in *Proc. 7th Int. Symp. Environmental Degradation of Materials in Nuclear Power Systems—Water Reactors,* Breckenridge, Aug. 7–12, 1995, R. Gold and A. McIlree (eds.), National Association of Corrosion Engineers, 1995.
31. W. Wu and C. Tsai, "Hot Cracking Susceptibility of Fillers 52 and 82 in Alloy 690," *Metall. Trans.* **30A,** 417 (1999).
32. M. Collins and J. Lippold, "An Investigation of Ductility Dip Cracking in Nickel-Based Filler Materials—Part I," *Welding Journal* **82**(10), 288s (2003).
33. M. Collins, A. Ramirez, and J. Lippold, "An Investigation of Ductility Dip Cracking in Nickel-Based Filler Materials—Part II," *Welding Journal* **82**(12), 348s (2003).
34. M. Collins, A. Ramirez, and J. Lippold, "An Investigation of Ductility Dip Cracking in Nickel-Based Filler Materials—"Part III," *Welding Journal* **83**(2), 39s (2004).
35. H. Hanninen, A. Toivonen, A. Brederholm, T. Saukkonen, U.Ehrnsten, and P. Aaltonen, "Environment-Assisted Cracking and Hot Cracking of Ni-Base Alloy Dissimilar Metal Welds," Paper 17, *Proc. 13th Int. Conf. Environmental Degradation of Materials in Nuclear Power Systems*, Whistler, Aug. 19–23, 2007, P. King and T. Allen (eds.), The Canadian Nuclear Society, 2008.
36. H. Hanninen, A. Toivonen, A. Brederholm, T. Saukkonen, U. Ehrnsten, and P. Aaltonen, "EAC Crack Initiation in Nickel-Based Dissimilar Metal Welds Using Doped Steam Test," p. 333 in *Proc. 14th Int. Symp. Environmental Degradation of Materials in Nuclear Power Systems*, Virginia Beach, Aug. 23–27, 2009, T. Allen and J. Busby (eds.), American Nuclear Society, 2010.
37. H. Hanninen, A. Toivonen, A. Brederholm, T. Saukkonen, W. Karlsen, U.Ehrnsten, and P. Aaltonen, "Effects of Hot Cracks on EAC Crack Initiation and Growth in Nickel-Base Alloy Weld Metals," p. 197 in *Proc. 15th Int. Conf. Environmental Degradation of Materials in Nuclear Power Systems—Water Reactors,* Colorado Springs, Aug. 7–11, 2011, J. Busby and G. Ilevbare (eds.), The Minerals, Metals and Materials Society, 2012.
38. G. A. Young, T. E. Capabianco, M. A. Penik, B. W. Morris, and J. J. McGee, "Mechanism of Ductility Dip Cracking in Nickel-Chromium Alloys," *Welding Journal* **87**(2), 31s (2008).
39. P. Combrade, P. M. Scott, M. Foucault, E. Andieu, and P. Marcus, "Oxidation of Ni Base Alloys in PWR Water: Oxide layers and Associated Damage to the Base Metal," p. 883 in *Proc. 12th Int. Conf. Environmental Degradation of Materials in Nuclear Power Systems—Water Reactors,* Salt Lake City, Aug. 14–18, 2005, L. Nelson, P. King and T. R. Allen (eds.), The Minerals, Metals and Materials Society, 2007.
40. M. Sennour, L. Marchetti, F. Martin, S. Perrin, R. Molins, and M. Pijolat, "A detailed TEM and SEM study of Ni-base alloys oxide scales formed in primary conditions of pressurized water reactors," *Journal of Nuclear Materials* **402,** 147 (2010).
41. J. B. Ferguson and H. F. Lopez, "Oxidation Products of Alloy 600 and 690 in PWR Environments and Their Role in Intergranular Stress Corrosion Cracking." *Metallurgical Transactions* **37A,** 2471 (2006).
42. M. J. Olszta, D. K. Schreiber, L. E. Thomas, and S. M. Bruemmer, "Penetrative Internal Oxidation from Alloy 690 Surfaces and Stress Corrosion Crack Walls during Exposure to PWR Primary Water," p. 331 in *Proc. 15th Int. Conf. Environmental Degradation of*

Materials in Nuclear Power Systems—Water Reactors, Colorado Springs, Aug. 7–11, 2011, J. Busby and G. Ilevbare (eds.), The Minerals, Metals and Materials Society, 2012.

43. S. Asada et al., "PWSCC Life Time Evaluation on Alloy 690, 52 and 152 for PWR Materials," *PWSCC of Alloy 600 Int. Conf. & Exhibition,* Atlanta, Electric Power Research Institute, June 2007.

44. P. L. Andresen, M. Morra and K. Ahluwalia, "SCC of Alloy 690 and Its Weld Metals," *Int. Boiling Water Reactor and Pressurized Water Reactor Materials Reliability Conference,* July 2012.

45. M. B. Toloczko, M. Olszta and S.M. Bruemmer, "Stress Corrosion Crack Initiation Testing on Nickel-Base Alloys in PWR Primary Water," International Cooperative Group on Envirnment-Assisted Cracking, Quebec City, Canada, May 2012.

46. P. L. Andresen, *Development of Advanced Testing Techniques to Quantify the Improved PWSCC Resistance of Alloy 690 and its Weld Metals (MRP-123),* Technical Report 1010269, Electric Power Research Institute, 2004.

47. D. J. Paraventi and W. C. Moshier, "Alloy 690 SCC Growth Rate Testing," *Workshop on Cold Work in Iron- and Nickel-Base Alloys,* Electric Power Research Institute, June 2007.

48. D. J. Paraventi and W. C. Moshier, "Alloy 690 SCC Growth Rate Testing," *Proc. EPRI Alloy 690 Workshop,* Atlanta, October 2007, Electric Power Research Institute.

49. P. L. Andresen, M. M. Morra, J. Hickling, A. Ahluwalia, and J. Wilson, "PWSCC of Alloys 690, 52 and 152," Paper 97 in *Proc. 13th Int. Conf. Environmental Degradation of Materials in Nuclear Power Systems*, Whistler, Aug. 19–23, 2007, P. King and T. Allen (eds.), The Canadian Nuclear Society, 2008.

50. P. L. Andresen, M. M. Morra, J. Hickling, K. Ahluwalia, and J. A. Wilson, "Effect of Deformation and Orientation on SCC of Alloy 690," p. 846 in *Proc. 14th Int. Symp. Environmental Degradation of Materials in Nuclear Power Systems*, Virginia Beach, Aug. 23–27, 2009, T. Allen and J. Busby (eds.), American Nuclear Society, 2010.

51. B. Alexandreanu, "The Stress Corrosion Cracking Behavior of Alloys 690 and 152 Weld in a PWR Environment," p. 239 in *Proc. 14th Int. Symp. Environmental Degradation of Materials in Nuclear Power Systems*, Virginia Beach, Aug. 23–27, 2009, T. Allen and J. Busby (eds.), American Nuclear Society, 2010.

52. M. B. Toloczko and S. M. Bruemmer, "Crack Growth Response of Alloy 690 in Simulated PWR Primary Water," p. 706 in *Proc. 14th Int. Symp. Environmental Degradation of Materials in Nuclear Power Systems*, Virginia Beach, Aug. 23–27, 2009, T. Allen and J. Busby (eds.), American Nuclear Society, 2010.

53. S. Bruemmer, M. Olszta, D. Edwards, and M. Toloczko, "Microstructural Effects on IGSCC of Cold-Rolled Alloy 690," *MRP Alloy 690/152/52 Research Meeting,* Electric Power Research Institute, December 2011.

54. M. B. Toloczko and S. M. Bruemmer, "One Dimensional Cold Rolling Effects on Stress Corrosion Crack Growth in Alloy 690 Tubing and Plate Materials," p. 91 in *Proc. 15th Int. Conf. Environmental Degradation of Materials in Nuclear Power Systems—Water Reactors,* Colorado Springs, Aug. 7–11, 2011, J. Busby and G. Ilevbare (eds.), The Minerals, Metals & Materials Society, 2012.

55. P. L. Andresen, M. M. Morra, and K. Ahluwalia, "SCC of Alloy 690 and Its Weld Metals," p. 161 in *Proc. 15th Int. Conf. Environmental Degradation of Materials in Nuclear Power*

Systems—Water Reactors, Colorado Springs, Aug. 7–11, 2011, J. Busby and G. Ilevbare (eds.), The Minerals, Metals & Materials Society, 2012.

56. D. R. Tice, S. L. Medway, N. Platts, and J. W. Stairmand, “Crack Growth Testing on Cold Worked Alloy 690 in Primary Water Environment,” p. 71 in *Proc. 15th Int. Conf. Environmental Degradation of Materials in Nuclear Power Systems—Water Reactors,* Colorado Springs, Aug. 7–11, 2011, J. Busby and G. Ilevbare (eds.), The Minerals, Metals & Materials Society, 2012.

57. S. M. Bruemmer and M. B. Toloczko, “Update on PNNL SCC Growth Rate Testing on Alloy 690 Materials,” *MRP Alloy 690/152/52 Research Collaboration Meeting,* Electric Power Research Institute, December 2011.

58. P. L. Andresen, M. M. Morra, and K. S. Ahluwalia, “SCC of Alloy 690 and Its Weld Metals,” Paper A010-T04, *Proc. Fontevraud 7 Int. Symp.: Contribution of Materials Investigation to Improve the Safety and Performance of LWRs,* Société Française d'Energie Nucléaire, Avignon, Sept. 26–30, 2010.

59. L. E. Thomas and S. M. Bruemmer, “High-Resolution Characterization of Intergranular Attack and Stress Corrosion Cracking of Alloy 600 in High-Temperature Primary Water," *Corrosion Journal* **56**(7), 572 (2000).

60. S. M. Bruemmer and L. E. Thomas, “Crack-Tip Examinations of Primary-Water Stress Corrosion Cracking in Alloy 600,” p. 603 in *Proc. Fontevraud 6 Int. Symp.: Contributions of Materials Investigations to Improve the Safety and Performance of LWRs,* Société Française d'Energie Nucléaire, Paris, Sept. 18–22, 2006.

61. S. M. Bruemmer and L. E. Thomas, “Insights into Stress Corrosion Mechanisms from High Resolution Measurements of Crack-Tip Structures and Compositions,” Paper 1264-BB01-09, *Proc. 2010 MRS Spring Meeting,* Vol. 1264, Materials Research Society, 2010.

62. S. M. Bruemmer and L. E. Thomas, “High-Resolution Characterizations of Stress-Corrosion Cracks in Austenitic Stainless Steel from Crack Growth Tests in BWR-Simulated Environments,” p. 189 in *Proc. 12th Int. Conf. Environmental Degradation of Materials in Nuclear Power Systems—Water Reactors,* Salt Lake City, Aug. 14–18, 2005, L. Nelson, P. King and T.R. Allen (eds.), The Minerals, Metals & Materials Society, 2007.

63. S. M. Bruemmer and L. E. Thomas, “Comparison of IGSCC Crack-Tip Characteristics in BWR Oxidizing Water and BWR Hydrogen Water Chemistry Conditions,” Paper 144, *Proc. EPRI Alloy 690 Workshop,* Atlanta, October 2007.

64. P. L. Andresen and M. Morra, “SCC Growth Rates of Alloy 152/52/52i Welds,” *MRP Alloy 690/152/52 Research Collaboration Meeting,* Electric Power Research Institute, December 2011.

65. M. B. Toloczko and S. M. Bruemmer, “Crack-Growth Response of Alloy 152 and 52 Weld Metals in Simulated PWR Primary Water,” p. 690 in *Proc. 14th Int. Symp. Environmental Degradation of Materials in Nuclear Power Systems—Water Reactors*, Virginia Beach, Aug. 23–27, 2009, T. Allen and J. Busby (eds.), American Nuclear Society, 2010.

66. M. B. Toloczko, M. Olszta, and S. M. Bruemmer, “Stress Corrosion Crack Growth of Alloy 52M in Simulated PWP Primary Water,” p. 225 in *Proc. 15th Int. Conf. Environmental Degradation of Materials in Nuclear Power Systems—Water Reactors,* Colorado Springs, Aug. 7–11, 2011, J. Busby and G. Ilevbare (eds.),The Minerals, Metals & Materials Society, 2012.

67. B. Alexandreanu, Y. Chen, K. Natesan, and W. Shack, “SCC Behavior of Alloy 152 Weld in PWR Environment,” p. 179 in *Proc. 15th Int. Conf. Environmental Degradation of Materials in Nuclear Power Systems—Water Reactors,* Colorado Springs, Aug. 7–11, 2011, J. Busby and G. Ilevbare (eds.), The Minerals, Metals & Materials Society, 2012.

68. G. Young, M. J. Hackett, J. D. Tucker, and J. M. Pyle, “Ni-Cr Weld Characterization,” *Alloy 690 Experts Meeting,* Electric Power Research Institute, December 2009.

69. P. L. Andresen, M. Morra, and A. Ahluwalia, “SCC Growth Rates of Alloy 690 and HAZ,” *NRC/Industry Alloy 690 Expert Meeting,* U.S. Nuclear Regulatory Commission, June 2011.

70. B. Alexandreanu, Y. Chen, K. Natesan, and W. Shack, “Cyclic and SCC Behavior of Alloy 690 HAZ in PWR Environment,” p. 109 in *Proc. 15th Int. Conf. Environmental Degradation of Materials in Nuclear Power Systems—Water Reactors,* Colorado Springs, Aug. 7–11, 2011, J. Busby and G. Ilevbare (eds.), The Minerals, Metals and Materials Society, 2012.

71. M. Higuchi et al., “Revised and new proposal of environmental fatigue life correction factor for carbon and low alloy steels and nickel base alloys in LWR water environments,” *Proc. ASME Pressure Vessels and Piping Division Conference,* PVP2006-ICPVT-11-93194, 2006.

72. R. Etien et al., “EAC Behavior and Mechanical Properties of Improved Alloy 690 Filler Metals,” *MRP PWSCC Expert Panel Meeting,* Electric Power Research Institute, November 2007.

73. A. Jenssen, K. Norring, and P. Efsing, “Swedish Activities on Alloy 690 and its Weld,” *MRP PWSCC Expert Panel Meeting*, Electric Power Research Institute, November 2008.

74. K. Tsutsumi, “Fatigue Crack Growth Rate Curve for Nickel Based Alloys in PWR Environment,” *Proc. Fontevraud 7 Int. Symp.: Contribution of Materials Investigations to Improve the Safety and Performance of LWRs,* Société Française d'Energie Nucléaire, Avignon, Sept. 26–30, 2010.

75. W. J. Shack and T. F. Kassner, *Review of Environmental Effects on Fatigue Crack Growth of Austenitic Stainless Steels*, NUREG/CR-6176, ANL-94/1, U.S. Nuclear Regulatory Commission, May 1994.

76. B. Alexandreanu, “SCC CGRs of Alloys 690 and 52/152 Welds in PWR Water,” *Alloys 690/52/152 PWSCC Research Test Materials Meeting,* Industry/NRC RES, U.S. Nuclear Regulatory Commission, July 2008.

77. J. A. Gorman, J. E. Harris, R. W. Staehle, and K. Fruzzetti, “Secondary Side Corrosion of 600MA Tubing in PWR Steam Generators—Causes, Implications for Alloys 600TT and 690TT and Need Research,” p. 362 in *Proc. 11th Int. Conf. Environmental Degradation of Materials in Nuclear Power Systems—Water Reactors,* Stevenson, Aug. 10–14, 2003, G. Was and L. Nelson (eds.), American Nuclear Society, 2003.

78. R. W. Staehle, “Clues and Issues in the SCC of High Nickel Alloys with Dissolved Lead,” *MRP Alloy 690/152/52 Research Collaboration Meeting,* EPRI, December 2011, p. 1163; and “Assessment of and Proposal for a Mechanistic Interpretation of the SCC of High Nickel Alloys in Lead-Containing Environments,” p. 381 in *Proc. 14th Int. Symp. Environmental Degradation of Materials in Nuclear Power Systems*, Virginia Beach, Aug. 23–27, 2009, T. Allen and J. Busby (eds.), American Nuclear Society, 2010.

79. T. Sakai, T. Senjuh, K. Aoki, T. Shigemitsu, and Y. Kishi, “Study on Corrosion Resistance of Alloy 600 and 690 in High Temperature Water Containing Lead,” p. 83/1 in *Corrosion 1992*, National Association of Corrosion Engineers, 1992.

80. K. K. Chung, J. K. Lim, S. Moriya, Y. Watanabe, and T. Shoji, “Lead Induced Stress Corrosion Cracking of Alloy 690 in High Temperature Water,” p. 233 in *Proc. 7th International Symposium on Environmental Degradation of Materials in Nuclear Power Systems—Water Reactors*, Breckenridge, Aug. 7–12, 1995, R. Gold and A. McIlree (eds.), National Association of Corrosion Engineers, 1995.

81. F. Vaillant, D. Buisine, B. Prieux, D. Gomez Briceno, and L. Castano, “Influence of Lead on the Secondary Side Cracking of Alloys 600, 690 and 800,” p. 13/1 in *Eurocorr’96*, Centre Francais de L’Anticorrosion Societe de Chimie Industrielle, Nice, 1996.

82. H. Takamatsu, B. P. Miglin, P. A. Sherburne, and K. Aoki, “Study on Lead-induced Stress Corrosion Cracking of Steam Generator Tubing under AVT Water Chemistry Conditions,” p. 216 in *Proc. 8th Int. Symp. Environmental Degradation of Materials in Nuclear Power Systems—Water Reactors*, Amelia Island, Aug. 10–14, 1997, A. McIlree and S. Bruemmer (eds.), American Nuclear Society, 1997.

83. J. M. Sarver, “IGSCC of Nickel Alloys in Lead Contaminated High Purity Water,” p. C11/1 in *1987 EPRI Workshop on Secondary Side Intergranular Corrosion Mechanisms*; NP-5971, Electric Power Research Institute, 1987.

84. J. Lumsden and A. R. McIlree, “Factors Affecting PbSCC in Alloy 600 and Alloy 690 Steam Generator Tubing,” PWR Secondary-III, Paper 40, *Proc. Fontevraud 7 Int. Symp.,* Société Française d'Energie Nucléaire, Avignon, Sept. 26–30, 2010.

85. H. Kim, S. Hwang, J. Kim, and J. Hong, “Stress Corrosion Cracking of Steam Generator Tubing Materials in Lead Containing Solution,” PWR Secondary-III, Paper 38, *Proc. Fontevraud 7 Int. Symp.,* Société Française d'Energie Nucléaire, Avignon, Sept. 26–30, 2010.

86. M. G. Burke et al., Evidence for a Corrosion Slot/Tunneling Mechanism for Lead-Induced Transgranular SCC of Alloy 690 in PbO + 10% NaOH Solution,” PWR Secondary-III, Paper 37 in *Proc. Fontevraud 7 Int. Symp.: Contribution of Materials Investigations to Improve the Safety and Performance of LWRs,* Société Française d'Energie Nucléaire, Avignon, Sept. 26–30, 2010.

87. L. E. Thomas and S. M. Bruemmer, “Observations and Insights into Pb-Assisted Stress Corrosion Cracking of Alloy 600 Steam Generator Tubes,” p. 1143 in *Proc. 13th Int. Conf. Environmental Degradation of Materials in Nuclear Power Systems*, Whistler, Aug. 19–23, 2007, P. King and T. Allen (eds.), The Canadian Nuclear Society, 2008.

88. L. E. Thomas and S. M. Bruemmer, *Summary of Analytical Electron Microscopy Observations of Intergranular Attack and Stress Corrosion Cracks in Alloy 600 Steam Generator Tubing,* Topical Report 1011683, Electric Power Research Institute, April 2005.

89. R. W. Staehle, “Reasonably Expected Performances of Alloy 690 and 800 Based on their Properties and Environment,” *7th CNS Int. Steam Generator Conference,* Toronto, November 2012.

90. *Pressurized Water Reactor Secondary Water Chemistry Guidelines—Revision 6,* Report 1008224, Electric Power Research Institute, 2004.

91. C. Mansour, “Behavior of Sulfur Species in Steam Generator Conditions of PWRs,” PWR Secondary 1, paper 10, *Proc. Fontevraud 7 Int. Symp.,* Société Française d'Energie Nucléaire, Avignon, Sept. 26–30, 2010.

92. Y. Yamamoto et al., “Evaluation of Crack Growth Rate for Alloy 600TT Steam Generator Tubing in Primary and Faulted Secondary Water Environments,” p. 1243 in *Proc. 14th Int.*

Symp. Environmental Degradation of Materials in Nuclear Power Systems, Virginia Beach, Aug. 23–27, 2009, T. Allen and J. Busby (eds.), American Nuclear Society, 2010.

93. O. de Bouvier et al., "Stress Corrosion Cracking of Nickel Alloys in Complex (Liquid and Vapor) Environments," p. 1255 in *Proc. 14th Int. Symp. Environmental Degradation of Materials in Nuclear Power Systems*, Virginia Beach, Aug. 23–27, 2009, T. Allen and J. Busby (eds.), American Nuclear Society, 2010.

94. P. L. Andresen, "SCC of High Cr Alloys in BWR Environments," p. 267 in *Proc. 15th Int. Conf. Environmental Degradation of Materials in Nuclear Power Systems—Water Reactors,* Colorado Springs, Aug. 7–11, 2011, J. Busby and G. Ilevbare (eds.), The Minerals, Metals & Materials Society, 2012.

95. C. M. Brown, and W. J. Mills, "Effect of Water on Mechanical Properties and Stress Corrosion Behavior of Alloy 600, Alloy 690, EN82H Welds, and EN52 Welds," *Corrosion Journal* **55,** 173 (1999).

96. W. J. Mills and C. M. Brown, "Fracture Behavior of Ni-Base Alloys in Water," p.167 in *Proc. 9th Int. Symp. Environmental Degradation of Materials in Nuclear Power Systems—Water Reactors*, Newport Beach, Aug. 1–5, 1999, S. Bruemmer, F. P. Ford and G. Was (eds.), The Minerals, Metals & Materials Society, 1999.

97. C. M. Brown and W. J. Mills, "Fracture Toughness of Alloy 690 and EN52 Welds in Air and Water," *Metallurgical and Materials Transactions A* 33, 1725 (2002).

98. A. Demma, A. McIlree, J. Peng, and P.J. King, "Effects of Dissolved Hydrogen and Hydrogen Peroxide on the Fracture Resistance of Weld Metals 182, 52, and 152 in Simulated PWR Shutdown Environment," Paper 32 in *Proc. 13th Int. Conf. Environmental Degradation of Materials in Nuclear Power Systems*, Whistler, Aug. 19–23, 2007, P. King and T. Allen (eds.), The Canadian Nuclear Society, 2008.

99. K. Tsutsumi, Y. Nomura, H. Kanasaki and S. Asada, "Intergranular Cracking Susceptibility of Alloy 152 in Low Temperature Water with Hydrogen," *Transactions of the Japan Society of Mechanical Engineers A* **726,** 265 (2007).

100. M. Ahonen, U. Ehrnstén, and H. Hanninen, "Low Temperature Crack Propagation of Nickel-Based Weld Metals in Hydrogenated PWR Primary Water," Paper A016-T04, *Proc. Fontevraud 7 Int. Symp.,* Société Française d'Energie Nucléaire, Avignon, Sept. 26–30, 2010.

101. T. Shoji, Y. Ito, Zhanpeng Lu, and T. Yonezawa, "Mechanistic Understanding of Low Temperature Crack Propagation for Alloy 690 in Hydrogenated Water," p. 98 in *Proc. 13th Int. Conf. Environmental Degradation of Materials in Nuclear Power Systems*, Whistler, Aug. 19–23, 2007, P. King and T. Allen (eds.), The Canadian Nuclear Society, 2008.